

ÓBUDAI EGYETEM
ÓBUDA UNIVERSITY

DOCTORAL (PhD) THESIS FOR HOME DEFENSE

XUANZHEN CEN

Stiffness-Related Coupling Analysis of the Biomechanical Functions of the Human Foot-Ankle Complex

Supervisor: Prof. Dr. Bíró István

Content

Motivation of the work	1
Research objectives	4
1 LITERATURE REVIEW	5
1.1 Biomechanical function of the human foot arch structure	5
1.1.1 Morphology-related arch motor function.....	7
1.1.2 Biomechanical coupling of the foot-ankle complex	12
1.2 Human gait characteristics and biomechanical analysis	16
1.2.1 Locomotion patterns and biomechanical function adjustment of the lower limbs.....	18
1.2.2 Gait termination biomechanics and compensatory strategy adjustment	21
1.3 Applications of finite element modeling in biomechanical analysis of foot arch	26
1.3.1 Overview of finite element model design	27
1.3.2 Main challenges in computational foot modeling	32
2 MATERIAL AND METHODS	40
2.1 Overview of the experimental and computational workflow	40
2.2 Ethics statement	41
2.3 Participants	42
2.4 Biomechanical functional analysis	43
2.4.1 Experimental protocol and procedures.....	43
2.4.2 Data collection and processing.....	45
2.4.3 Statistical analysis	47
2.5 Foot finite element analysis	48
2.5.1 Geometry reconstruction and mesh creation.....	48
2.5.2 Material properties	49
2.5.3 Boundary and loading conditions.....	50
2.5.4 Model validation	51

3 RESULTS.....	52
3.1 Statistical nonparametric mapping analysis	52
3.1.1 Ankle kinematics	52
3.1.2 Metatarsophalangeal kinematics	54
3.2 Inter-joint coupling coordination analysis	56
3.2.1 Coupling coordination.....	56
3.2.2 Coordination variability	57
3.2.3 Ground reaction impulse	58
3.3 Foot finite element analysis.....	60
3.3.1. Finite element model validation.....	60
3.3.2 Stress distribution.....	60
3.3.3 Force transmission	61
4 DISCUSSION.....	63
4.1 Foot-ankle temporal kinematics.....	63
4.2 Inter-joint coupling coordination and ground reaction impulse.....	65
4.3 Internal foot mechanics.....	68
4.4 Limitations	70
5 CONCLUSIONS AND FUTURE WORKS	72
NEW SCIENTIFIC THESIS POINTS	73
LIST OF PUBLICATIONS.....	79
REFERENCE.....	84
ABBREVIATION	104
LIST OF TABLES.....	105
LIST OF FIGURES	105
ACKNOWLEDGEMENTS	107

*“The human foot is a masterpiece of engineering
and a work of art.”*

Leonardo Da Vinci

Italian polymath

Motivation of the work

A well-functioning foot-ankle structure is significant in daily locomotor tasks [1]. As the primary part for adjusting foot stiffness, the foot arch is springlike, as it compresses during the early stance phase and recoils during the late stance phase, which could improve gait efficiency by storing and returning mechanical work [1-3]. Given the stiffness of arch-spanning tissues, the windlass mechanism indicates that metatarsophalangeal (MTP) dorsiflexion produces the winding of the plantar fascia (PF) about the head of the metatarsus, thereby shortening and raising the arch, and inverting the subtalar joint [4]. On the other hand, considering the impact of altering MTP kinematics on the PF strain, the arch-spring mechanism further emphasizes the significant contribution of ligamentous structures, represented by the PF, to elastic energy absorption and dissipation [1]. Welte et al. [2] investigated the interaction between the above two mechanisms and found that the engagement of the windlass through MTP dorsiflexion reduced arch stiffness (AS), and increased energy storage and return. MTP dorsiflexion may consequently influence foot movement by adjusting the mechanical energy pattern. Kirsty et al. [5] also found that the PF demonstrated a characteristic elastic stretch-shortening cycle, with most of the strain produced through compressing the arch. The energy transfer mechanism of the PF between the MTP (energy absorption) and the foot arch (energy produced during recoil) reduces the strain required for the PF to produce positive mechanical work at the arch.

From the perspective of morphological evolution and functional adaptation, structural changes in the foot arch will inevitably lead to variations in the lower-limb biomechanics, increasing the potential risk of foot damage and musculoskeletal problems [6-8]. Although arch height is overwhelmingly cited as a predictive factor for podiatry, there is emerging evidence that AS (or arch flexibility) might also be a critical contributor [9]. It is also considered to be a standard for evaluating injury susceptibility considering the association among ground reaction force (GRF), foot pronation/supination, and foot injury [9, 10]. Despite some studies demonstrating links

between arch morphological characteristics and discrete biomechanical data, little work has examined the correlation between AS and temporal kinematics. Statistical parametric mapping (SPM) has proven to be helpful in biomechanical data with time-varying characteristics in previous studies [11, 12]. Statistical nonparametric mapping (SnPM), as an SPM nonparametric equivalent, permits hypothetical testing on the whole waveform rather than concentrating on specific data points, thus compensating for regional focus bias [13, 14]. The amplitude of the loading on the arch would further increase in comparison to steady-state gait during gait termination (GT) [15]. Furthermore, the GT task was performed as a valuable tool for gait analysis, and it is widely used to assess motor function in patients with balance disorders [16, 17]. As the closest anatomically to the arch, the biomechanical properties between the MTP and ankle joint are also worth exploring during GT induced by unplanned stimuli.

Another area that has yet to be explored is the implications of AS on lower extremity coupling coordination in gait. Traditional biomechanical gait assessments have typically used discrete measures, such as range of motion (ROM) and peak plantar pressure. Nevertheless, isolated joint kinematics can neither effectively reflect the segmental coordination information producing resultant angular positions nor provide a comprehensive insight into the altered movement patterns caused by functional differences in the foot [18]. A continuous approach, in contrast, enables the quantification of movement coordination patterns throughout the gait cycle and can provide spatial-temporal details of the locomotion [19]. Coupling coordination analysis allows for assessing the timing and magnitude of relative motion between body segments, while coordination variabilities (CVs) further quantify the degree of fluctuation in coordination patterns [18, 19]. While numerous studies have shown relationships between kinematic coupling behavior and arch biomechanical function, and between foot morphology and injury susceptibility, few have investigated the association between lower extremity inter-joint coordination and AS [20, 21].

The etiology of biomechanical metatarsalgia has been recognized as alterations in weight distribution to the MTP joints due to functional or structural changes [22].

Nevertheless, these laboratory-based experimental results may be limited since they cannot allow direct assessment of detailed mechanical changes in the foot structure, particularly for the internal stress and strain distribution in the metatarsal region [23, 24]. To overcome the above-mentioned intrinsic difficulties, computational modeling techniques, represented by the finite element (FE) analysis, provided the feasibility for methodological purposes. Therefore, the present work aimed to combine biomechanical functional analysis and FE analysis of the foot-ankle complex to reveal foot-specific functional coupling mechanisms related to AS during motion. An understanding of the morphological arch biomechanical function may provide additional insights into foot injury prediction and the comprehensive compensatory adjustment of lower-limb joints.

Research objectives

Based on the work motivation, the main research objectives of this dissertation are as follows.

The first research objective: To investigate the foot-ankle temporal kinematic characteristics of stiff- and flexible-arched individuals during planned and unplanned GT using an SnPM method. Since more flexible arches tend to have a greater tendency to drop under load, I hypothesized that flexible arches would exhibit greater dorsiflexion angles in the sagittal plane during GT. Furthermore, subjects would have large ankle and MTP joint angles during GT caused by unexpected stimulation in all motion planes.

The second research objective: To examine the influences of AS on the lower extremity segment CVs and anterior-posterior ground reaction impulses (AP-GRIs). I assumed that the CVs of the selected inter-joint couplings and the GRIs in the AP directions would be affected due to differences in AS and that the flexible arch group would exhibit greater CVs and GRIs because of the tendency for the flexible medial longitudinal arch (MLA) to deform during walking and running.

The third research objective: To reconstruct a subject-specific FE model of the foot-ankle complex utilizing the exact three-dimensional geometry of foot bone and soft tissue, and examine the influences of PF stiffness on metatarsal stress distribution and joint force transmission. Based on previous reports, I hypothesized that variations in PF stiffness would lead to stress redistribution in the metatarsal region, while peak stress would be gradually reduced as stiffness decreased until PF release. Besides, I also assumed that as the PF stiffness increases, the joint contact forces related to the metatarsals would increase.

1 LITERATURE REVIEW

1.1 Biomechanical function of the human foot arch structure

The human foot arch is the elastic and constrictive cambered structure comprising of tarsal bones, metatarsal bones, and surrounding ligaments and tendons. In general, the anterior transverse arch and the medial and lateral longitudinal arches together form this arch structure. Moreover, the MLA is considered as a significant feature that is different from other primates in the process of evolution [25]. The most important contribution of the longitudinal arch in human locomotion, such as running and jumping, is to absorb loading impact and to improve the efficiency of ambulation [26, 27]. The windlass mechanism of the human foot illustrates well the positive effects of the longitudinal arch in the push-off phase during gait (**Figure 1**) [25, 28].

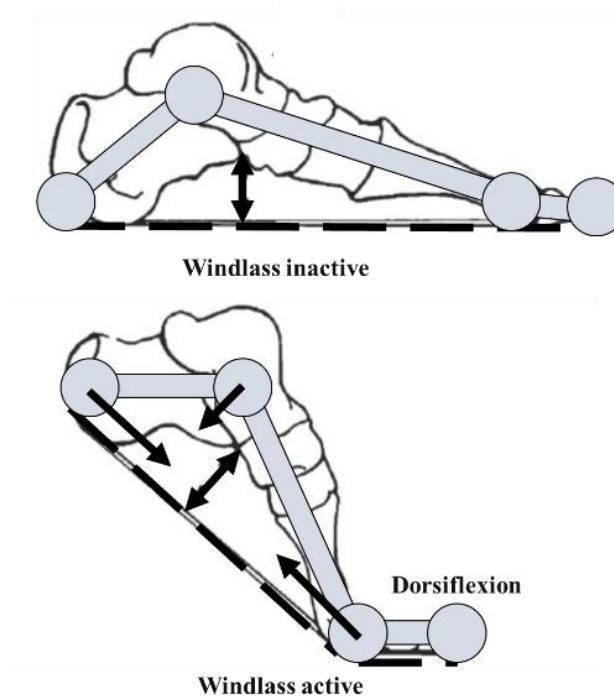


Figure 1 The windlass mechanism of the human foot

The active elastic subsystem composed of the intrinsic and extrinsic muscles on the foot plays an important role in maintaining arch stability and foot motion [29]. The plantar intrinsic muscles support the foot arches in dynamic activities and have synergistic and

modulating effects on the foot arches [29, 30]. The extrinsic muscles provide both absorption and propulsion abilities to the longitudinal arch during gait [29]. The difference in arch type is a contributory factor in sports injuries, which could influence physical performance [27]. Furthermore, poor exercise behaviors might also lead to progressive deformation in arch morphology, resulting in foot problems and affecting the quality of life [31].

A complete foot arch serves as a cushion during running or jumping actions, where the foot structure resembles a triangular truss structure (**Figure 2**). The distance from the metatarsal neck corresponds to the top structure of the truss, while the distance from the metatarsal head to the phalanges and the calcaneus corresponds to the front and rear struts of the truss, respectively. The PF acts as the tension member or crossbeam of the truss structure [32, 33]. The struts on both sides of the truss model experience vertical pressure, while the PF experiences horizontal tension. When the truss tension member elongates, the top of the truss descends correspondingly, increasing the horizontal force and weakening the compressive strength. During the stance phase of gait, the PF experiences increased horizontal tension, leading to a descent of the longitudinal arch. Conversely, when the truss tension member shortens, the top of the truss rises, increasing compressive strength and the corresponding increase in the load at the ends of the tension member[32].

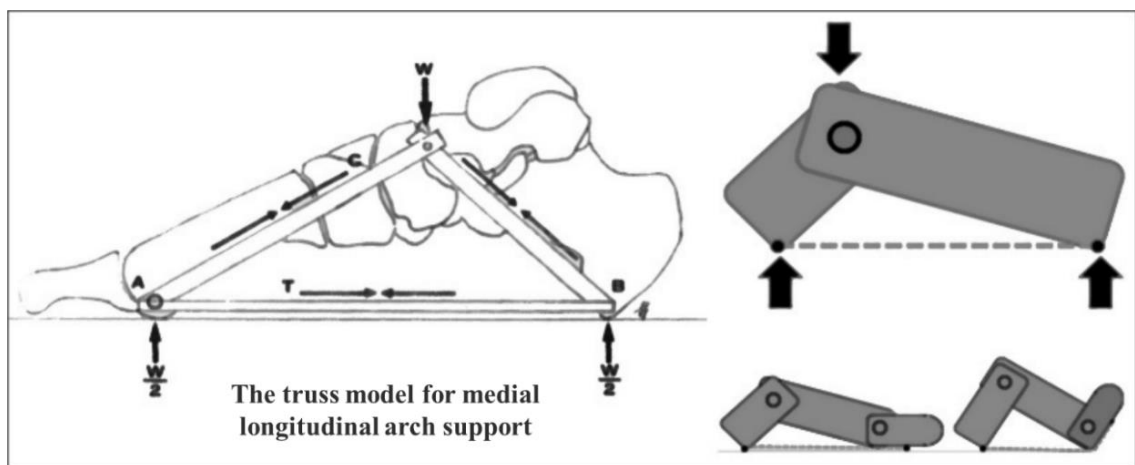


Figure 2 The triangular truss model for medial longitudinal arch support

1.1.1 Morphology-related arch motor function

With a transformation of locomotor habits related to terrestrial bipedality, foot structure and function have altered during evolution and the transition from ape-like species to human species [29]. Among the changes observed, a representative change in the human species is the addition of MLA protected by plantar tensile elements. In the course of human movements such as running and jumping, the foot arch implements the effective transmission of force between the lower limbs and the ground through the synergy between the facet joints [15, 34]. During the stance phase, the arch deforms to absorb the impact load as elastic strain energy. AS is changed by the windlass mechanism during the terminal phase, and the passive elastic rebound of the PF produces positive work to improve the efficiency of ambulation [28, 35]. When performing a GT task, compared with steady-state gait, the impact load on the arch may further increase [36, 37]. This is especially true during UGT, and due to unknown stimulus, the initial dynamic balance of the body will be disrupted. The human body needs to increase the braking force and reduce the push-off force in a short period, thereby creating a sufficient net braking impulse to form a modified body balance perspective [38, 39].

1.1.1.1 Morphology-related arch assessment parameters

Improving insight into complex human locomotion of the lower limb requires sophisticated gait analysis using a biomechanical approach. Morphologically related foot parameters have been widely investigated in biomechanical research [36]. For example, high arches and low arches have been classified as abnormal foot configurations formed by extreme arch structures, which are commonly associated with a higher risk of sports injuries [40, 41].

1) Arch height index. In the past two decades, the arch height index (AHI) has been recognized as a valid and reliable indicator for evaluating arch structure [26, 27], which was outlined by Williams and Mcclay in 2000 [42]. Nevertheless, Wendi and Justin [43] proposed that it is not recommended to use pure AHI to classify foot arch types due to

the interference of ethnicity, gender, and other factors. Moreover, in the course of human movement, the arch of the foot effectively transfers power between the lower limb and the ground through the interaction between the facet joints. In the stance phase, the foot arch will undergo a process of compression-recoil. Meanwhile, the impact load will be absorbed as elastic strain energy and then released at the terminal stance to improve gait efficiency [28]. Therefore, the static foot height index alone may not be able to reveal fully the characteristics of dynamic gait.

2) *Arch stiffness index*. The arch stiffness index (ASI) can effectively reflect the dynamic load adaptability of the foot arch by comparing the arch height difference between the standing and sitting posture of the human body and is also used as an effective risk assessment index for physical activities [26]. According to previous studies, there are different methods used to calculate AS (or arch rigidity, arch flexibility, etc.), all of which are essentially based on changes in subjects' arch height between the sitting and standing positions (**Figure 3**) [9, 26, 44].

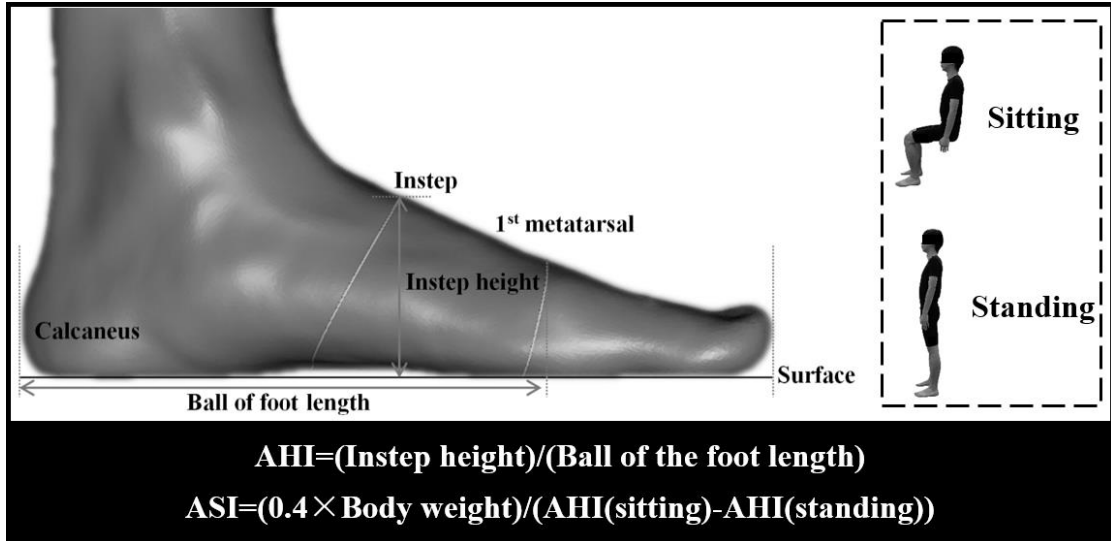


Figure 3 Illustration of foot morphology variables and arch indexes

Zifchock et al. [26] found that there were no significant differences in the AHI between male and female subjects, but the arches of female subjects were more flexible than those of male subjects. In addition, the AHI of the dominant foot was significantly higher than that of the non-dominant foot, while the ASI showed no significant

difference. There was a significant but weak correlation between the AHI and ASI ($p < 0.01$, $R^2 = 0.09$). Combining the relationship between medial-lateral (ML) GRFs and chronic running injuries, AS has been reported as a criterion to assess injury susceptibility [9]. It has been widely recognized that more flexible arches tend to splay during the stance phase and shift load from the midfoot to the forefoot and rearfoot concurrently along the longitudinal axis of the foot [9]. However, other studies have noted that flexible arches exhibited a smaller and larger proportion of total plantar impulse in the forefoot and rearfoot than stiff arches, respectively, in both walking and running (**Figure 4**) [9, 15]. The unidirectional impulse transmission on the plantar longitudinal axis could be related to the fact that in the asymmetric and irregular triangular truss model formed by the PF and the arch bones, the shorter proximal side attached to the calcaneal tuberosities would suffer more impulses during arch compression[32, 33].

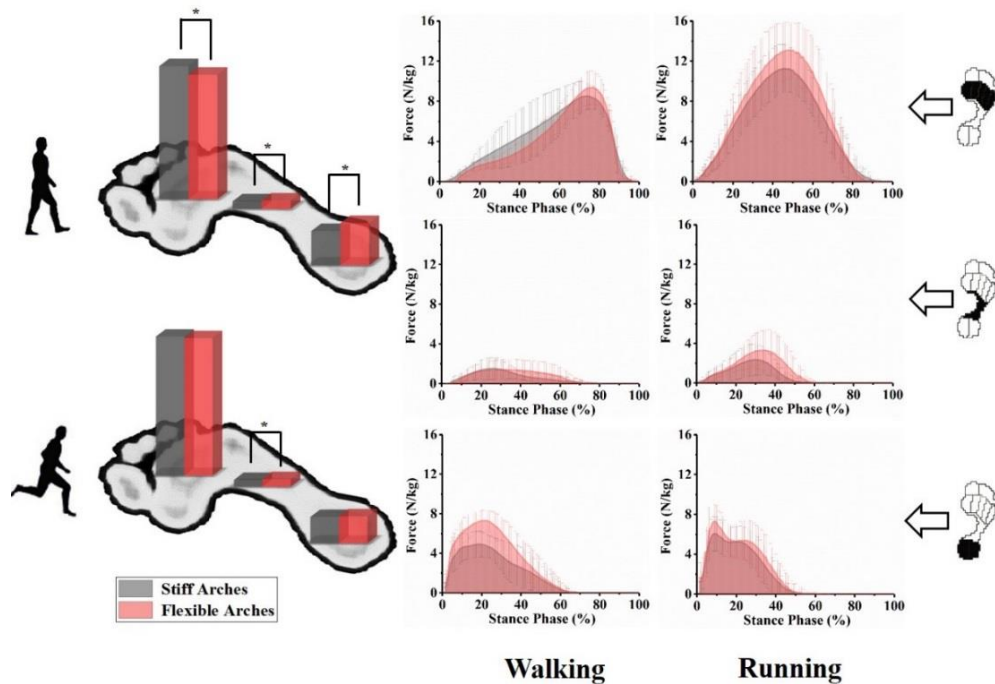


Figure 4 Comparison of impulse distribution between different arch stiffness index

1.1.1.2 Pathological assessment of foot arch morphology

The curvature of the foot arch generally depends on the balance between the muscles in the foot, and researchers often use the Ombre Danne Model to illustrate this issue. The

foot arch may be influenced by the body weight and the muscles attached to the arch (mainly the calf muscles, anterior tibialis muscle, long toe extensor muscle, and long toe flexor muscle contraction), which compresses the arch [36]. The long toe extensor muscle and long toe flexor muscle only come into play when the proximal metatarsal bones are constrained by interosseous muscles. In addition, the foot arch is elevated when muscles such as the posterior tibialis, gastrocnemius, and toe extensor muscles contract or attach to the convex surface of the foot arch. It is worth noting that the loss of function or contraction of any of these muscles can lead to overall instability and even various degrees of foot deformities [23, 36].

1) High arch. In patients with high arches, the height of the foot arch is significantly increased compared to a normal arch, resulting in increased pressure distribution in the forefoot and hindfoot regions and decreased load in the midfoot region [45]. The arch is stiff, and functions such as shock absorption and energy return are reduced or lost. High arches can occur in adults or children, and if they occur during childhood or adulthood, they are usually caused by genetic factors. Unilateral high arches resulting from trauma are usually caused by accidental injuries. However, when unilateral high arches occur without trauma-related factors, magnetic resonance imaging (MRI) of the brain and spinal cord is required to exclude treatable progressive lesions, such as brain tumors or spinal cord tethering caused by congenital abnormalities. In general, the main causes of high arches are: 1) hereditary motor or sensory diseases; 2) post-traumatic skeletal deformities or ligament imbalances causing post-traumatic deformities; 3) untreated or incompletely treated deformities of the foot; 4) idiopathic or other reasons, such as rheumatoid arthritis, ankle osteoarthritis, plantar fibromatosis, tarsal coalition, and diabetic foot syndrome. Delayed diagnosis of worsening deformities in patients can lead to fixed and rigid deformities and severe cases often require joint fusion surgery[46]. If underlying bony deformities are not corrected properly, there is a risk of tendon transfer for patients. Complications of high arches include ankle instability and inversion, peroneal tendon disorders, metatarsal stress fractures, plantar fasciitis, claw toe

deformity, etc., which may eventually extend to proximal joints such as knee joint disorders, increasing the risk of knee osteoarthritis [47].

2) *Low arch*. Patients with low arches exhibit collapsed arches, with the entire foot approaching or fully contacting the ground. In severe cases, it is referred to as flatfeet, a combination of dynamic and static arch deformity with a decrease in the MLA [48]. Flat feet are a common foot abnormality in children and adolescents. The development of the foot arch gradually occurs during infancy as part of the musculoskeletal growth process. As children grow into puberty, flat feet may gradually develop into high arches. For pediatric patients, the risk of knee, hip, and back pain is higher. In addition, flat feet are often associated with hereditary musculoskeletal disorders such as movement disorders and ligament laxity. For adult patients, low arches may be due to foot injuries or diseases, or even part of the normal aging process. It is most common in women over 40 years of age, and common risk factors include obesity, hypertension, and diabetes. It is worth noting that for pregnant women, the increased elastic protein in the feet during pregnancy may also lead to the appearance of low arches.

Low arches, or fallen arches, can cause structural abnormalities in the foot, including: 1) Contracture of the Achilles tendon: After the collapse of the longitudinal arch, the moment arm of the Achilles tendon acting on the ankle joint weakens, making it difficult for tensile forces to effectively transmit through the arch to the forefoot. To maintain body movement, the Achilles tendon is forced to become shorter, tighter, and more powerful; 2) Increased stress on the posterior tibial tendon: This may lead to tendon injuries, and in severe cases, it may even increase the risk of medial ligament injuries; 3) Displacement of the forefoot: The collapse of the medial arch may cause subluxation of the talus, making it difficult for the talus anterior process to support the metatarsal heads. In order to adapt to the new position, the forefoot and midfoot shift laterally, and the forefoot is forced to evert; 4) Subtalar joint pronation, accompanied by eversion of the calcaneus; 5) Relaxation of the midfoot, with the midtarsal joint unable to be locked [49].

1.1.2 Biomechanical coupling of the foot-ankle complex

The foot and ankle, comprising a complex system, encompass 28 bones, 33 joints, and 112 ligaments, and are under the control of 13 extrinsic and 21 intrinsic muscles. The biomechanical coupling of foot and ankle pathologies plays a crucial role in understanding the intricate relationship between various structures and their impact on kinematics and kinetics during gait [50]. Pathologies affecting the foot and ankle structures (e.g., first metatarsal-phalangeal joint stiffness) not only influence the related joint biomechanics but also have repercussions on other areas in the foot-ankle complex [51]. This can be attributed to the interconnectivity of active and passive structures that span multiple foot and ankle joints. Passive structures, including ligaments and fascia, serve as restraints for motion, while external loading and muscular forces act as movers and controllers of bone motions [23, 50]. The active and passive structures attached to adjacent bones govern the motion between those bones, while the ones attached to non-adjacent bones have the ability to influence the motion of non-adjacent bones. This intricate web of interconnected structures results in a coupling effect, where the motion of adjacent and non-adjacent bones becomes interdependent.

By comprehending this coupling mechanism, researchers can gain valuable insights into the complete kinematic and kinetic effects of localized foot and ankle pathologies. For example, a biomechanical study [48] quantified the efficacy of arch support orthosis in improving postural alignment and joint coordination during gait in patients with flatfoot by using an optimised vector coding technique for foot-ankle coordination and CV. In addition, Kawakami et al. [52] investigated foot joint coupling patterns and variability in young women with hallux valgus and found that hallux valgus exhibited altered inter-joint CV which may be related to the progression of the deformity. This understanding allows researchers to better evaluate and manage these conditions, as well as develop targeted diagnostic and therapeutic strategies that consider the broader biomechanical implications. Further research into the biomechanical coupling of the foot-ankle complex holds the potential to enhance understanding of these conditions and improve clinical outcomes for affected individuals[50].

1.1.2.1 Basic techniques for investigating the foot-ankle coupling mechanics

Various fundamental techniques have been utilized to study the biomechanical coupling patterns of the foot-ankle complex during dynamic movement [53]. However, cross-correlations, which assume linear relationships between adjacent segments, prove inadequate in evaluating non-linear linkages [54]. As a single value that represents the average joint coupling, the rearfoot eversion and tibial internal rotation (EV/TIR) excursion ratio was applied to measure the relative motion between the rearfoot and tibia from heel-strike to the respective peaks around midstance [53]. Also, this ratio proves valuable in determining if the tibia exhibits greater motion concerning rearfoot eversion, with people displaying lower EV/TIR ratios showing increased tibial internal rotation and a heightened risk of lower extremity injury [54]. Emerging evidence indicates that arch structure plays a significant role in influencing EV/TIR ratios[53]. Higher arch height leads to increased subtalar orientation, altering the EV/TIR ratio; subjects with high arches tend to exhibit relatively greater tibial internal rotation and lower EV/TIR ratios compared to those with low arches[20, 55]. Several studies on subjects with varying arch structures support these findings, demonstrating that differences in EV/TIR ratios can primarily be attributed to tibial internal rotation excursion rather than rearfoot eversion excursion during dynamic motions[10, 53].

The continuous relative phase (CRP) technique was introduced to biomechanics literature by Hamill et al. [56], aiming to describe the coupling motion relationships between adjacent segments. This technique quantifies the degree of in-phase or out-of-phase relationships between two segments, providing a continuous measure throughout the gait cycle[53]. By utilizing dynamical systems theory, biomechanists adopted the CRP measure from motor control science, which involves generating a phase plane portrait of normalized angular velocity against the normalized angular position for the segments of interest. The CRP angle is then calculated by subtracting the phase angle of the distal segment from that of the proximal segment, resulting in values ranging from -180° to 180° , where 0° indicates complete in-phase coupling and 180° or -180° indicates complete out-of-phase coupling (**Figure 5**) [53, 56-58].

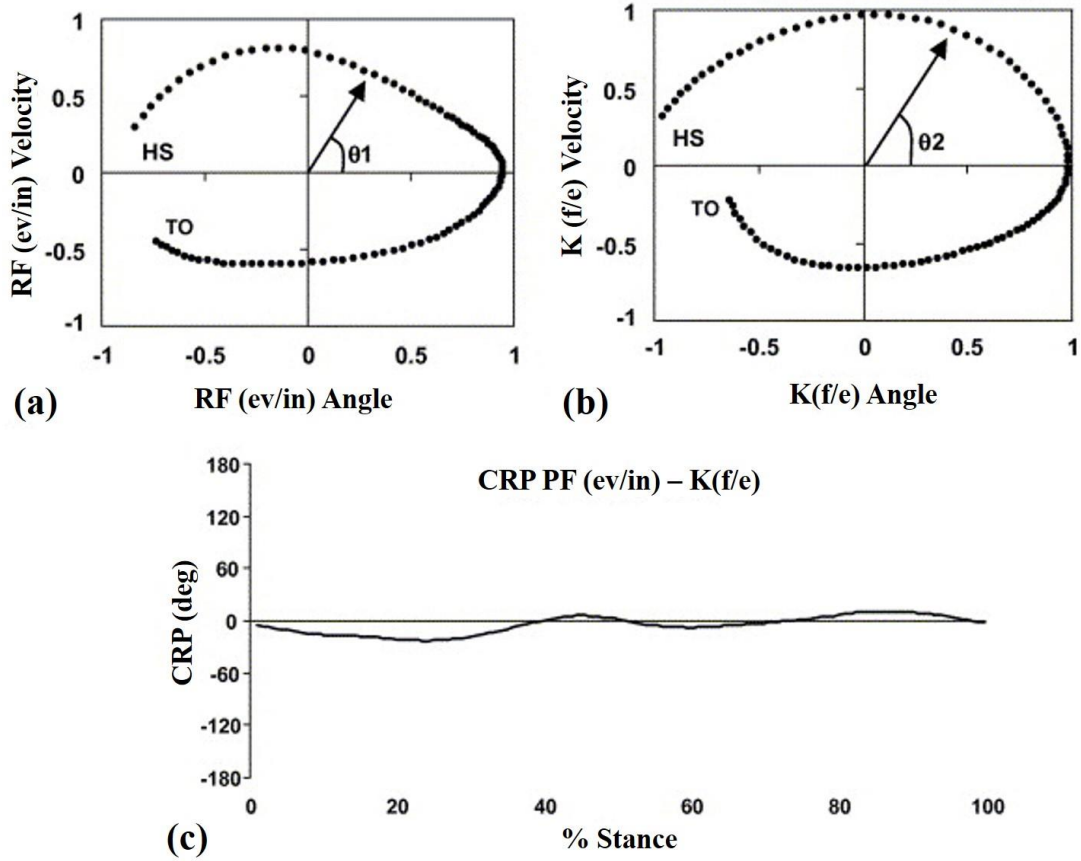


Figure 5 Illustration of continuous relative phase calculation [53]

Note: (a) Phase angle plots of position versus velocity curves for rearfoot eversion/inversion, (b) tibial rotation, and (c) the continuous relative phase plot for eversion and tibial internal rotation coupling.

1.1.2.2 Inter-joint coordination and coordination variability of the foot-ankle complex

Traditional biomechanical gait assessments have typically used discrete measures. Nevertheless, isolated joint kinematics can neither effectively reflect the segmental coordination information producing resultant angular positions nor provide a comprehensive insight into the altered movement patterns caused by functional differences in the foot [18, 48]. A continuous approach, in contrast, enables the quantification of movement coordination patterns throughout the gait cycle and can provide spatial-temporal details of the locomotion [19]. Coordination patterns can assess the timing and degree of relative movement of inter-segment of the human body,

allowing researchers to understand further the collaborative mechanism of the motor system [21]. Meanwhile, CV can play an essential role in controlling motion strategies by quantifying the coordination patterns' level of fluctuation and improving the adaptive capacity to movement disturbances and task constraints [18, 21, 59]. Coordination and CV during moving have also been associated with biological systems' health status [31]. A previous study [21] demonstrated that the 4-month usage of AS orthoses could significantly improve joint coordination between ankle, knee, and hip, in patients with flatfoot during walking. However, the coordination pattern between the MTP and ankle joint, which is the closest anatomically to the foot arch, has been ignored. Evaluation of MTP-ankle coordination and CV in flatfoot patients with AS through a vector coding method may provide valuable information about motion control, which is undoubtedly precious in a clinical setting [60]. Meanwhile, the efficacy of arch orthoses in posture adjustment and joint coordination improvement during steady-state gait is well documented; however, the biomechanical changes of gait sub-tasks caused by arch support, especially during GT, are poorly understood. Hence, a recent prospective exploration [48] investigated how the acute arch-supporting intervention affects foot-ankle coordination and CV in individuals with flatfoot during UGT. MTP-ankle coordination and CV were quantified using an optimized vector coding technique during the three sub-phases of UGT (**Figure 6**). Significant differences in the joint kinematics between non-arch-support and arch-support were exhibited only in the MTP transverse plane during the middle and later periods of UGT. Frontal plane MTP-ankle coordination under arch support during stimulus delay significantly decreased from $177.16 \pm 27.41^\circ$ to $157.75 \pm 32.54^\circ$ compared with under non-arch-support condition; however, the coordination pattern had not changed. Moreover, no significant difference was found in the coupling angle (CA) variability between non-arch-support and arch-support in three planes during sub-phases of UGT. These results might help understand the implications of manipulating foot or arch structure on foot injury during UGT. Related information might be necessary for further considering the utility of intrinsic foot manipulations such as foot surgical intervention and extrinsic foot manipulations

such as designing specific shoes. Besides, further studies are expected to reflect lower limb inter-joint coordination during GT through the long-term effects of arch support orthoses.

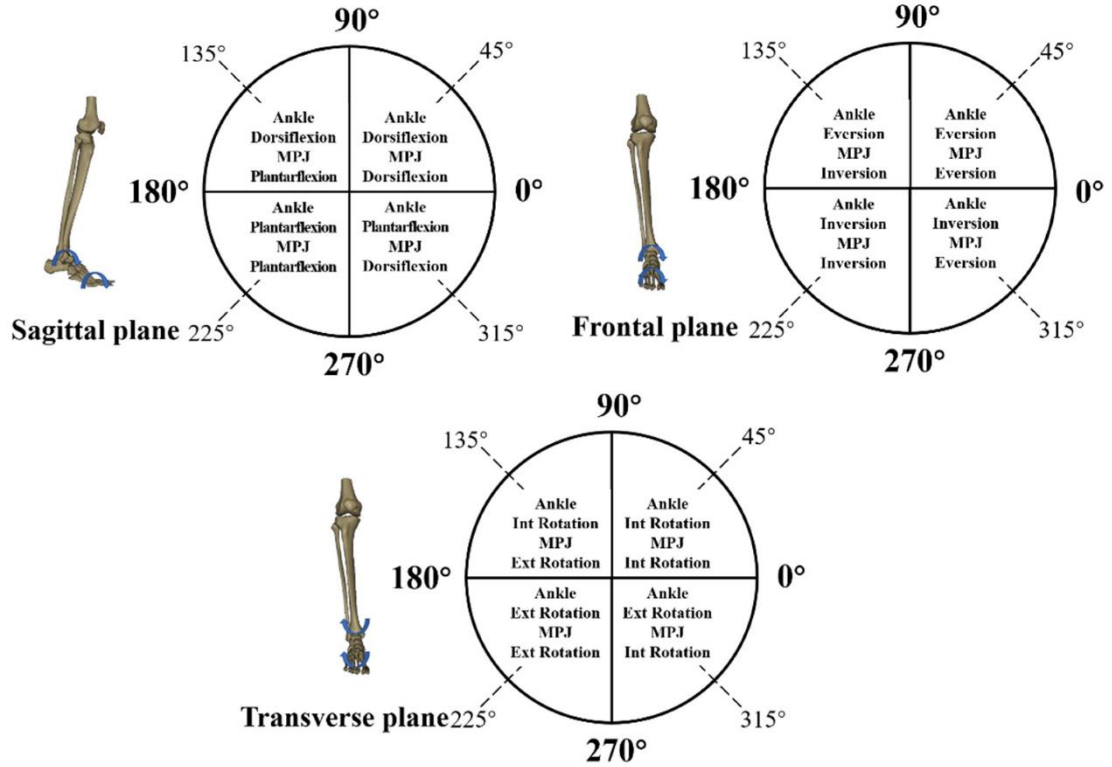


Figure 6 Classification of coordination model based on the coupling angle in sagittal, frontal, and transverse planes

1.2 Human gait characteristics and biomechanical analysis

Human locomotion is performed through coordinating body segments employing an interaction between internal and external forces. However, this phenomenon is considered an extremely complex process that needs to be described by multidisciplinary methods [61]. The most representative aspect is gait analysis by biomechanics approaches. Gait analysis is the process of using sports biomechanics analysis tools and techniques to quantitatively assess biomechanical parameters, including spatio-temporal parameters, kinematics, and kinetics, during human locomotion [62]. By comparing gait data from healthy individuals, it helps identify characteristics of gait abnormalities and sheds light on the key factors that contribute to

such abnormalities [63]. This analysis provides objective evidence and scientific guidance for clinical diagnosis, treatment, and rehabilitation purposes [63]. As a characteristic behavior of human beings, the process of gait control is highly complex, involving central commands, body balance, and coordinated control. It encompasses the synchronized movements of muscles and related joints in the foot, ankle, knee, hip, trunk, neck, shoulder, and arm. Any imbalance in any part of this process can potentially affect the overall gait characteristics. As shown in **Figure 7**, during the walking process, a complete gait cycle is formed from the initial contact of one heel to the subsequent contact of the same heel on the ground [64]. For a specific lower limb, one gait cycle activity can be divided into two phases: the stance phase and the swing phase. When one lower limb enters the stance phase, the other lower limb is still on the ground, and both limbs simultaneously bear the body weight, which is known as the double support phase.

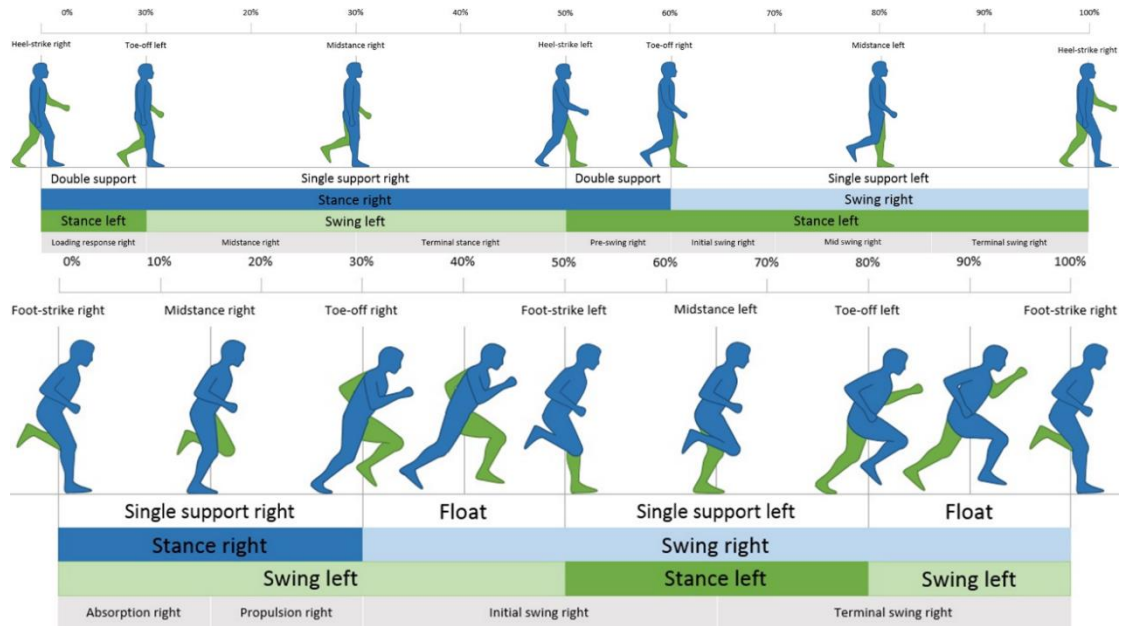


Figure 7 Phase division of the normal gait cycle

Gait characteristics could be influenced by various physiological factors, such as age and gender [65]. For instance, elderly individuals exhibit different gait patterns compared to younger individuals due to age-related physical decline. Age-related changes in the neuromuscular-skeletal system can affect gait control, leading to

decreased step length, reduced walking speed, and shorter single-limb support time in the elderly [66, 67]. Consequently, older individuals adopt a gait strategy of increasing double-limb support time while decreasing walking speed and step length to maintain dynamic balance [68]. Furthermore, researchers recognize the significance of considering gender differences in gait impact in biomedical and clinical studies. Gait patterns also vary between males and females due to disparities in height, body mass, and skeletal muscle fiber length [66, 69]. Gender differences in joint kinematics and kinetics during walking have also been reported, with females exhibiting larger ROM in ankle joint flexion-extension and smaller ROM in hip joint flexion-extension and hip joint flexion moments [70].

1.2.1 Locomotion patterns and biomechanical function adjustment of the lower limbs

The foot, as the starting point of the human kinetic chain and the interface with the external environment, undergoes morphological changes closely related to its functional performance [23]. The specific structure of the foot's skeletal system also serves corresponding functions, such as the foot arch that provides support, stress dispersion, and cushioning effects [23, 29]. Apart from the bones, complex muscles and ligamentous tissues are distributed from superficial to deep, controlling human movement through the neuromuscular function and proprioceptive system [29]. The sole of the foot, in particular, contains 104 mechanical sensory domains, with receptors mainly distributed in areas where the foot makes contact with the ground [71]. This highlights the significance of the foot in action control and maintaining balance. Understanding the adjustments in lower limb biomechanical function caused by foot movement patterns is a crucial research area, involving how the human body moves and adapts during various activities.

1.2.1.1 Effects of barefoot locomotion on the biomechanical function of lower limbs

The earliest footwear emerged approximately 40,000 years ago, and since then, human toe length has noticeably reduced due to wearing footwear, leading to a decreased reliance on toe grip function. Modern footwear has evolved from simple toe-separated

footwear to complex designs driven by aesthetics, often overlooking their impact on foot morphology and function [72, 73]. Prolonged use of ill-fitting or excessively protective footwear can result in foot and toe deformities, weakened foot arch-related muscle strength, ligament function, and compromised windlass mechanism [2, 4, 74]. In children, wearing simple footwear without arch support and shock absorption leads to a flatfoot incidence of about 6%, while using technology-enhanced footwear increases the incidence to 13% [75]. Long-term use of high-heeled footwear with a heel height over 5 cm causes passive dorsiflexion and forward-leaning of the body, increasing knee joint load and ankle sprain risk, and resulting in hallux valgus deformity [76, 77].

Form and function are closely related, and changes in form can lead to functional compensations or even degenerative changes. Barefoot and minimalist footwear running have become prominent topics in biomechanics. Embracing a more natural state through barefoot activities reduces injury risk, strengthens foot and lower limb muscles, and improves foot arch function [78-80]. From an evolutionary perspective, long-distance running was a vital survival skill for early humans, and the foot shape of habitual barefoot individuals is closer to a natural foot shape. Studies suggest incorporating barefoot running as a means to prevent injuries, enhance muscle strength, and improve running economy [81, 82].

Lower limb biomechanical functions undergo various adjustments during barefoot activities. Short-term barefoot intervention in shod populations showed biomechanical characteristics similar to those of habitual barefoot individuals. Both walking and running exhibited traits of short stride length in temporal-spatial parameters [83]. Kinematic features showed reduced foot strike angle, ankle dorsiflexion, and increased knee flexion [84-86]. In terms of kinetic features, both peak GRF and vertical loading rate decreased in both walking and running for both habitual shod and barefoot individuals [87, 88]. However, compared to habitual barefoot individuals, habitually shod individuals demonstrated increased peak pressure and pressure impulse in the heel and metatarsal regions during walking [89]. Changes in foot morphology and partial functional inhibition were observed in habitually shod individuals, such as decreased

cross-sectional area of foot muscles (e.g., intrinsic foot muscles), narrower forefoot, and increased toe-out angle [90, 91]. These morphological changes might inhibit certain foot functions in habitually shod individuals, such as the foot arch's torsional mechanism and toe gripping function [92]. Therefore, while an immediate or short-term transition to barefoot activities may exhibit some biomechanical similarities to long-term habitual barefoot individuals, it is essential to consider the morphological and functional differences and adopt a progressive approach to barefoot-style activities [93].

1.2.1.2 Effects of strike pattern on the biomechanical function of lower limbs

The impact of striking techniques on the load distribution in the lower limbs has become a prominent topic in the field of biomechanics in recent years. Two common striking techniques are forefoot strike and rearfoot strike [94, 95]. In the forefoot strike process, the ankle joint first undergoes a slight plantarflexion and then dorsiflexion. Compared to the rearfoot strike, the forefoot strike tightens the foot arch, elongates the Achilles tendon, and reduces the eccentric contraction of the calf muscles, thus reducing the direct impact on the brain during the impact phase [80].

During the forefoot strike, the center of pressure (COP) on the foot moves backward in the direction of movement before moving forward. Initially, this process was believed to increase energy consumption, but it has been found to provide cushioning for runners during landing [96]. Subjects who are accustomed to forefoot strike and were tested running with a rearfoot strike approach demonstrated a significant decrease in vertical loading rate when transitioning from rearfoot strike to non-rearfoot strike [97]. A previous study [80] indicated that the force-time curve of a typical forefoot strike process does not exhibit a clear impact transient, with the GRF steadily increasing throughout the gait cycle. In contrast, the force-time curve of a typical rearfoot strike shows an additional peak, the impact transient, before the vertical GRF reaches its peak. The vertical GRF during the rearfoot strike may be three times higher than that of habitual barefoot forefoot strike runners [80]. During the rearfoot strike, impact absorption primarily relies on the cushioning effect of the heel pad or shoe sole, leading

to higher impact peaks and shock waves. The resulting high stress and strain may directly cause running injuries [98]. This explains why wearing minimalist footwear can reduce foot injuries by promoting a return to a more natural gait. Although the above research indicated that habitual barefoot runners experience a decrease in vertical loading rate during forefoot strike, the forefoot strike pattern places increased stress on the metatarsal bones compared to rearfoot strike or midfoot strike. Therefore, the forefoot strike pattern may potentially increase the risk of metatarsal injuries [99].

1.2.2 Gait termination biomechanics and compensatory strategy adjustment

Human gait sustains progression from initiation to termination, and the dynamic balance should be maintained in position movement. Although the steady-state pace has been extensively studied, GT as a gait sub-task has received less attention. Sparrow & Tirosh [37] defined GT in the review as when both feet stop moving either forward or backward based on displacement and time characteristics. Compared with steady-state gait, the process of executing GT demands higher control of postural stability and complex integration and cooperation of the neuromuscular system [3, 100]. During GT, the body needs to rapidly increase braking impulse and decrease propulsion impulse to form a new body balance [38, 39]. GT also can be divided into planned gait termination (PGT) and unplanned gait termination (UGT) according to different control processes. In PGT conditions, individuals can know when and where they will stop. UGT is a stress response to an unknown stimulus. When confronted by an unexpected stimulus that requires one to stop suddenly, the initial dynamic balance will be disrupted. Due to the need for continuous control of the body's center of mass (COM) and feedback control, UGT poses a more significant challenge to the ability of postural control [37, 101].

In the process of GT, maintaining body stability is crucial by keeping COM within the support surface formed by the feet [37, 102]. Based on the previously established human inverted pendulum model [103], Tirosh and Sparrow [104] suggested that the key parameters determining the stability of GT are the horizontal velocity of the COM,

normalized by body height, and its relative position on the base of support provided by the feet. During the transition from walking to standing, the COM velocity becomes zero and remains within the base of support, resulting in a new state of balance. Furthermore, research indicates that if the body state exceeds the upper boundary of the appropriate range of COM velocity (the COM reaches the most anterior position of the foot support base), forward falling or additional steps may be required for termination; whereas if it exceeds the lower boundary (when the COM just reaches the support surface), backward falling may occur [104]. Additionally, Jian et al. [105] argued that the vector connecting the COP of the foot to the COM is the primary determining factor for decelerating and smoothly stopping the COM. The AP and ML positions of the foot define the stability boundaries of the COP, thereby determining the magnitude and direction of the COP-COM vector. Therefore, the aforementioned model of human stability is significant for explaining the foot positions during GT, especially in UGT. While maintaining stability, the adaptability to reduce forward impulse is limited by the available response time (ART) [106]. For example, Cao et al. [102] investigated the success rate of GT based on ART in their experiment by requiring participants to complete GT before a specified boundary. Moreover, response time is influenced by various variables such as walking speed, signal delay, and signal probability.

1.2.2.1 Gait termination and human ageing mechanisms

From the perspective of motor control, GT is considered a complex process in which the central nervous system predicts, controls, and prevents forward impulses [37, 107]. As the body ages, the functionality of the neuromuscular control system responsible for movement gradually declines, affecting motor execution. Tirosh and Sparrow [37] emphasized that investigating the characteristics of the neuromuscular control system during GT plays a significant role in understanding the mechanisms of aging and neuropathology. For example, in the experiment conducted by Cao et al. [102] to explore the success rate of GT based on ART, they found that older participants (mean age: 72.6 years) had a significantly lower success rate in completing GT before the specified boundary compared to younger participants (mean age: 23.4 years).

Furthermore, their study revealed that when ART was set at 525 milliseconds, the success rate for younger participants reached 58%, while for male older participants and female older participants, it was 51% and 23%, respectively. When ART increased to 600 milliseconds, the success rates for the three groups rose to 84%, 72%, and 57%, respectively. Gehring et al. [108] also found that in conditions where the success rate of GT was 50%, younger male participants, older male participants, and younger female participants required 520, 530, and 590 milliseconds, respectively, to complete the action. The results from these studies collectively suggest that aging may be an important factor contributing to the decline in GT ability.

Age-related differences in GT may be attributed to different muscle recruitment strategies. Tirosh and Sparrow [109] found that muscle activity during GT in younger participants occurred significantly earlier than in older participants, resulting in increased ground contact time and reduced propulsive force during the stance phase [23]. During GT using a swing leg, older participants exhibited synchronous recruitment of the soleus (SOL), vastus lateralis (VL), and gluteus medius (GM) muscles in only 75% of the gait trials. Reduced muscle activation during GT may lead to insufficient braking force and increase the likelihood of requiring two steps for termination. Other studies have also highlighted the significant role of SOL muscle recruitment in gait deceleration during GT [110]. Additionally, a related study [111] indicated that the GM muscle partially affects the ML stability of the hip joint, and control deficiencies in ML displacement may impact overall stability during movement. Slower muscle recruitment and weaker muscle activity during GT result in increased time and distance required for termination, and reduced activation of the GM may impair dynamic stability during the process.

1.2.2.2 Pathological effects on strategy adjustments during gait termination

Aging has been an essential factor in difficulties precisely terminating gait [37]. However, many diseases such as diabetes could accelerate the neurodegenerative process, which results in a further decline in motor control during GT [112]. Besides,

many other diseases may also reduce the patient's ability to GT. For example, patients with balance disorders such as vestibular hypofunction and cerebellar damage show significantly slower velocity in the forward direction to enter the final stride during PGT compared to healthy controls [113]. Although these diseases may cause changes in gait parameters for patients during GT, the body will take a series of compensatory strategies to attenuate postural instability and adjust abnormal movement patterns [109, 114].

1) Parkinsonism. Parkinsonism has been studied more than any other disease regarding GT research and has been one of the diseases with the most significant impact on the gait characteristics of patients. Compared with the control group, the gait characteristics of Parkinson's patients showed longer time, lower speed, and shorter step length during PGT [115]. These gait characteristics alterations were also observed in the UGT of the patients. Also, patients may need additional steps to maintain body stability and complete GT. The degree of disease, age, slippery surface, and unexpected perturbation will affect the GT performance of patients with parkinsonism [115-117].

Bishop et al. [114] observed the activity of related muscles in Parkinson's patients during UGT. They found similar patterns of muscular activation of SOL, tibialis anterior, and GM to control subjects, although at significantly reduced amplitude levels. Moreover, they indicated that Parkinson's patients might not produce enough braking force in GT, so they required extra steps to stop walking [118].

2) Cerebellar Ataxia. The primary clinical manifestation of cerebellar ataxia is balance disorder, which will produce an irregular gait pattern. Compared to the healthy subjects, the GT parameters of patients with cerebellar ataxia showed a reduced step length, greater step width, and additional steps to stop [100]. Moreover, researchers found that the patients could not generate a flexor extensor pattern to coordinate the lower limb joint and appropriate braking forces to decelerate the sagittal plane's body progression [119]. This multistep compensation strategy may help the patient stop walking more safely to some extent.

O’Kane et al. [113] compared the kinetic parameters of GT in patients with balance disorders, including vestibular hypofunction and cerebellar damage, with healthy subjects. During GT, poor eccentric muscle control would lead to excessive energy transfers for patients with cerebellar damage in the final stride. And they dissipated forward kinetic energy by using a transfer of upper body energy from onwards to lateral. Lateral stability could be affected for patients with vestibular hypofunction once they have stopped walking due to vestibular feedback’s weakness regarding changes in forwarding velocity. In general, converting excessive kinetic energy from forward into lateral as a termination strategy may be used by patients with balance disorders.

3) *Multiple Sclerosis*. Roeing et al. [16, 120] reported PGT and UGT successively in multiple sclerosis patients in two studies. On the level of macro-control strategy, patients with multiple sclerosis had a similar failure rate compared with controls during the planned transition from dynamic to static posture. Nevertheless, under cognitively distracting conditions, the failure rate of GT had a fold increase for patients with multiple sclerosis owing to cognitive-motor interference. Similarly, during UGT, patients with multiple sclerosis need more time to stop walking. And assistive devices might improve the termination behavior.

At present, it is generally accepted that patients with multiple sclerosis have gait disorders due to muscle weakness, sensory impairment, decreased coordination, and other symptoms [121]. As a result, they show a slower gait speed in the characterization of temporal-spatial parameters. Because of the loss of somatosensory processing, the patient passively adjusted the gait strategy (e.g., more significant foot displacement, higher loading force, etc.) to prevent falls. Especially during the cognitively distracting dual-task, strategy adjustment was more significant due to limited attentional resources being competed by cognitive and motor tasks [16].

4) *Other Diseases*. Besides, there were also studies involving GT in patients with Type II diabetes and Prader-Willi syndrome [112, 122].

Aging has been reported to be an essential factor in the ability decline of GT [37]. Type II diabetes, a common disease in the elderly, might further worsen the performance of GT. Compared with healthy elderly, diabetic subjects exhibited lower velocity of AP-COP and larger ML- and AP-COP and COM overshoots. The slowness strategy was considered partial compensation for the pathology-related decrease in postural stability during goal-oriented GT [112].

1.3 Applications of finite element modeling in biomechanical analysis of foot arch

The importance of well-functioned foot arches has long been recognized while performing daily locomotion tasks. The arch structure enables it to function as a stabilizer and an absorber in weight support and loading absorption [123]. Many foot deformities are related to abnormalities in the function of the foot arch [124]. Liang et al. [125] examined the involvement of the associated ligaments in the biomechanics of the foot arch and found significant collapse and elongation of the MLA due to the release of the plantar ligaments without the role of tendons and external stabilizers. From the perspective of morphological evolution and functional adaptation, structural changes in the foot arch will inevitably lead to variations in the lower-limb biomechanics, increasing the potential risk of foot damage and musculoskeletal problems [3, 123]. It has been reported that excessively high arches might increase the potential for low-extremity stress fractures, foot pain, and ankle injuries [40, 126, 127]. At the same time, low arches are frequently associated with MTP osteoarthritis, soft tissue injuries, plantar fasciitis, and patellar tendonitis [123, 128, 129]. Despite the low strength and partially contradictory evidence for the potential relationship between these non-neutral foot types associated with arch deformation and lower extremity injury [6], further exploration of the arch deformation mechanisms and their application in the clinical setting is of undeniable general interest.

Three-dimensional motion capture and plantar pressure collections could be employed to evaluate the risks of foot and ankle injuries due to mechanical loading [130, 131]. These laboratory-based experiments provide essential information on overall foot

biomechanics. However, because of technological limitations, detailed mechanical changes in the foot structure cannot be directly evaluated, particularly for the arch region's internal stress and strain distribution [132]. To overcome the above-mentioned intrinsic difficulties, computational modeling techniques, represented by the FE analysis, have been widely used to simulate the mechanical responses of biological systems for methodological purposes [23, 133, 134]. Over the last two decades, with biomechanical simulation techniques and related software development, the computational orthopedics research scope has extended to areas consisting of complex components and loading definitions, especially involving the foot-ankle complex [23, 133-136]. Previous clinical studies have also demonstrated the critical contribution of passive stabilizers, represented by the PF and associated plantar ligaments, in plantar arch maintenance and foot pronation [124, 137]. Loading information on the primary soft tissues of the foot is crucial for a better insight into the association between arch deformation mechanisms and foot-related pathological conditions [138, 139]. Cheung et al. [140] quantified the biomechanical response of ankle-foot complexes with different PF stiffnesses by FE analysis and verified that the PF has a substantial stabilizing contribution to the longitudinal arch of the human foot. Cifuentes-Dela Portilla et al. [137] also evaluated the relative contribution of passive soft tissue stabilizers of the foot arch, such as spring ligaments, in arch maintenance by reconstructing an FE model.

1.3.1 Overview of finite element model design

While the capability to employ computational foot modeling is determined by its cost-effectiveness and noninvasiveness, the potential to improve clinical performance is highly dependent on the precision and correlation of the information provided [133]. Specifically, these biomechanical models were developed with a high sensitivity to the assumptions made in defining modeling parameters (especially true for boundary and loading conditions, element types, and material properties) that could lead to discrepancies in prediction accuracy, thus limiting the generalizability of their predictions [141, 142].

1.3.1.1 Model reconstruction and configuration

The reconstructions of initiative structures (e.g., intrinsic/external foot muscles and tendons) and passive structures (e.g., ligaments and PF) of the foot are essential for exploring the arch deformation mechanisms by FE models (**Figure 8**). These models were mainly reconstructed from computed tomography (CT) [27, 125, 137, 139, 143-149] or MRI [124, 138, 140, 150-152] to replicate the anatomical contours of the foot segments. Specialized software such as MIMICS was employed to segment the different tissues in a series of acquired images. Among them, the geometries of bone structures can be created separately or fused for simplification. For example, the second to fifth intermediate and distal phalanges were fused into one bony structure to reduce computational effort (**Figure 8**) [138]. For arch passive stabilizers represented by ligaments and PF, studies other than those focusing on the specific tissue usually connect anatomical origins and terminations via two-dimensional tension-only truss in a reverse engineering environment rather than reconstructing three-dimensional solid geometry [27, 124, 125, 138, 140, 144-146, 149-152]. Similarly, most studies maintained the simplification of cartilage, which is considered to be an isotropic linear elastic material with no interstitial fluid flow [27, 124, 140, 143, 149, 150]. In contrast, considering the rigidity issue, Cifuentes-Dela Portilla et al. [137, 147, 148] modeled the cartilage material as nonlinear and hyper-elastic using the Ogden model while maintaining the cartilage morphology in the FE foot model. It is exceedingly difficult to measure the subject-specific mechanical properties of most tissues (e.g., ligaments, tendons, and cartilage). Therefore, most of the material data were referenced from previous publications. Specifically, most components were idealized as homogeneous, isotropic, and linearly elastic, except soft tissue, which was commonly assumed hyper-elastic by some models [138, 144-146, 149-152].

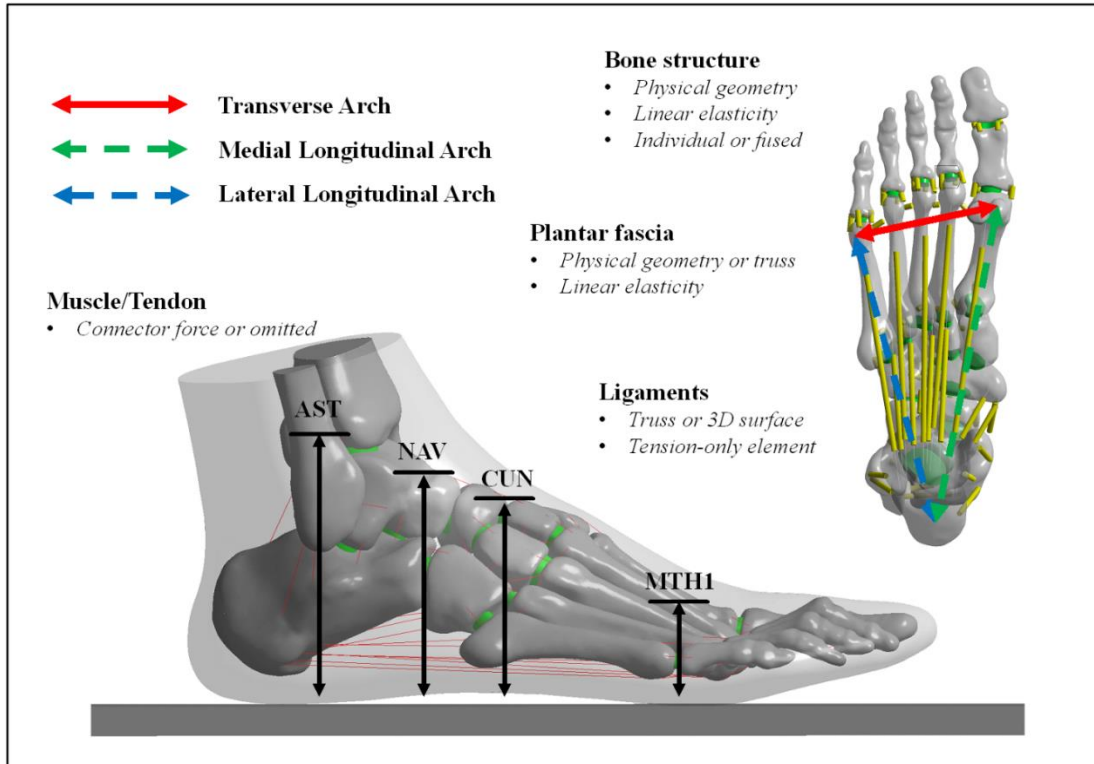


Figure 8 The main components of the foot finite element model

1.3.1.2 Boundary and loading conditions

Most of the boundary and loading settings for most existing simulations were determined for experimental purposes. For example, the foot-plate system approach with balanced standing as the motion pattern was applied to simulate the ankle-foot complex with the ground [27, 125, 137, 139, 140, 145-147, 150, 152]. Specifically, the superior surface of the soft tissue, distal tibia, and fibula or ground plate was fixed, while muscle forces and GRF were assessed based on body weight estimates. As for dynamic motions represented by gait, subject-specific boundary and loading situations could be acquired from the three-dimensional motion analysis with inverse dynamics involving kinematic and kinetic parameters, thus simulating the motion states more accurately [138, 151]. The foot intrinsic and extrinsic muscle forces were calculated from the electromyography (EMG) signals and respective physiological cross-sectional areas based on the assumption of muscle gain or estimated from recorded motion and GRFs via multi-body musculoskeletal modeling [138, 151]. For the interaction

behaviors between the foot and ground, the connection modes were selected as the frictional contact surface with a factor of 0.5-0.6.

1.3.1.3 Model verification and validation

Model verification and validation are critical for the application of clinically relevant foot FE modeling, and this process is a challenging aspect of computational biomechanics. Direct or indirect model validation procedures were performed in most of the literature [27, 125, 137-140, 143-148, 150-152]. With direct experimental validation of in vivo data, most papers measured plantar pressure distribution and displacements visible in radiographic images [27, 137, 139, 140, 147, 148, 151, 152]. In addition, several studies utilized cadaveric measurement experiments for model validation [125, 138, 150]. A part of the studies performed indirect validation by comparing the predicted plantar pressure or tissue-specific stress/strain behavior with relevant results from the literature [143-146, 151].

1.3.1.4 Grouping of foot arch deformation mechanisms

The present papers presented extensive applications in exploring the biomechanical and deformation mechanisms of the foot arch with computational simulation strategies. Specifically, some articles employed FE models of healthy feet [124, 125, 138, 140, 143, 150], while others reconstructed FE models of pathological feet, including midfoot deformities such as progressive collapsing foot deformity [27, 137, 139, 144-149], valgus foot [152], and posterior tibial tendon dysfunction [151].

1) Finite element model of the healthy foot. The first group investigated the mechanisms of foot arch deformation by reconstructing the FE model of a healthy foot. Of these studies, a few aimed to reveal the arch deformation and internal biomechanical characteristics under different movement patterns/states [138, 143], while the remaining studies focused on exploring the biomechanical responses caused by the tissue properties associated with the foot arch [124, 125, 140, 150].

To precisely reproduce the mechanical responses within the PF during different foot postures, a study simulated a quasi-static gait with Achilles tendon force applied on the calcaneus simultaneously as displacement was imposed on the distal tibia and fibula [143]. Moreover, considering that foot strike patterns might also contribute to PF overload, Chen et al. simulated running with rearfoot strike and forefoot strike with a dynamic explicit solver [138]. Furthermore, the time series data input as boundary conditions (e.g., segmental kinematics and joint reaction forces) were obtained from the musculoskeletal motion model via three-dimensional capture. The PF and major ligaments, as primary foot tissues that maintain the static structure of the arch, were also widely focused on in the study of FE models of healthy feet. In two studies, Cheung et al. investigated the effect of Achilles tendon loading on PF tension and the effect of PF stiffness on the ligament stress/strain distribution by reconstructing an ankle-foot FE model incorporating geometric and contact nonlinearities, respectively [140, 150]. Some studies examined the relative contribution of the PF and the major ligaments represented by the spring and plantar ligaments in the foot arch biomechanics by simulating the release of the tissues mentioned above individually [124, 125]. Moreover, these studies all applied linear trusses to approximate the nonlinear profile of the PF and ignored the interface between the PF and peripheral tissue.

2) *Finite Element Models of the Pathological Foot.* Another group presented FE modeling of pathological feet, including midfoot deformation represented by progressive collapsing foot deformity, valgus foot, and posterior tibial tendon dysfunction.

FE modeling of non-healthy feet in most papers simulated pathology by modifying the standard subject model. For example, Sun et al. [27] established low and high arch FE models based on reconstructed standard arch FE models by adjusting the AHI varied by the arch length and height. Malakoutikhah et al. demonstrated extensive research interest in the role of ligaments in progressive collapsing foot deformity [144-146]. Their studies simulated collapsed feet by modeling the breakdown of ligaments participating in progressive collapsing foot deformity (e.g., PF, spring ligament, deltoid

ligament, and plantar ligaments). In addition, the studies by Cifuentes-De la Portilla et al. focused on the significant soft tissues related to progressive collapsing foot deformity [137, 147, 148]. In addition to passive tissues such as arch stabilizers, tendons such as the posterior tibial tendon, peroneus longus tendon, and peroneus brevis tendon were also included in their study to investigate the ability of these soft tissues to support the plantar arch. Zhang et al. assessed equivalent stress on the articular surface of the MLA joints and the principal stress in the periarticular ligaments of the ankle joint to further explore progressive collapsing foot deformity development in the second stage characterized by flexible arch deformity [139]. The study by Wang et al. is the only included paper that employed a large sample size in constructing the FE model [149]. A total of 140 subjects (including 30 with healthy feet, 30 with flatfoot, 30 with clubfoot, and 50 with Lisfranc injury) were included in their study to reconstruct the foot FE model and thus verify the differences in von Mises stress levels in the mid-foot between groups.

Furthermore, considering the potential influence of posterior tibial tendon dysfunction on the onset of progressive collapsing foot deformity, Wong et al. simulated the pathological condition by unloading the posterior tibial tendon. Parameters of interest involved the tensile strains of plantar ligaments such as the plantar first metatarsocuneiform, intermetatarsal, tarsometatarsal, intercuneiform, cuneocuboid, naviculocuneiform, cuboideonavicular ligaments [151]. For the biomechanical behavior of the valgus foot in children with cerebral palsy, Guo et al. [152] compared the internal bone locus and stress of the standard and valgus foot by FE models. The results indicated that the locus of the forefoot, downward rotation of the talus head, and navicular drop might be of interest in quantifying the MLA collapse.

1.3.2 Main challenges in computational foot modeling

Overall, most of the studies focused on the construction of problem-specific models that did not include the individual characteristics of each patient but rather represented certain pathological conditions. The development of these models has undoubtedly

contributed to establishing an essential foundation to improve our understanding of arch biomechanics [153]. Nevertheless, many FE analyses were performed under the simplification of geometry and linear assumptions of material properties. At the same time, the complexity of the foot arch problem led to substantial gaps in the further development of precise models for clinical practices.

1.3.2.1 Model Design

The first crucial challenge in achieving clinically applicable FE modeling is to obtain credible information for geometry design and reconstruction in a cost-effective and non-invasive manner [133, 134]. It is evident that MRI and CT are currently the most accepted imaging modalities that could provide high-quality images capable of accurately reconstructing the geometry of bones or soft tissues. The primary distinction between both techniques is that CT precisely outlines the internal bone structure, while MRI provides finer details of the soft tissues [154]. Given the complexity of the foot arch structure, the reconstruction methods of related ligament and PF geometries depend on the analytical focus. Among others, in order to assess specific ligament stress distribution, detailed three-dimensional geometries are usually extracted from MRI scans or generated with ligament insertions from CT images [155]. For instance, Zhang et al. [139] reconstructed PF, spring ligaments, tendons, and fat pads based on anatomical images obtained from atlases and autopsies dissection with the suggestion of professional foot-ankle surgeons. In contrast, when the analysis was focused on assessing foot joint kinematics, related studies often used one-dimensional elements (such as link and spring) to represent the whole ligament [155]. It is worth noting that given the small bending and compression stiffness of real ligaments, three-dimensional isotropic solid elements might not adequately reflect the tension-only properties of ligaments [142]. On the other hand, although tension-only elements ignore the anatomical shape of the ligament and cannot adequately model ligament behavior, they avoid transmitting unrealistic bending and twisting moments and compressive forces [142, 146]. The above operation also raises a new issue in model design: the balance between exact details and proper simplifications (i.e., computational cost) [133]. To

simplify the FE analysis, associated ligaments and connective tissue (e.g., the joint capsules), as well as plantar flat pad and muscles, might not be considered due to the lack of evidence of their correlation with passive plantar arch maintenance or arch deformity [137, 140, 148, 150]. The foot arch is a synergic structure, and any local alteration might occur at the modified site and adjacent areas, even over the whole foot. The structural simplification of the FE model would also reduce the foot joint stability and increase predictions of foot arch deformation [150].

For exploring foot arch deformation based on FE models, most researchers need to modify the standard subject model, which could result in actual model objects that are difficult to represent in populations with the targeted clinical conditions or demographic characteristics [135]. Patient-specific FE models are usually required to involve personal characteristics, especially in pathological conditions. Most studies used regular subjects to build the model or create pathological models from the regular models, considering the time-consuming nature of constructing individual FE models involving all details [141]. For example, Malakoutikhah et al. [144-146] simulated progressive collapsing foot deformity by removing involved ligaments (e.g., the PF, deltoid ligament, spring ligament, and plantar ligaments) and unloading the posterior tibial tendon. Furthermore, the potential impact of individualized differences in the patients' feet (e.g., foot morphological differences in foot length and width, etc.) could be attenuated by modifying the healthy foot model to simulate foot deformities. Sun et al. [27] established low and high arch FE models based on reconstructed normal arch FE models by adjusting the AHI value varied by the arch length and height. Nevertheless, the patient-specific model is suggested for foot problems with significant structural deformities, such as progressive collapsing foot deformity, given that a modified standard foot may potentially affect pathological features [141].

1.3.2.2 Material Property Assignment

The major problem with the assignment of material properties is that most studies assumed elasticity linearly for foot arch tissues referring to previously published articles,

whereas biological tissues exhibit complex nonlinear and time-varying mechanical behavior [133]. Especially true for cartilage tissues that displace water under compression, this assumption may increase the rigidity of the model, reducing the bone rotation and the foot structure deformation; thus, it may not be entirely accurate to consider it to be a quasi-incompressible material [137, 147, 148]. Several existing studies [137, 147, 148] have considered using the Ogden model to create nonlinear and hyper-elastic cartilage materials to enhance the model behavior and its convergence. For bony structures, the current trend is to use an elaborate model that distinguishes between cortical and trabecular bone and to consider more complex simulations involving anisotropic and hyper-elastic behavior [137, 147, 148, 154]. With further simplifying the bone structure, the model material properties should be further calculated, particularly under large deformations and dynamic situations, as excessive neglect of the bone structure might significantly impact the model's rigidity [134, 141].

Besides that, it is also worth mentioning that a wide range of material properties/coefficients have been used to model ligaments. Thus, the challenge of a practically applicable and meaningful FE model of the ligament is to have the flexibility and reliability to model with patient-specific material properties and ligament geometries. Characterizing the time-dependent behavior of ligaments could significantly increase the computational complexity and information needed to develop an accurate ligament model. Simplifying the material model was often used as a compromise to achieve satisfactory accuracy with an acceptable computational complexity. However, when the aim of the study involves investigating ligament property change, for example, healthy and degenerative conditions, or dynamic loading conditions, time-dependent material models are often necessary to achieve accurate predictions.

1.3.2.3 Boundary and loading conditions

Another significant difficulty in implementing a practical FE analysis is setting boundary and loading conditions that can correlate with a given movement pattern or clinical setting without requiring specialized devices and time-consuming

measurements. Based on the current literature, most FE models tend to apply simplified loading conditions, such as balanced standing considering only GRF or vertical forces estimated from body weight, while ignoring all foot muscle forces or including only simplified Achilles tendon forces [27, 124, 125, 137, 140, 147, 148, 150, 152]. However, in cases where accurate measurement of specific loadings is critical to the reliability of the analysis, calculating loading using this approach might limit the usability and validity of the model as well as the patient specificity [133, 155]. It was also found that the boundary and loading conditions were not always determined from the same model subjects [143]. This may be acceptable if the characteristics specified for the subjects are limited or not the focus of the study. It is critical to obtain relevant loading and boundary data by performing biomechanical tests on the subjects involved, especially for clinically relevant scenarios where the model's accuracy is a prerequisite [134]. For example, Wong et al. [151] obtained boundary and loading conditions for FE analysis from gait experiments with model subjects to investigate the effect of load transfer alteration due to unloading the posterior tibial tendon on progressive collapsing foot deformity. Besides, in terms of arch deformation under different movement states, Chen et al. [138] derived kinematic and kinetic data from a musculoskeletal model of the same subject as boundary conditions for FE analysis to simulate running with different strike patterns.

1.3.2.4 Model Validation.

The eventual challenge in performing foot FE analysis in clinical practice is to ensure that it produces a credible model for a specific population with the targeted clinical scenarios or demographic characteristics [133]. Especially for the complex issue of foot arch deformity, the model accuracy must be verified in further experimental studies to have the ability to formulate clinically relevant recommendations. The two main types of validation include direct and indirect validation. The former requires researchers to perform experiments explicitly designed to validate the proposed model, while the latter tends to compare model predictions with previous studies, where the setup of the experiments cannot be controlled [154, 156]. Currently, experimental validation of FE

models focused on comparing predicted plantar pressures with data measured by a platform system, matching parameters such as plantar pressure distribution, peak regional pressure, and contact area [27, 140, 144-146, 150]. However, the predicted plantar pressure data were significantly higher than the experimental measurements due to resolution differences between the measurement system and the model or mismatched comparison parameters (e.g., measured plantar pressures were compared with predicted von Mises stresses) [154]. Furthermore, in terms of validation of arch deformation displacements, some studies also compared the vertical displacements visible in radiographic images concerning the FE model predictions by measuring anatomical parameters from sagittal views [137, 139, 147, 148]. Overall, future biomechanical analyses of foot arch deformation need more explicit validation for FE models to optimize accuracy. Especially considering the limited knowledge of the prestress and the complexity of deformation patterns of passive arch stabilizers such as the PF and main ligaments, it is difficult to determine whether the simulation results match in stress distribution of actual tissues [157]. Consequently, a combination of in vivo non-invasive mechanical testing, imaging, and computational modeling techniques is needed to make the foot FE model more recognized for future clinical applications [133, 155].

1.3.2.5 Model Applications

The existing FE foot models provide vast simulation data that could be useful in different fields. These model applications can be grouped into two main areas: biological applications and clinical applications, covering topics such as the effects of motion status/pattern on arch deformation [138, 143], the relevance of PF and main ligaments in foot arch function [124, 125, 140, 150], and analysis of pathology and foot disorders associated with arch deformity [27, 137, 139, 144-149, 151, 152, 158].

Since direct measurement of stress distribution within the foot arch (PF and main ligaments) is not feasible, it is necessary to use the FE methods in simulating the mechanical behavior of the foot [155, 159]. Simulating the dynamic motion of the ankle

and foot complex is often challenging due to the complex muscle forces and position changes during locomotion. Chen et al. [143] performed a quasi-static gait simulation to investigate the biomechanical responses of the PF during the stance phase and linked the increase in fascial tension and peak stress with the windlass mechanism of the foot arch. Furthermore, other researchers proposed a more accurate dynamic FE model with running gait characteristics using a dynamic explicit solver to improve the simulation accuracy [138]. The simulation results of the above study also provide further evidence about the association between arch deformation, PF overloading, and risk of plantar fasciitis.

The PF and associated ligaments (spring ligament and long and short plantar ligaments) are the primary stabilizing structures of the foot arch, and knowledge of their functional biomechanics is critical in determining the establishment of rehabilitation, orthotics, and surgical treatments related to pathological foot arch deformities. Increased PF stiffness significantly increases the strain on the associated ligaments [140]. When simulating the release of the PF (zero fascia Young's modulus), the peak stress shift resulted in a stress surge in the midfoot and metatarsals [125, 140]. At the same time, lateral and forward shifts of the COP and a reduction in the arch height were found. Besides, although predictions showed no complete arch collapse after the release of each soft tissue structure individually, the internal mechanical behavior was significantly altered [124]. Notably, arch support function was lost only when all major passive arch stabilizers, including PF, spring ligament, and long and short plantar ligaments, were severed simultaneously, emphasizing the reciprocal compensatory role of these soft tissues for controlling arch deformation [124, 125, 140].

Regarding pathomechanics, a rational understanding of foot disease, particularly associated with arch deformity, is essential to identify the best treatment [160, 161]. The midfoot is a relatively stable structure with less motion during locomotion than the hind and forefoot [141]. However, midfoot deformation is the main pathological issue for the reviewed foot FE models. Among them, progressive collapsing foot deformity is the most studied foot pathology, which has a direct clinical manifestation of progressive

flattening of the arch associated with ligament deficiency and posterior tibial tendon dysfunction [162]. It might not be sufficient to simulate flatfoot by simply reducing the ligament stiffness of the foot model, since progressive collapsing foot deformity occurs due to repeated loading of the plantar arch, resulting in long-term elongation of the ligaments and consequent loss of function [145]. As torn or stretched ligaments are nonfunctional and bear no or little tension under normal working conditions, their absence simulates their failure to function as foot stabilizers [144]. Therefore, most studies simulated the collapsed foot by removing all involved ligaments and unloading the posterior tibial tendon [144-146].

2 MATERIAL AND METHODS

2.1 Overview of the experimental and computational workflow

As illustrated in **Figure 9**, the present work combined biomechanical functional analysis and FE analysis of the foot-ankle complex to reveal foot-specific functional coupling mechanisms related to AS during motion. An understanding of the morphological arch biomechanical function may provide additional insights into foot injury prediction and the comprehensive compensatory adjustment of lower-limb joints during motion.

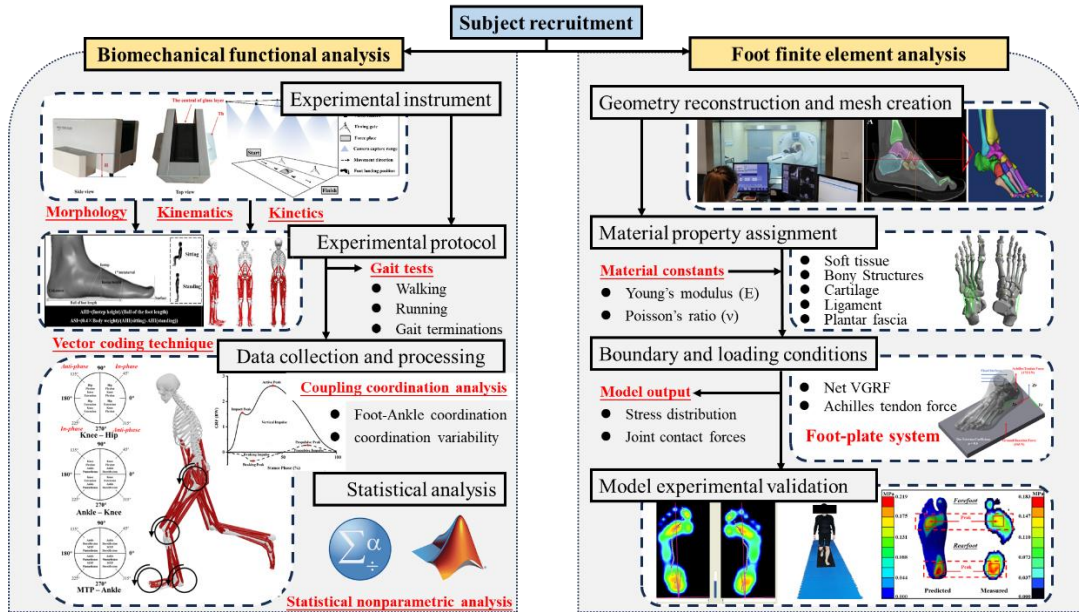


Figure 9 Experimental and computational process flowchart

The dissertation began with foot morphological measurements to classify the foot AS of recruited subjects based on the calculation of three-dimensional arch parameters under different loading conditions. All subjects were then required to complete gait tests in a standard biomechanical laboratory, including walking, running, PGT and UGT. Kinematic and kinetic parameters from the gait tests were collected to perform the subsequent musculoskeletal modelling. The SnPM approach was employed to assess the impacts of AS on foot-ankle kinematics during PGT and UGT. Inter-joint coordination

and variability were calculated from the angle-angle plots of knee-hip, ankle-knee, and MTP-ankle couplings based on an optimized vector coding technique.

Regarding the computational simulation, reverse engineering technology was used to acquire geometrical data of the right foot of the subject and establish a subject-specific FE model of the foot-ankle complex. A sensitivity investigation was conducted to evaluate the effects of varying PF stiffness on the metatarsal stress distribution and joint force transmission. The foot FE model was further validated by comparing plantar pressure acquired from computational simulations and experimental collections.

The details about the biomechanical functional analysis and FE analysis of the foot-ankle complex are listed in 2.2-2.5 sessions. Based on these results, a generalized methodology workflow that considers stiffness-related biomechanical functional coupling of the human foot-ankle complex, together with the musculoskeletal modelling, vector coding and reverse engineering techniques, was introduced for the quantitative exploration of foot biomechanical function and injury mechanism.

2.2 Ethics statement

This dissertation was performed in compliance with the declaration of Helsinki and was approved by the Institutional Ethics Committee of Ningbo University (Authorization No. RAGH20211220). Before taking part in the dissertation, all subjects were informed of the corresponding experimental protocol, study objectives, requirements, and procedures. All subjects gave consent to participate in this dissertation, as shown in **Figure 10**.



<div style="text-align: center;">  <p>Research Academy of Grand Health, Ningbo University</p> </div> <div style="text-align: right;"> <p>Human Informed Consent Form</p> </div> <hr/> <p>Instructions to the Student Researcher(s): An informed consent/assent/permission form should be developed in consultation with the Adult Sponsor, Designated Supervisor or Qualified Scientist. This form is used to provide information to the research participant (or parent/guardian) and to document written informed consent, minor assent, and/or parental permission.</p> <ul style="list-style-type: none"> When written documentation is required, the researcher keeps the original, signed form. Students may use this sample form or may copy ALL elements of it into a new document. <p>If the form is serving to document parental permission, a copy of any survey or questionnaire must be attached.</p> <p>Student Researcher(s): _____</p> <p>Title of Project: _____</p> <p>I am asking for your voluntary participation in my science fair project. Please read the following information about the project. If you would like to participate, please sign in the appropriate area below.</p> <p>Purpose of the project: _____</p> <p>If you participate, you will be asked to:</p> <p>Time required for participation: _____</p> <p>Potential Risks of Study: _____</p> <p>Benefits: _____</p> <p>How confidentiality will be maintained: _____</p> <p>If you have any questions about this study, feel free to contact:</p> <p>Adult Sponsor/QS/DS: _____ Phone/email: _____</p> <p>Voluntary Participation: Participation in this study is completely voluntary. If you decide not to participate there will not be any negative consequences. Please be aware that if you decide to participate, you may stop participating at any time and you may decide not to answer any specific question. By signing this form I am attesting that I have read and understand the information above and I freely give my consent/assent to participate or permission for my child to participate.</p> <p>Adult Informed Consent or Minor Assent Date Reviewed & Signed: _____</p> <p>Research Participant Printed Name: _____ Signature: _____</p> <p>Parental/Guardian Permission (if applicable) Date Reviewed & Signed: _____</p> <p>Parent/Guardian Printed Name: _____ Signature: _____</p>	<div style="text-align: center;">  <p>宁波大学 NINGBO UNIVERSITY</p> </div> <p style="text-align: right;">中国浙江宁波市江北区风华路818号 邮编: 315211 电话 Tel: (866)-574-87600253 No 818, Fenghua Road, Ningbo, Zhejiang, China 315211 传真 Fax: (866)-574-87604161</p> <p style="text-align: center;">Research Academy of Grand Health Ningbo University</p> <p style="text-align: center;">Institutional Review Board Procedures</p> <p>At the Research Academy of Grand Health, Ningbo University, all human subjects' research activities come under the purview and oversight of the Research Support Services Office and the Institutional Review Board (IRB), irrespective of whether the research is funded or non-funded, minimal risk or more. The Human Subjects Protection policy applies to all Research Academy of Grand Health, Ningbo University faculty, staff, and students conducting human subjects' research on or off-campus (domestic or international sites) as well as visitors conducting research at the Research Academy of Grand Health Ningbo University.</p> <p>Researchers, including the faculty advisors of student researchers, must successfully complete online human subjects' protection training before submission to the IRB.</p> <p>Human subjects protection is a collaborative effort by the researcher and the Research Academy of Grand Health, Ningbo University. The IRB is charged with the responsibility of protecting the rights and welfare of human subjects involved in research. The composition of the IRB and the number of members on the committee are in accordance with national regulations. IRB members are appointed by the Vice Provost for Research on the recommendation of the chairperson of the IRB. Members are appointed for renewable, three-year terms and include faculty and community members with expertise in the various disciplines engaged in human subjects' research on campus.</p> <p>Scope of Review</p> <p>The IRB reviews research involving human subjects if one or more of the following apply:</p> <ul style="list-style-type: none"> the research is sponsored by CN, regardless of the location of the project; the research is conducted by, or under the direction of, any staff, faculty, student, or other agent of CN in connection with his or her institutional responsibilities; the research is conducted by or under the direction of any employee or agent of CN using any property or facility of CN; the research involves the use of CN's non-public information to identify or contact human research subjects or prospective subjects.
---	---

Figure 10 The human informed consent form and institutional review board procedures

2.3 Participants

A minimum sample size of fifty-two was required for the present research, as calculated by G*Power software (effect size = 0.8, α = 0.05, and power = 0.8). Thus, fifty-four physically active adults were recruited and completed the following gait experiments. All participants had to meet the following requirements: (i) each subject was a physically active male adult; (ii) the right-side leg was the dominant leg; (iii) there were no foot deformities or medical problems that might potentially affect gait performance; (iv) there was no hearing disorder; (v) there had been no history of disorders or injuries to the lower limbs in the first half of the year preceding data collection. For the SnPM analysis, twenty-eight subjects (age: 23.53 ± 1.92 years, height: 1.76 ± 0.03 cm, mass: 68.88 ± 5.92 kg, BMI: 22.17 ± 1.65) were randomly selected from the total sample size. For the FE simulation test, a male adult subject (age: 28 years, height: 178 cm, mass: 69 kg) without neurological involvement was enrolled. This subject had no neurological disorders or biomechanical abnormalities resulting from suffering acute foot injury or having undergone previous osseous foot surgery.

2.4 Biomechanical functional analysis

2.4.1 Experimental protocol and procedures

2.4.1.1 Foot morphology measurements

Compared with traditional foot dimensional measurements (e.g., digital caliper and digital footprint), three-dimensional foot morphological scanning for acquiring foot anthropometric parameters has relatively higher precision and robustness [163]. Therefore, before performing the gait task, three-dimensional foot morphological parameters were collected from all participants during standing and sitting conditions using the Easy-Foot-Scan instrument (OrthoBaltic, Kaunas, Lithuania) following a previously developed protocol [15]. Participants' foot morphology was only measured for their dominant feet. The variables of the foot structure were calculated with AutoCAD version 2018 software (Autodesk, San Rafael, CA, USA) according to the three-dimensional foot images acquired from the foot morphology scanner in standing and sitting postures. MLA was calculated as the height between the ground and the dorsal surface at half the foot length. Forty per cent bodyweight (BW) was standardized because of variation in the load placed on the feet during sitting (10% BW) and standing (50% BW)[7]. Therefore, this study calculated arch height flexibility as the difference between MLA height at two body positions, normalized to 40% BW [4]. A previous study [7] on a large sample derived a median arch height flexibility, which was utilized in the present study to classify the FA (> 14.8 mm/kN) and SA (< 14.8 mm/kN). The arch height flexibility of each participant was measured as representative of AS to establish stiff arch (SA) and flexible arch (FA) groups (**Table 1**).

Table 1 Anthropometric characteristics of two groups

Variable	Total	Groups		p-Value
		FA	SA	
Number (n)	54	27	27	NA
Age (y)	24.1 ± 2.0	24.7 ± 2.1	23.3 ± 1.7	0.164
Height (m)	177.8 ± 5.6	177.7 ± 5.4	177.9 ± 6.1	0.936
Weight (kg)	71.9 ± 7.3	70.1 ± 8.1	73.7 ± 6.4	0.309

BMI (kg/m ²)	22.8 ± 2.3	22.1 ± 1.8	23.4 ± 2.6	0.265
AS (mm/kN)	14.2 ± 3.7	17.0 ± 2.6	11.3 ± 2.1	0.000*

Note: * indicates a significant difference between the two groups, $p < 0.05$.

2.4.1.2 Gait Task Measurements

After completing foot morphological measurements, participants underwent a 5-minute warm-up before gait task measurements. The lower extremity kinematics and GRF were obtained from the dominant side in the gait experiments. The walking and running speeds were controlled to 1.6 ± 0.2 m/s and 2.7 ± 0.2 m/s, respectively, via a timing gate to attenuate the effect of gait speed on biomechanical parameters [160, 164]. Prior to data collection, each participant was asked to familiarize themselves with the laboratory environment in order to adapt to walking and running speeds. Participants were asked to complete a dataset of ten successful gait trials, including five walking and five running trials. Besides, all participants were instructed to perform two types of GT tests, PGT and UGT, within a laboratory setting following a previously established protocol [3]. First, they were asked to walk barefoot along a 20 m walkway at a self-selected speed. If they received a transmitted auditory signal with a bell during this process, they needed to stop walking immediately and remain stationary. Otherwise, they had to stop systematically at a designated location at the end of the walkway. Of the GT tests, 20% included a ringing signal, while the remaining 80% did not. A 2-minute rest interval was provided between trials to reduce the effect of tiredness on experimental results to a minimum. Each participant was requested to provide a dataset of 10 successful GT tests comprising 5 PGT tests and 5 UGT tests.

Joint movements were collected by an 8-camera motion capture system (Vicon Motion System Ltd., Oxford, UK) with sampling at 200 Hz synchronously with GRFs from an AMTI force platform (AMTI, Watertown, MA) embedded in the center of the walkway, at 1000 Hz. Each participant was fitted with thirty-eight retroreflective markers as per a customized lower limb kinematic marker set and model (**Figure 11**) [131].

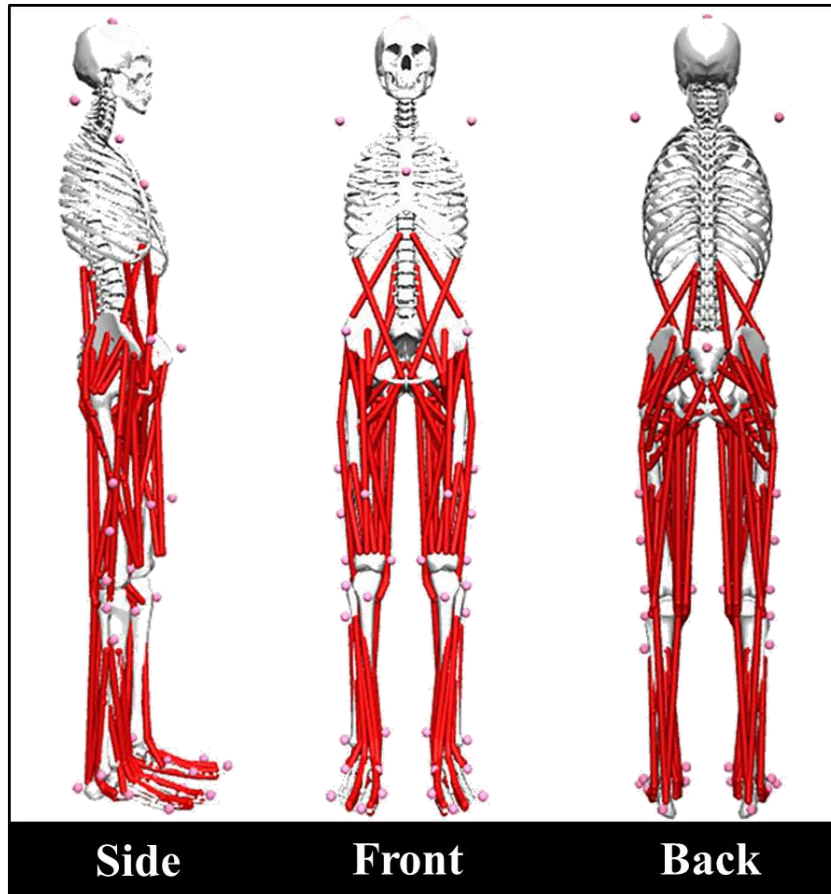


Figure 11 Illustration of reflective markers attached to the human body

2.4.2 Data collection and processing

The marker trajectory and the GRF data acquired by the gait trials were processed and transformed by the self-designed MATLAB script, and the standardized OpenSim workflow was performed following a previously established scheme [165]. Moreover, the inverse kinematics algorithm was applied to compute the lower limb joint angles for the minimum error. For each gait trial, time-series data, including the hip, knee, ankle, and MTP joint angles on the sagittal plane, as well as GRF in the vertical and AP directions, were extracted to adjust to 101 time points.

As a non-linear method, the vector coding analysis technique quantifies the coordination pattern by inferring CA in the angle-angle diagram, so as not to miss segmental spatial data of motion [166]. In this study, I used an optimised vector coding technique to calculate inter-joint coordination and CV, following the procedure reported

by Needham et al. [167]. The CA (γ_i) was computed according to the successive proximal segment angles ($\theta_{P(i)}$) and distal segments angles ($\theta_{D(i)}$). Mathematically, γ_i was inferred as:

$$\gamma_i = \begin{cases} \tan^{-1} \left(\frac{\theta_{D(i+1)} - \theta_{D(i)}}{\theta_{P(i+1)} - \theta_{P(i)}} \right) \cdot \frac{180^\circ}{\pi}, & \text{if } \theta_{P(i+1)} - \theta_{P(i)} > 0^\circ \\ \tan^{-1} \left(\frac{\theta_{D(i+1)} - \theta_{D(i)}}{\theta_{P(i+1)} - \theta_{P(i)}} \right) \cdot \frac{180^\circ}{\pi} + 180^\circ, & \text{if } \theta_{P(i+1)} - \theta_{P(i)} < 0^\circ \end{cases} \quad (1)$$

where i is the corresponding time point of the standardised stance phase (i_1 = the first stride in 101 time points, ... i_n = the n th stride in 101 time points).

The following supplementary conditions were adopted [167]:

$$\gamma_i = \begin{cases} 90, & \text{if } \theta_{P(i+1)} - \theta_{P(i)} = 0 \text{ and } \theta_{D(i+1)} - \theta_{D(i)} > 0 \\ -90, & \text{if } \theta_{P(i+1)} - \theta_{P(i)} = 0 \text{ and } \theta_{D(i+1)} - \theta_{D(i)} < 0 \\ -180, & \text{if } \theta_{P(i+1)} - \theta_{P(i)} < 0 \text{ and } \theta_{D(i+1)} - \theta_{D(i)} = 0 \\ \text{undefined}, & \text{if } \theta_{P(i+1)} - \theta_{P(i)} = 0 \text{ and } \theta_{D(i+1)} - \theta_{D(i)} = 0 \end{cases} \quad (2)$$

The γ_i for two joints was further adjusted in the range of 0° - 360° based on the following equation [19, 167, 168]:

$$\gamma_i = \begin{cases} \gamma_i + 360, & \text{if } \gamma_i < 0 \\ \gamma_i, & \text{if } \gamma_i \geq 0 \end{cases} \quad (3)$$

Selected inter-joint couplings included hip vs. knee, knee vs. ankle, and ankle vs. MTP on the sagittal plane, with reference to the previously defined coordination modes' classification from the CA on the sagittal plane [169]

Given the directivity of the CA, the average CA ($\bar{\gamma}_i$) were calculated according to the average horizontal and vertical components by circular statistics [167, 170]. Where \bar{x}_i and \bar{y}_i denotes the horizontal and vertical elements of the $\bar{\gamma}_i$ at per time point (i) during the stance phase, and $\bar{\gamma}_i$ for two joints was further adjusted in the range of 0° - 360° .

$$\bar{x}_i = \frac{1}{n} \sum_{i=1}^n \cos \gamma_i \quad (4)$$

$$\bar{y}_i = \frac{1}{n} \sum_{i=1}^n \sin \gamma_i \quad (5)$$

$$\bar{\gamma}_i = \begin{cases} \tan^{-1} \left(\frac{\bar{y}_i}{\bar{x}_i} \right) \cdot \frac{180^\circ}{\pi}, & \text{if } x_i > 0^\circ \text{ and } y_i > 0^\circ \\ \tan^{-1} \left(\frac{\bar{y}_i}{\bar{x}_i} \right) \cdot \frac{180^\circ}{\pi} + 180^\circ, & \text{if } x_i < 0^\circ \\ \tan^{-1} \left(\frac{\bar{y}_i}{\bar{x}_i} \right) \cdot \frac{180^\circ}{\pi} + 360^\circ, & \text{if } x_i > 0^\circ \text{ and } y_i < 0^\circ \\ 90^\circ, & \text{if } x_i = 0^\circ \text{ and } y_i > 0^\circ \\ -90^\circ, & \text{if } x_i = 0^\circ \text{ and } y_i < 0^\circ \\ \text{undefined}, & \text{if } x_i = 0^\circ \text{ and } y_i = 0^\circ \end{cases} \quad (6)$$

Finally, CV_i was computed as the circular standard deviation of γ_i , where \bar{r}_i is the length of the average coupling:

$$CV_i = \sqrt{2 \cdot (1 - \bar{r}_i)} \cdot \frac{180^\circ}{\pi}, \text{ where } \bar{r}_i = \sqrt{\bar{x}_i^2 + \bar{y}_i^2} \quad (7)$$

The GRF data of the gait trial was filtered through a fourth-order Butterworth filter with a lowpass frequency of 50 Hz. A threshold of 10 N on the vertical GRF was used to recognize the time interval from initial contact and toe-off as the stance phase. Then, the GRF data for each participant were standardized to their BW. The following GRF parameters of interest were included: i) peak vertical impact force; ii) peak vertical active force; iii) vertical impulse; iv) peak braking force; v) peak propulsive force; vi) braking impulse; vii) propulsive impulse. As a self-normalizing metric, the ratios of anterior: vertical and posterior: vertical GRI were computed to describe the force distribution in the vertical, anterior and posterior directions [9].

2.4.3 Statistical analysis

Due to the one-dimensional time-varying properties of the joint kinematics, a factorial SnPM was applied in MATLAB R2018a (The MathWorks, Natick, MA, USA) using open-access one-dimensional SPM scripts [14, 171]. Two-way repeated-measures ANOVA was used to assess the effect of AS on foot-ankle kinematics during PGT and

UGT. Bonferroni correction was applied to adjust the alpha risk of post hoc tests in the case of significance.

To assist in the interpretation of the time-series waveforms and coordination patterns, the stance phase of walking was categorized into three sub-phases: early (0-33%), middle (34-66%), and late stance (67-100%), while running was defined as early (0-24 %), middle (25%-50%), and late stance (51%-100%) [18, 19]. An independent sample t-test was used in SPSS 23.0 (Chicago, IL, USA) to examine discrete CA, CV, and GPF data. For time-varying GRF waveforms in the vertical and AP directions, data variability was verified in MATLAB software using a one-dimensional SPM package (independent t-test). The significance level for all statistical analyses was set at 5%.

2.5 Foot finite element analysis

2.5.1 Geometry reconstruction and mesh creation

The medical CT images of the patient's right foot were collected via the Optima CT540 scanner (GE Healthcare, USA). The slice thickness of the coronal plane of the foot was set as 0.625 mm when CT scans were performed under neutral and non-weight-bearing conditions. Subsequently, the DICOM imagery was segmented and reconstructed using the software MIMICS 19.0 (Materialise Co., Ltd., Belgium) to acquire the geometries of bony structures and soft tissues to reconstruct the 3D foot-ankle complex model. In order to simplify the analysis, the distal and intermediate phalanxes of the 2nd - 5th toes were fused as a single bony structure [160]. A total of twenty-four bones were thus segmented, including 1st - 5th metatarsals (M1-M5), as shown in **Figure 12**. The geometry was smoothed via Geomagic Wrap 2021 (3D Systems. Rock Hill, USA) and subsequently imported into Solidworks 2022 (Dassault Systèmes, France) to create solid components. According to the contact surfaces of bones, twenty-four cartilaginous structures were reconstructed to allow articulation and relative movement between the bony segments in this model. Volume Boolean operations were performed to yield an encapsulated soft tissue by subtracting the bone and cartilage structures from the entire soft tissue volume. The PF and major ligaments responsible for maintaining the static

foot arch structure, including the long and short plantar ligaments as well as spring ligaments, were modeled utilizing tension-only link elements according to the anatomical positions on their respective bones [124].

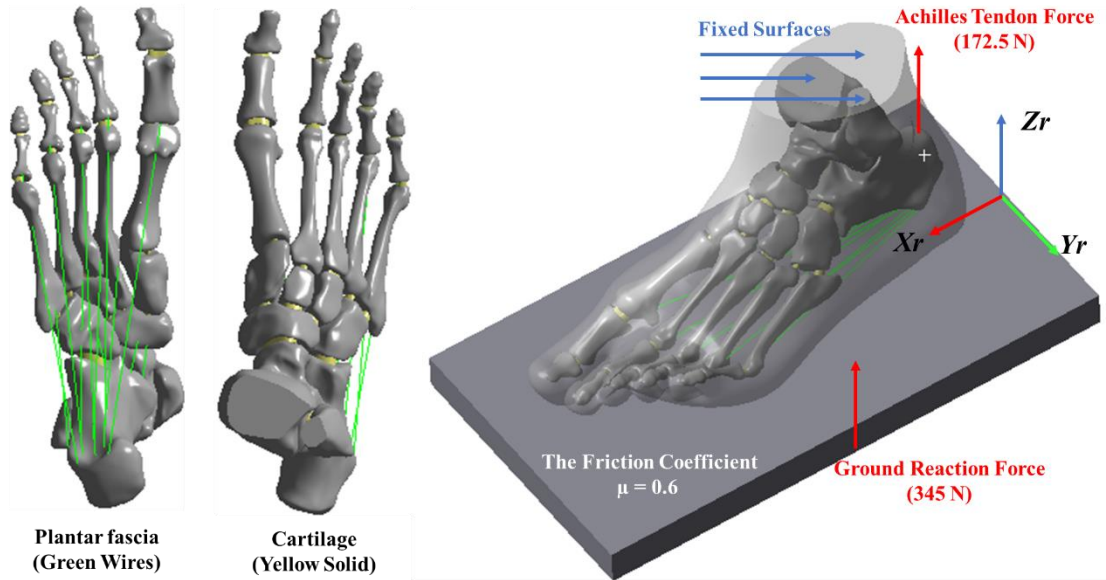


Figure 12 The three-dimensional finite element model and the application of boundary and loading conditions.

A convergence analysis was performed during the meshing process in Ansys Workbench 2022 (ANSYS, Inc., United States) to ensure both model accuracy and optimal computational resource utilization. Virtual topology techniques were employed to adjust the surface of each part [172]. The meshing scheme involved using hexahedral elements for the ground plate and tetrahedral solid elements for all other components. The mesh sizes were set as follows: 2.0 mm for the cartilage, 3.5 mm for the bony structures, and 5.0 mm for the soft tissue and ground plate. The resulting mesh consisted of a total of 252,096 nodes and 139,238 elements, encompassing the entire foot model.

2.5.2 Material properties

All materials used in this FE analysis were assumed to be homogeneous, isotropic, and linearly elastic (**Table 2**). The elastic properties were defined by two material constants: Young's modulus (E) and Poisson's ratio (ν). In particular, a Young's modulus of 350 MPa was selected as the reference value to indicate the regular PF stiffness. Meanwhile,

to evaluate the influence of PF stiffness on load distribution, various Young's modulus values ranging from 0 to 700 MPa (representing 0%-200% of the reference values) were assigned to the PF [140].

Table 2 Material properties of the components in the finite element model

Component	Element Type	Young's Modulus E (MPa)	Poisson's Ratio ν	Cross-Section Area (mm ²)	Reference
Bony Structures	Tetrahedral solid	7300	0.30	N/A	Gefen, 2002[173]
Soft tissue	Tetrahedral solid	1.15	0.49	N/A	Cho et al., 2009[174]
Cartilage	Tetrahedral solid	1	0.40	N/A	Gu et al., 2010[132]
Ligament	Tension-only truss	260	0.40	18.4	Siegler et al., 1988 [175]
Plantar fascia	Tension-only truss	350 (0-700)	0.40	58.6	Brilakis et al., 2012 [176]
Ground plate	Hexahedral solid	17,000	0.10	N/A	Gu et al., 2010[132]

2.5.3 Boundary and loading conditions

A foot-plate system method was utilized to simulate the interaction between the ankle-foot complex and the ground plate, as illustrated in **Figure 12**. A solid plate that was restricted to vertical movement only was applied to represent the supporting ground. The superior surfaces of the encapsulated soft tissue, distal tibia, and distal fibula components were fixed in all directions. Two separate extra forces, net vertical GRF equal to half of the body weight (345 N) and Achilles tendon force estimated to be half of the ground support force in a balanced stance (172.5 N), were exerted at the inferior surface of the plate and the superior surface of the calcaneus [140]. Regarding the interaction between the foot and ground plate, a frictional contact connection was defined, with a coefficient of 0.6.

In this study, a sensitivity analysis was conducted to examine the impact of different PF stiffnesses (ranging from 0 to 700 MPa) on the metatarsal stress distribution and force transmission. Specifically, I computed the peak von Mises stresses of the metatarsal region and joint contact forces transmitted through the metatarsals. The evaluation includes the MTP and tarsometatarsal (TMT) joints.

2.5.4 Model validation

The foot FE model was validated by comparing plantar pressure acquired from computational simulations and experimental collections through the Footscan system (RSscan International, Belgium) in a standing position. The experimental measurement was performed on the same participant who had previously undergone medical image scanning. Two plantar anatomical regions, the forefoot and rearfoot, were divided to compare the differences between experimentally measured and FE predicted regional peak pressure. The forefoot area consisted primarily of the phalanges and the metatarsal bones, while the rearfoot area was composed of the calcaneus and the talus [27].

3 RESULTS

3.1 Statistical nonparametric mapping analysis

3.1.1 Ankle kinematics

Kinematic differences in ankle angles in the sagittal plane are displayed in **Figure 13**. There was an interaction effect, with an F-value above the significant threshold of 8.64 during 23-51% of the stance phase (**Figure 13A**). Specifically, compared to PGT, FA and SA had significantly smaller ankle plantarflexion angles during 10-21% and 8-51% of the stance phase of UGT, respectively. Moreover, FA exhibited a significantly increased ankle plantarflexion angle in the sagittal plane during 10-21% and 53-65%, and 4-65% of the stance phase under PGT and UGT conditions, respectively (**Figure 13B, C**).

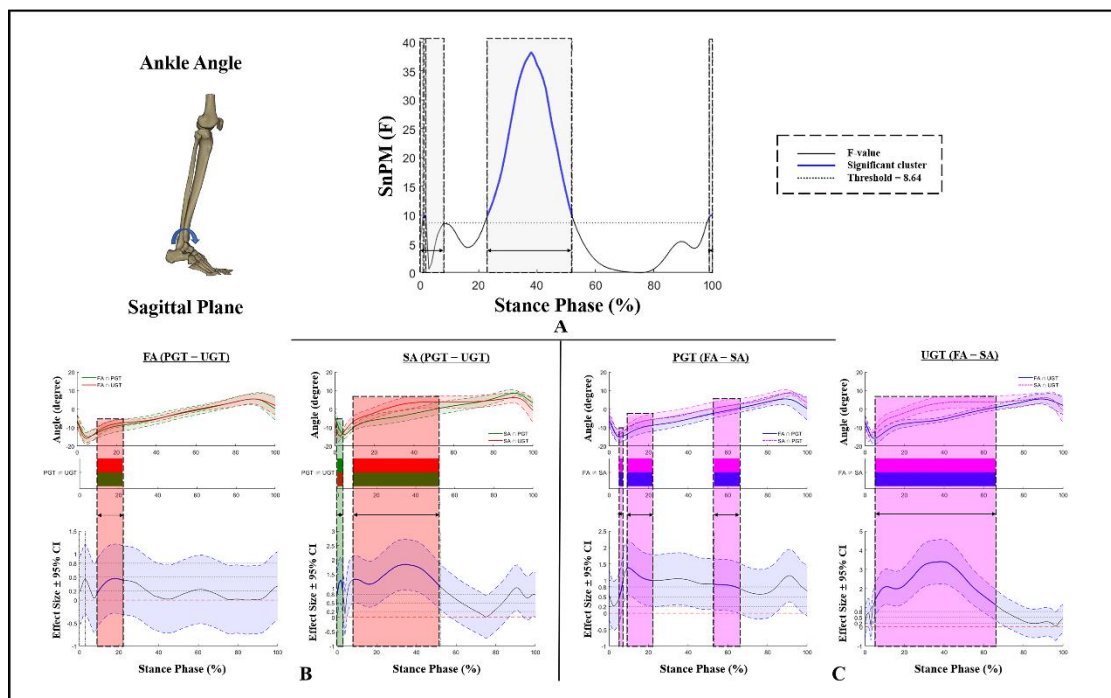


Figure 13 Kinematic differences of ankle angles in the sagittal plane

Note: (A) Interaction, (B) post hoc test for GT, and (C) post hoc test for AS. Shaded gray vertical bars represent the areas where interaction effects exist. Shaded red and green vertical bars represent the area where data during UGT were significantly greater or smaller than during PGT. Shaded purple vertical bars represent the area where data

for SA were significantly greater than for FA.

As for ankle angles in the frontal plane, no $GT \times AS$ interaction effects or main effects of AS were found (**Figure 14**). Additionally, at the early stance phase (4-25%), a GT effect with an F-value above the significant threshold of 7.65 presented (**Figure 14A**). During that phase, compared to PGT, a significantly greater ankle inversion angle was exhibited during UGT (**Figure 14B**).

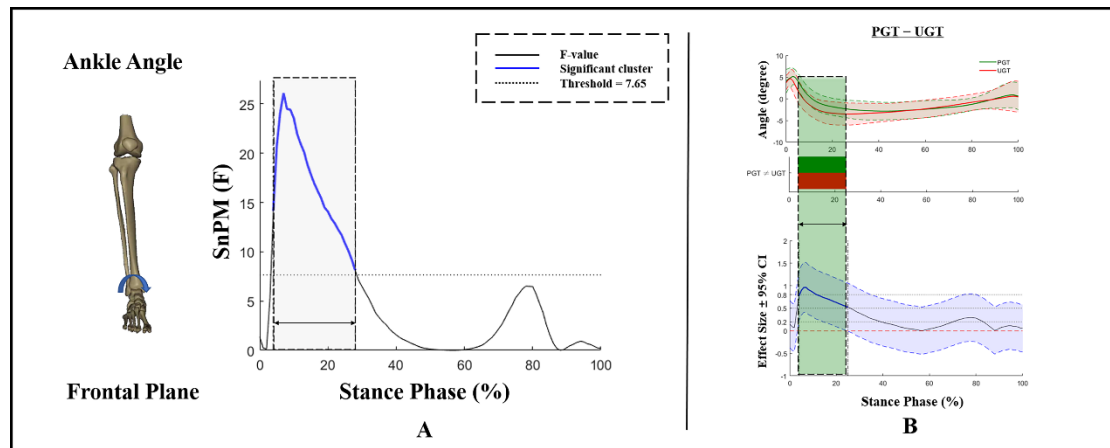


Figure 14 Kinematic differences of ankle angles in the frontal plane

Note: (A) Main effects of GT and (B) post hoc test for GT. Shaded gray vertical bars represent the areas where the main effects of GT exist. Shaded green vertical bars represent the area where data during UGT were significantly smaller than during PGT.

Figure 15 exhibits differences in ankle angles in the transverse plane under different ASs and GTs. There were significant $GT \times AS$ interaction effects for ankle angles in the transverse plane during 4-6% and 16-18% of the stance phase. The ankle external rotation angles of FA and SA during 40-52% of PGT were significantly greater than those at UGT. Moreover, a significant decrease in the external rotation of SA during the stance phase of PGT and UGT (22-100%) was found (**Figure 15B, C**).

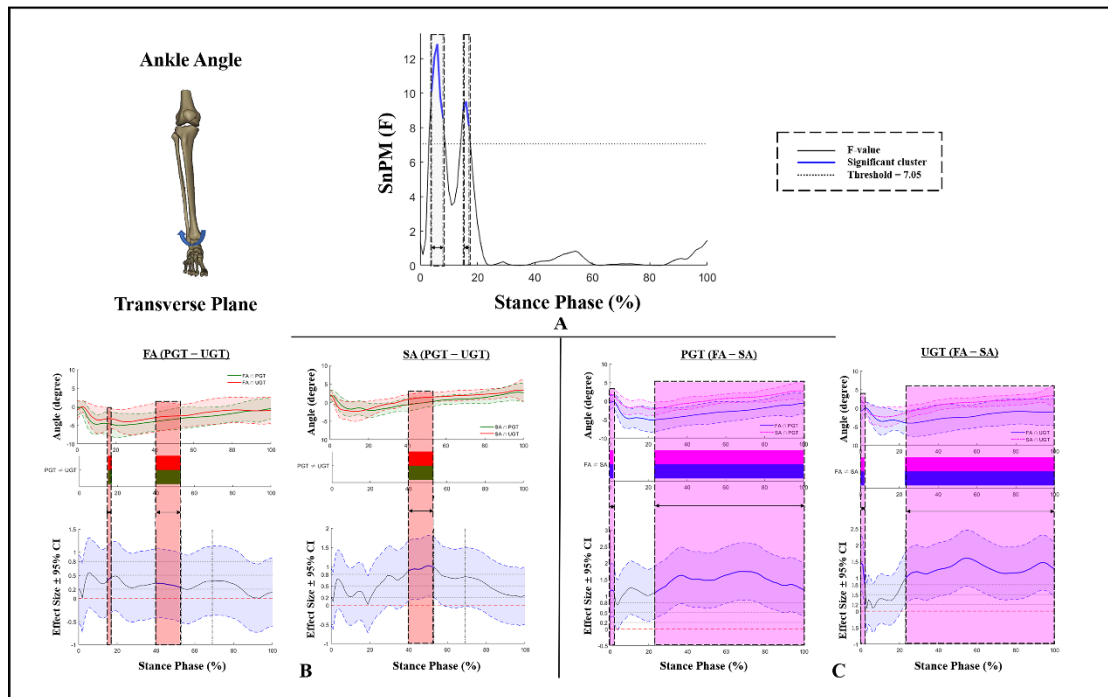


Figure 15 Kinematic differences of ankle angles in the transverse plane

Note: (A) Interaction, (B) post hoc test for GT, and (C) post hoc test for AS. Shaded gray vertical bars represent the areas where interaction effects exist. Shaded red vertical bars represent the area where data during UGT were significantly greater than during PGT. Shaded purple vertical bars represent the area where data for SA were significantly greater than for FA.

3.1.2 Metatarsophalangeal kinematics

As for MTP angles in the sagittal plane, no significant kinematic differences were found on the basis of the results of SnPM.

Kinematic differences in MTP angles in the frontal plane are exhibited in **Figure 16**, and no GT \times AS interactions or main effects of AS were found during PGT and UGT. There was a GT effect with an F-value above the significant threshold of 9.4 during 4-57% of the stance phase (**Figure 16A**). During that phase, compared to PGT, a significantly smaller MTP inversion angle was exhibited during UGT (**Figure 16B**).

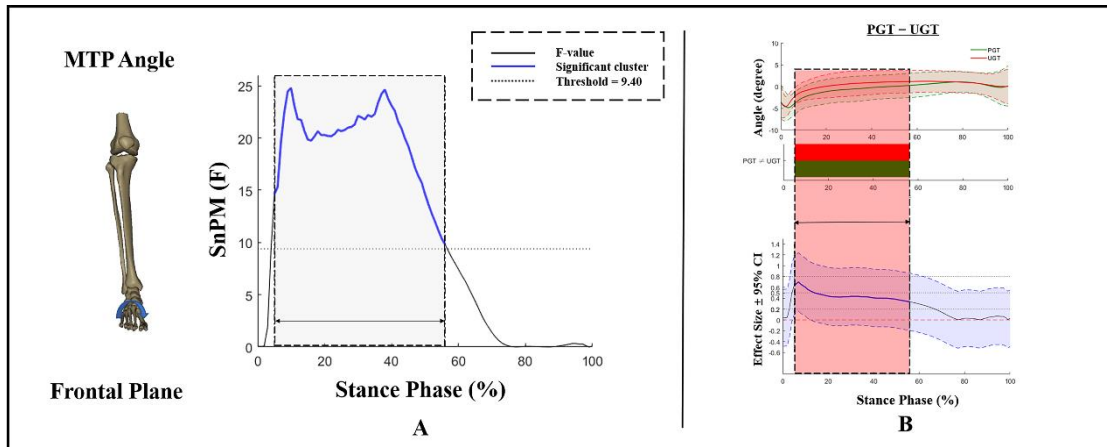


Figure 16 Kinematic differences of MTP angles in the frontal plane

Note: (A) Main effects of GT and (B) post hoc test for GT. Shaded gray vertical bars represent the areas where the main effects of GT exist. Shaded red vertical bars represent the area where data during UGT were significantly greater than during PGT.

No GT \times AS interaction effects were found for MTP angles in the transverse plane. **Figure 17A** shows a GT effect with an F-value above the significant threshold of 10.3 (18-48% of the stance phase).

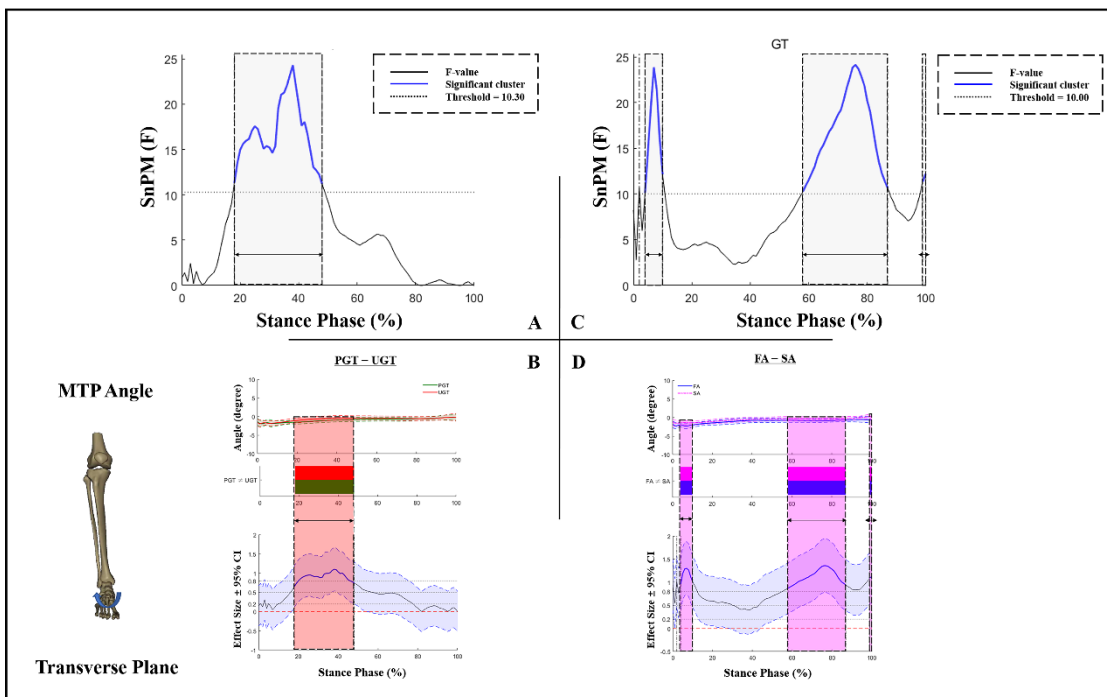


Figure 17 Kinematic differences of MTP angles in the transverse plane

Note: (A) Main effects of GT and (B) post hoc test for GT; (C) main effects of AS and

(D) post hoc test for AS. Shaded gray vertical bars represent the areas where the main effects of GT or AS exist. Shaded red vertical bars represent the area where data during UGT were significantly greater than during PGT. Shaded purple vertical bars represent the area where data for SA were significantly greater than for FA.

During that phase, compared to PGT, a significantly smaller MTP external rotation angle was exhibited during UGT (**Figure 17B**). During 4-10% and 58-87% of the stance phase, an AS effect with the F-value above the threshold of 10 was observed (**Figure 17C**). Moreover, FA exhibits a significantly increased MTP external rotation than SA (**Figure 17D**).

3.2 Inter-joint coupling coordination analysis

3.2.1 Coupling coordination

Comparisons of mean CAs for different MLA flexibilities during each sub-phase are shown in **Table 3**. In both the FA and SA groups, and either gait sub-phase, the CA was in the range of 157.5° and 202.5°, indicating that the joint coordination patterns were in the distal phase.

During mid-stance of walking, the knee-hip coordination CA of FA was $185.63 \pm 16.16^\circ$, while that of SA was $173.99 \pm 20.06^\circ$ ($p = 0.012$). For ankle-knee coordination, FA moved both the ankle and knee into plantarflexion and extension during the early stance of running ($176.42 \pm 16.51^\circ$), whilst SA moved the ankle into plantarflexion while moving the knee into flexion ($186.54 \pm 19.25^\circ$) ($p = 0.025$).

Table 3 Coupling angle between different arch flexibility in each sub-phase.

Joints Coordination	Motion	Sub-phase	Groups		Mean difference (95% CI)
			FA	SA	
Knee-Hip	Walking	ES	181.84 ± 16.83	177.61 ± 22.01	4.22 (-5.41 – 13.86)
		MS	185.63 ± 16.16	173.99 ± 20.06	11.64 (2.69 – 20.60) *
		LS	174.64 ± 21.63	174.89 ± 22.24	0.25 (-11.04 – 10.54)
	Running	ES	180.34 ± 18.62	176.16 ± 16.18	4.19 (-4.39 – 12.76)
		MS	175.72 ± 16.25	181.06 ± 20.99	5.34 (-14.57 – 3.89)
		LS	181.67 ± 16.00	179.07 ± 22.50	2.61 (-7.01 – 12.23)

Ankle-Knee	Walking	ES	180.78 ± 21.52	182.12 ± 20.93	1.34 (-11.78 – 9.10)
		MS	175.77 ± 18.15	181.25 ± 22.44	5.47 (-15.51 – 4.56)
		LS	179.42 ± 20.06	179.42 ± 17.50)	0.00 (-9.25 – 9.26)
	Running	ES	176.42 ± 16.51	186.54 ± 19.25	10.13 (-18.94 – -1.31) *
		MS	178.34 ± 22.08	182.48 ± 27.45	4.14 (-16.47 – 8.19)
		LS	180.89 ± 20.64	180.72 ± 19.65	0.17 (-9.74 – 10.08)
MTP-Ankle	Walking	ES	176.26 ± 18.71	173.39 ± 19.50	2.87 (-6.53 – 12.27)
		MS	180.34 ± 20.00	178.60 ± 23.36	1.74 (-8.95 – 12.44)
		LS	176.86 ± 21.80	176.73 ± 20.63	0.14 (-10.30 – 10.57)
	Running	ES	179.14 ± 22.26	176.55 ± 22.33	2.59 (-8.37 – 13.55)
		MS	177.37 ± 22.77	175.93 ± 17.85	1.44 (-8.62 – 11.50)
		LS	180.54 ± 23.30	179.37 ± 20.90	1.17 (-9.71 – 12.06)

Note: The unit for the values is degrees; The sub-phases are categorized into three events: early stance (ES), middle stance (MS), and late stance (LS).

3.2.2 Coordination variability

Figure 18 compares CVs between the two groups during each gait sub-phase of walking and running.

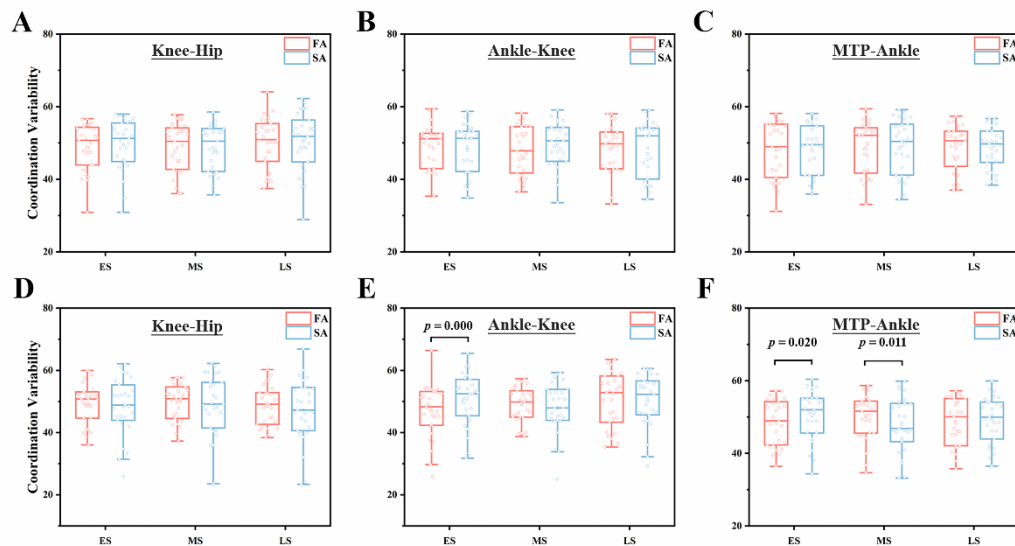


Figure 18 Comparison of coordination variabilities between different arch flexibilities.

Note: Knee-hip coordination (A), ankle-knee (B), and MTP-ankle (C) coordination during walking and knee-hip coordination (D), ankle-knee (E), and MTP-ankle (F) coordination during running

No statistically significant differences in CV were found between the FA and SA in each sub-phase of walking ($p > 0.05$). Compared to the FA, the CVs of SA were significantly larger for the ankle-knee ($p < 0.001$) and MTP-ankle coordination ($p = 0.020$) during the early stance of the running. However, for the MTP-ankle coordination during MS of the running stance phase, a significantly smaller CV value was found in the SA than in FA ($p = 0.011$).

3.2.3 Ground reaction impulse

Figure 19 exhibits GRF waveforms in the vertical and anterior-posterior directions and the braking and propulsive impulse ratio between FA and SA.

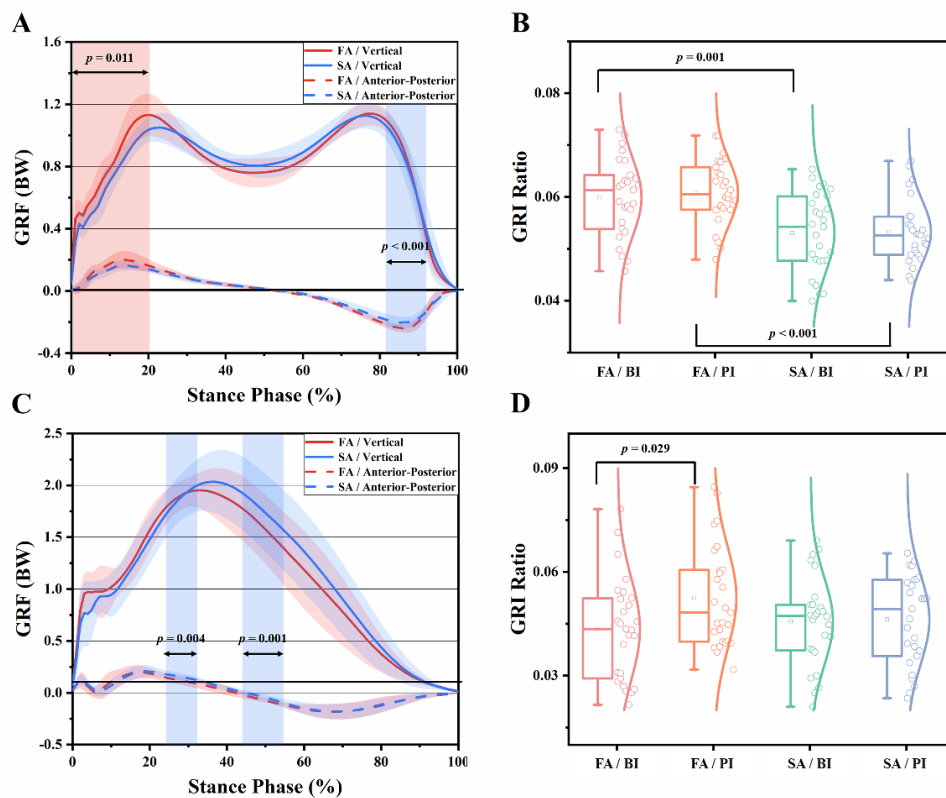


Figure 19 Comparison of ground reaction forces and impulses between different ASI.

Note: GRFs waveforms in the vertical and anterior - posterior directions of FA and SA during walking (A) and running (C); The ratio of anterior: vertical and posterior: vertical ground reaction impulses (GRIs) of FA and SA during walking (B) and running (D). Note: shaded red and blue vertical bars indicate significant differences in GRFs in the vertical and anterior - posterior directions

During the stance phase of walking, FA showed a larger vertical GRF in the early stance (0-20%, $p = 0.011$) and a larger propulsive force in the late stance (82-92%, $p < 0.001$) (**Figure 19A**). In addition, compared with SA, FA also presents higher ratios of braking and propulsive impulses ($p = 0.001$ and $p < 0.001$) (**Figure 19B**). As shown in **Figure 19C**, no significant difference in vertical GRF between FA and SA was found during running. However, in the anterior-posterior direction, FA presents an increased braking force and a decreased propulsive force in 25-32% ($p = 0.004$) and 44-55% ($p = 0.001$). Moreover, a larger ratio of propulsive impulse than in the posterior direction ($p < 0.029$) (**Figure 19D**).

All discrete GRF data in the vertical and anterior-posterior directions are presented in **Table 4**. FA demonstrated greater peak vertical impact forces than SA during both walking and running ($p = 0.006$ and $p = 0.007$). In the anterior-posterior direction, significantly greater peak braking force and propulsive force were found in FA during walking ($p = 0.001$ and $p < 0.001$). Additionally, during walking, FA also presents greater braking and propulsive impulses than SA ($p = 0.001$ and $p < 0.001$).

Table 4 Ground reaction forces and impulses between different arch flexibility

Variable	Motion	Groups		<i>p</i> -Value
		FA	SA	
Peak Vertical Impact Force (BW)	Walking	1.14 ± 0.12	1.06 ± 0.09	0.006*
	Running	1.30 ± 0.21	1.18 ± 0.21	0.007*
Peak Vertical Active Force (BW)	Walking	1.15 ± 0.08	1.14 ± 0.09	0.608
	Running	2.04 ± 0.19	2.10 ± 0.25	0.081
Vertical Impulse (BW%·s)	Walking	54.45 ± 3.99	54.20 ± 2.33	0.601
	Running	36.31 ± 2.79	36.76 ± 1.99	0.227
Peak Braking Force (BW)	Walking	0.21 ± 0.07	0.18 ± 0.04	0.001*
	Running	0.19 ± 0.08	0.19 ± 0.07	0.974
Peak Propulsive Force (BW)	Walking	0.24 ± 0.03	0.21 ± 0.04	0.000*
	Running	0.22 ± 0.07	0.23 ± 0.05	0.754
Braking Impulse (BW%·s)	Walking	3.26 ± 0.80	2.90 ± 0.62	0.001*
	Running	1.61 ± 0.90	1.70 ± 0.50	0.459
Propulsive Impulse (BW%·s)	Walking	3.38 ± 0.47	2.94 ± 0.57	0.000*
	Running	1.92 ± 0.54	1.78 ± 0.58	0.112

3.3 Foot finite element analysis

3.3.1. Finite element model validation

Figure 20 illustrates the comparison of predicted pressure distribution against the plantar pressure data collected with the Footscan system. With a reference value of the PF stiffness, this FE model closely matched the experimentally measured plantar peak pressure in the forefoot area, with values of 0.168 MPa and 0.152 MPa, respectively. In the rearfoot area, the predicted peak pressure was approximately 0.219 MPa, while the experimental measurement yielded a value of 0.183 MPa.

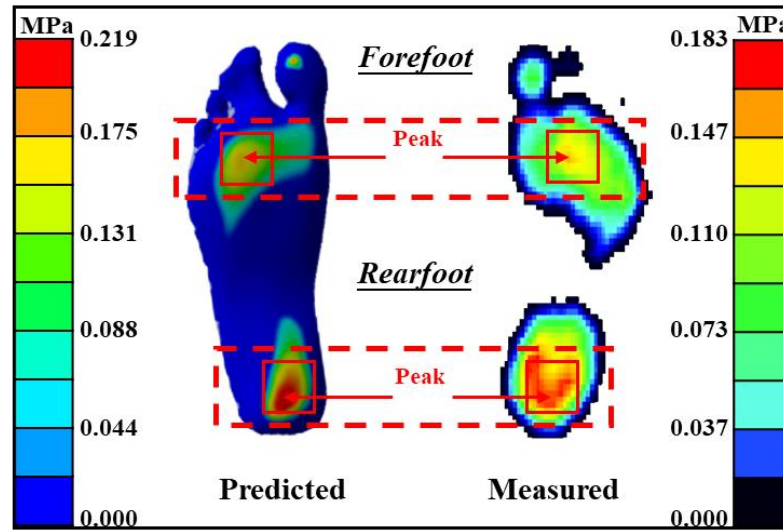


Figure 20 Comparison of FE predicted (left) and experimentally measured (right) peak pressure during balanced standing for model validation

3.3.2 Stress distribution

There was a general rise in the peak metatarsal stress as Young's modulus of PF increased, except for the M5 (**Figure 21**). With two folds of the reference value of 350 MPa, increases of 29.8%, 12.9%, 12.4%, and 11.5% from M1 to M4, and a decrease of 10.2% from M5, were predicted, respectively. Reducing Young's modulus of the PF to zero led to a significant decrease in peak stress in the M1 (27.3%), M3 (22.4%), and M4 (21.5%). Meanwhile, an increase of 19.4% was predicted in M1.

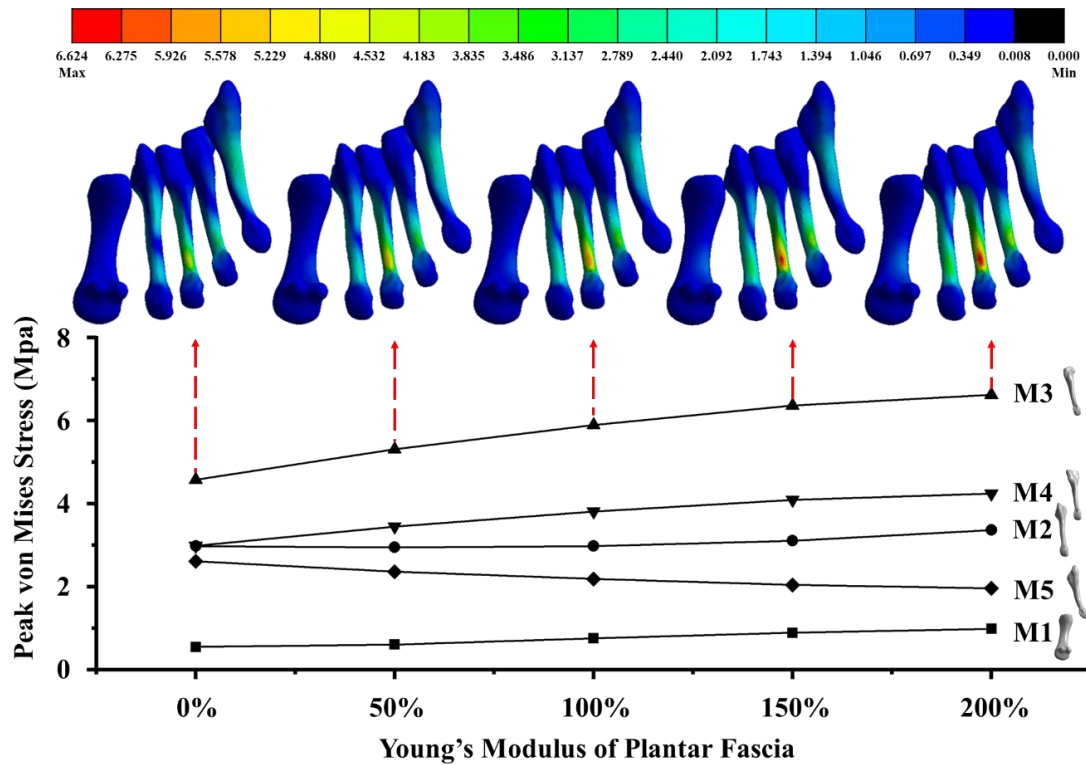


Figure 21 Effects of varying Young's modulus of the plantar fascia on peak von Mises stress of metatarsals

3.3.3 Force transmission

Figure 22 illustrates the force transmission through the MTP and TMT joints under different PF stiffnesses. There was a general increase in the joint contact forces as Young's modulus of PF increased. In terms of the magnitude of forces, the influence of Young's modulus of the PF on MTP joint contact mechanics is negligible compared to the TMT joint. Compared to the reference value of $E=350$ MPa, a 3% to 23% increase in force transmission through the TMT joint was predicted with twofold the reference value. And fasciotomy (Young's modulus of fascia, $E=0$ MPa) led to a pronounced decrease in force transmitted through the TMT joint ranging from 7% to 36%. Adjusting the PF stiffness to twice the reference value led to an increment of 83%, 59%, 36%, 116%, and 44% in the forces transmitted through the 1st to 5th MTP joints, respectively. Besides, with simulated fasciotomy, the predicted reductions in the forces transmitted through the 1st to 5th MTP joints were approximately 66%, 72%, 53%, and 67%, while the fifth MTP joint increased by about 23%.

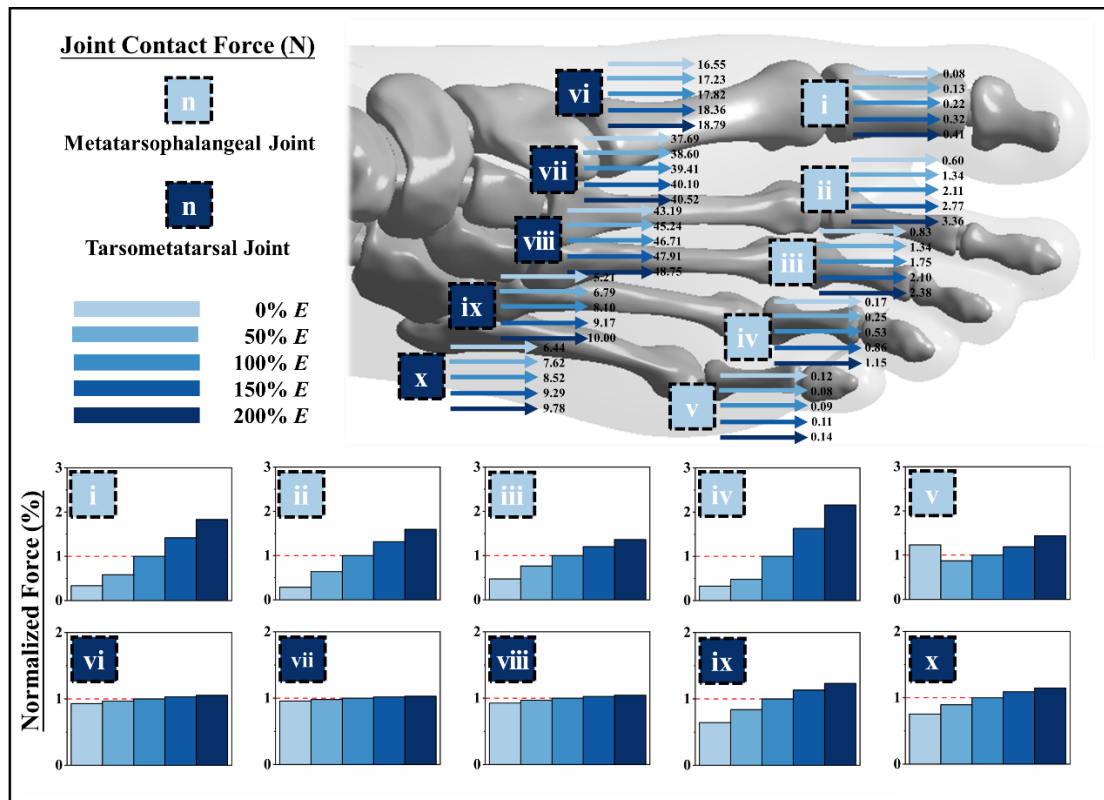


Figure 22 Effects of varying Young's modulus of the plantar fascia on changes in the force transmission through the metatarsophalangeal and tarsometatarsal joints

4 DISCUSSION

4.1 Foot-ankle temporal kinematics

The present study defined AS as the change in arch height in the sitting and standing conditions, standardized to 40% BW [15]. Although not a dynamic index, the AS is easily obtained and captures two phases of the foot load pattern (i.e., loading and unloading), thus indicating how the foot dynamically adapts to the load [9]. FAs tend to splay during the stance phase and shift the load from the midfoot to the forefoot and rearfoot concurrently along the longitudinal axis of the foot. However, other studies noted that FAs exhibited a greater percentage of overall plantar impulse in the hindfoot than that of SAs [9, 15]. The transfer of unilateral impulse on the foot longitudinal axis might be associated with the fact that, in the asymmetric and irregular triangular truss model formed by the PF and the arch bones, the shorter proximal side attached to the calcaneal tuberosities would suffer more impulses during arch compression [32, 33]. Considering the relationship between AS and arch height (i.e., the low arch tends to be more flexible, while the high arch is more likely to be stiffer), FAs may stretch the soft tissues to create enough moment for toe-off during gait, while SAs may be less flexible and lack shock absorption [26, 123].

Compared to steady-state gait, the arch receives an increase in the magnitude of load during GT, which can be inspected in the observable biomechanical parameters [15]. The experimental designs based on the GT model would allow for investigating the effect of morphological arch differences on foot-ankle biomechanics. As a multisegmental system, hip, knee, and ankle joint motion is associated with the lower limb kinetic chain; however, a previous study showed no significant effect of morphological differences in the foot arch on the kinematic compensation of proximal joints such as the hip and knee [3, 177]. The FA group had significantly greater MTP and ankle-joint angle periods than those of the SA group during the stance phase of GT, which is also supported by the results found in this study. FA exhibits a significantly increased ankle plantarflexion in the sagittal plane during the braking and transitional

phases of GT, while external rotation was significantly greater than that of SA during the transitional and stabilization phases. The elastic storage-return mechanism of the foot suggests that the human arch can compress when loaded, allowing for the storage of elastic strain energy [5]. The FA tends to splay along the longitudinal axis of the foot, resulting in the ankle joint exhibiting greater ROM (e.g., greater plantarflexion) in the sagittal plane during GT [3, 9]. The more significant ankle external rotation of FA may be related to the morphology and function of the medial and lateral longitudinal arches, i.e., the former is higher, softer, and more flexible [32]. With the lateral longitudinal arch acting as weight-bearing support, the foot tends to compress the MLA, resulting in external rotation of the ankle joint. Similarly, the present experiment found a significant main effect of AS for MTP angles in the transverse plane, i.e., FA exhibited a greater external rotation of the MTP joint than that of SA. No significant differences in MTP angles in the sagittal plane were found according to the results of SnPM. The potential reasons for this may be related to the fact that the ROM of the MTP joint is limited in the sagittal plane due to its anatomical structure, although it may be smaller in the frontal and transverse planes [3]. However, the MTP movement in the sagittal plane, especially dorsiflexion, is the key driver. The GT experiments designed in this study might have resulted in a significantly greater impact on the foot than that of a normal gait (e.g., walking and running) [15]. Therefore, during the stance phase of GT, both FA and SA present larger MTP dorsiflexion in a shorter termination time, approaching the maximal limit.

As a transitional motor task, GT involves the transition from cyclic gait to quiet standing, and experiments based on this transitional task can be designed to challenge both feedforward (i.e., PGT) and feedback neuromuscular control (i.e., UGT) [17, 37]. Compared with PGT, subjects had significantly smaller ankle plantarflexion angles, greater inversion angles during the braking phase of UGT, and significantly smaller external rotation angles during the transitional phase (40-52%). The stimulus delay period is critical because subjects must determine whether they receive an unexpected stimulus to perform the appropriate GT strategy. The stimulus delay period is crucial

since participants must determine whether they received an unexpected stimulus to execute the adequate GT strategy [178]. Once they capture the stopping indication during this phase, the body adopts a series of adjustments to create a net braking impulse via increasing the initial braking impulse and decreasing the push-off impulse during the braking phase [3, 39, 101]. The SOL amplitude activity could also be enhanced to moderate tibial progression, while the activity of the tibialis anterior and GM could be augmented to limit plantarflexion and maintain limb extension during the transitional phase. Given the change in foot balance associated with GT patterns, these kinematic alterations could also lead to gait imbalance and an increased risk of joint injury [160]. As an essential contributor to lower-limb energetics, MTP requires energy storage and creates little or no energy during braking and transitional phases [3, 12, 48]. Notably, significantly smaller MTP inversion and external rotation angles are exhibited during UGT during braking and transitional phases, which might be related to an integrated response concerning the MTP-ankle coordination pattern to compensate for increased ankle inversion [48, 178].

4.2 Inter-joint coupling coordination and ground reaction impulse

In the present study, I quantified discrepancies in lower limb inter-joint coordination and CVs as well as AP-GRIs in individuals with different AS during walking and running to demonstrate the coordination pattern variation associated with foot arch structure and the potential risk of injury. An optimized vector coding technique was employed to examine knee-hip, ankle-knee, and MTP-ankle coupling coordination on the sagittal plane with the hypothesis that the FA would exhibit a larger CV of selected inter-joint couplings and GRF in the AP direction during gait. In partial support of this hypothesis, subjects with flexible arches experienced a greater proportion of braking impulse and propulsive impulse during walking, while significant differences in CV between groups were found only for individual inter-joint coupling coordination of interest.

Inter-joint coordination mode analysis delivers insight into the timing and amplitude of segmental motion and represents the organization of multiple degrees of freedom into a more straightforward control strategy [19, 179]. During the mid-stance of walking, the knee-hip CAs of the two groups were significantly different. This suggested that while the participants moved both knees into flexion, FA tended to move the hip into extension compared to SA. Additionally, results for ankle dorsiflexion/plantarflexion-knee flexion/extension joint coordination angle demonstrated that subjects with stiffer arches showed a pattern indicating more knee flexion during the early stance of running. Inter-joint coordination on the sagittal plane, particularly in the early and middle stance phase of gait, is the main component of the lower extremity kinematic chain for load response [180]. After the initial contact with the ground, adjacent lower limb joints typically move in opposite directions to generate negative work to cushion the landing [179]. Thus, concerning previous findings that FA prefers to consider the lower extremity joints as a multi-segmental system for comprehensive integration of compensatory adjustments during stabilization, individuals with more flexible arches might employ impact attenuation strategies in gait to allow for greater compliance in the lower limbs [3, 181].

Understanding the inter-joint CV is essential to elucidate the mechanism by which abnormal gait patterns (deviation from the “normal” CV range) and the occurrence of injury [21]. Exceeding this safe range at the early stance phase may result in excessive ground force and poor soft tissue engagement [182, 183]. Results show significantly greater CVs of SA for both ankle-knee and MTP-ankle coordination during the early stance of running relative to FA. Considering previously explored relationships between segment CV and running injuries, I speculated that individuals with more flexible arches might adopt a conservative coordination strategy to maintain stability in response to the impacts of the lower extremities at initial contact[18]. Notably, when transitioning to the mid-stance phase, the CV of SA for the MTP-ankle coordination progressively decreased and was significantly smaller than that of the FA. This finding is interesting given previous work, where healthy individuals (with either stiff or

flexible arches) appear to compensate by controlling joint coupling CV within a safe range to ensure optimal load distribution to the lower extremities [18]. Previous studies have also demonstrated that if increased CVs on the sagittal plane occur as expected, they would trigger disaccustomed strains in the internal structures and aggravate the risk of injury [183].

The kinetical results further support the hypothesis that the proportion of total GRI in the AP direction would be greater in those with more flexible arches because of the propensity of FA to splay under load. While vertical forces are the largest component of the GRF, the AP-GRF is closely linked to the braking and propulsion processes of human gait, again concerning the spring mechanism of the MLA in gait involving mechanical energy conservation and propulsion mechanics [2, 184]. Compared with SA, FA exhibits greater peak braking and propulsive forces and impulse ratios during the stance phase of gait. Both active and passive structures support MLA function in resisting MLA deformation, while more flexible arches may experience more deformation during the stance phase of gait [29, 185]. During the stretch-shortening cycle, the midfoot could be allowed to remain rigid, thus resulting in an efficient transfer of mechanical output from the forefoot to the support surface [186]. Besides, the association between AS and ML-GRF distribution was demonstrated in a previous study that SA tended to experience a larger proportion of GRF in the ML direction [9]. Kinetics results of the present study may involve a combined integrative response of compensatory adjustments in impact loadings to compensate for changes in the proportion of GRI in the ML plane of motion and stabilize the foot. Furthermore, clarifying the influence of different MLA flexibilities on GRF continuity data in addition to the eigenvalue is also of great value in assessing injury risk. Based on the examination of the differences between the two groups on GRF waveforms by SPM1d analysis, I found that FA experienced a greater propulsive force during the later stance of walking (82-92%) and a greater braking force during the early stance of running (25-32%). This would suggest that the foot with a more flexible MLA enables better

utilization of the arch-spring mechanism to function as a stabilizer and a propeller in the early and late phases, respectively [2, 123].

4.3 Internal foot mechanics

Although the metatarsalgia has been previously established in relation to inadequate load distribution in the foot, detailed information on the internal mechanical of foot structures, particularly in the metatarsal region, is limited [127]. To quantify the parametric impact of varying PF stiffness on the load-bearing properties of the internal foot structures, a patient-specific foot computational model was reconstructed, which applies the exact geometry of foot bones and soft tissues. My findings supported the hypothesis that the peak metatarsal stress and joint contact forces reduced as Young's modulus of the PF decreased. Even though the biomechanical stress values generated may not represent the exact stress values experienced by all patients due to inter-subject variability, I could quantify the relative differences in each case.

Structurally, it is widely recognized that a decreased ground contact region in the midfoot is related to a higher load per unit area on the rearfoot and forefoot [45, 127]. This conclusion regarding potential risk factors for lower extremity overload injury is further supported by my validation results of the foot FE model. Additionally, I also found that the peak plantar pressures are concentrated in the middle forefoot and hindfoot. Burns et al. [127] suggested that this increase in peak pressure might be a kind of compensatory strategy for inadequate load-bearing beneath the midfoot. Furthermore, the M2 and M3 are anatomically wedged between the cuneiform joints, which results in their less freedom of motion and poor ability to disperse the loads they receive[45]. Such a pattern of plantar pressure distribution might be the source of metatarsalgia owing to musculoskeletal overloading and consequent soft tissue injury, or alternatively metatarsalgia might be the source of elevated plantar pressure through a modified antalgic loading distribution pattern [36, 127].

The current study further provided detailed information on the internal biomechanics of the foot through FE simulation. Generally, the bony structure characteristic changes

such as pes cavus may result in a heightened PF because of the underlying deformity, and the foot is typically stiffer and less capable of absorbing impact loads than a neutral foot [123]. During movement, if the PF is shortened, the fascia experiences excessive strain during the toe-off phase. Additionally, a tight Achilles tendon could enhance the effect of the windlass mechanism as the foot experiences early heel lift during gait leading to further PF strain[187]. Repeated straining and tearing of the PF may irritate and increase the risk of plantar fasciitis, further exacerbating primary metatarsalgia due to forefoot overload [22]. My FE simulations yielded similar predictions that peak stress of the metatarsals generally increases with increasing PF stiffness. The above results are also consistent with those observed by previous researchers in FE modeling of the foot[140]. As fascial stiffness decreases, metatarsal stresses tend to be relatively reduced. In the third metatarsal, for example, the peak metatarsal stress was reduced by approximately 22.4% after fasciotomy ($E=0$ MPa), demonstrating the role of the PF in relieving metatarsal stresses [173]. It should be noted that the M5 showed an opposite trend, i.e., the FE model predicted 1.96 and 2.61 MPa peak von Mises stress in this zone with Young's modulus of PF, $E = 700$ MPa and with fasciotomy ($E = 0$ MPa), corresponding to an increment of 33%. Considering the relative contribution of the PF to the maintenance of static equilibrium in the foot, a potential explanation for the increase in fifth metatarsal stress is a compensatory response to decreased stress in other metatarsals [124].

The foot deformities could destabilize the balance between joint mobility and stability and cause abnormal force transmission throughout the joint [188]. In this study, I quantified the changes in joint contact mechanics through the MTP and TMT joints by FE analysis to further understand its association with the biomechanical mechanisms of metatarsalgia. The simulated results of a general reduction in joint contact forces as Young's modulus of the PF decreases may be related to the fact that PF release leads to arch collapse, although previous studies have demonstrated that isolated PF failure rather than a combined failure of PF and ligaments (e.g., spring ligament and long and short plantar ligaments) does not lead to complete arch deformity [23, 145, 146].

Besides, Malakoutikhah et al. [146] also found that foot collapse resulted in increased contact pressure on the subtalar, calcaneocuboid, and tibiotalar, which could predispose these joints to chondral degeneration leading to the development of arthritis. Interestingly, even though all TMT joints presented increased contact forces after PF release ($E = 0$ MPa), the magnitude of change in the lateral TMT joint, represented by the 4th and 5th TMT joints, was significantly greater than that in the medial TMT joint (36% and 24% decrease compared to the reference values $E = 350$ MPa). This tendency for load transfer occurring over the TMT joint may be similar to the mechanism of fasciotomy accompanied by the midfoot pronation [140]. The concentration of joint contact forces in the central metatarsals following fasciotomy highlights the regions susceptible to stress failure. Even though focal forces associated with metatarsalgia could be relieved by adjusting PF stiffness, a previous study suggested that fatigue damage to the metatarsals may be accelerated due to the fact that the dorsal aspects of the medial metatarsals are normally loaded in compression, and the bending loads on these bones would be elevated after fascial release [173]. Therefore, when surgical procedures such as plantar fasciotomy are considered, a decrease in the abilities of load-bearing and shock-attenuation of the foot should be taken into account.

4.4 Limitations

There are some limitations of the present study that need to be acknowledged. Firstly, the relatively homogenous nature of the participants in this study, in order to alleviate gender- and age-related effects, might be a limiting factor in generalizing the current findings to a wider and more diverse population [26, 123]. Secondly, as an easily-acquired indirect metric, the AS predicts MLA deformation during dynamic loading by comparing the adaptation of the arch height between two different static load-bearing conditions. Concerns have been raised that static (complex foot anatomical factors) variables and dynamic (foot neuromuscular control during locomotion) variables may confound the results of the study [9, 181]. Thirdly, while the SnPM was effective in ANOVA for biomechanical data with time-varying characteristics, post hoc tests with Bonferroni correction might be relatively approximate and conservative [14]. Lastly, in

the current foot FE model, several considerations related to the balance between exact details and proper simplifications (i.e., computational cost) need to be attended to for the predicted results and further practical applications. In order to simplify the computational model, the foot-ankle complex was assigned homogeneous and linearly elastic material properties. Tension-only elements were employed to simulate the PF and main ligamentous structures, avoiding the transmission of unrealistic bending, twisting moments, and compressive forces [23, 142]. Only the loading on the Achilles tendon was simulated, while the forces exerted by other intrinsic and extrinsic muscles were not considered, which may not fully reflect the actual mechanobiological conditions. Additionally, the analysis focused on balanced standing, and future studies should encompass more complex load-bearing phases, requiring further dynamic FE analyses.

5 CONCLUSIONS AND FUTURE WORKS

Firstly, the present study provides insights into how individuals with SA or FA regulate foot-ankle kinematics during the stance phase of different GT patterns. Since a greater tendency to splay under loads, FA exhibited significantly larger MTP and ankle angles than those of SA during the stance phase of GT except in the MTP sagittal plane. During UGT induced by unknown stimuli, the lower extremity kinetic chain requires a comprehensive integration of the compensatory adjustment due to the increased urgency for the dynamic stability to be activated spontaneously. My work gave a new understanding of the regulations of foot-ankle temporal kinematics during gait subtasks and might be instructive to foot injury prediction and arch orthotics development.

Secondly, this study revealed that FA experienced significantly smaller CVs for ankle-knee and MTP-ankle coordination during the early stance and a greater proportion of GRFs in the AP direction. The present kinematic and kinetic results indicate that individuals with a flexible MLA tend to adopt a conservative coordination strategy that better functions as an arch stabilizer and propeller during the stretch-shortening cycle via the arch-spring mechanism. Given the current limitations of this study, subsequent studies involving a more diverse subject population and employing more precise foot indicators to characterize MLA flexibility and control for dynamic activity of the muscles and tendons are warranted.

Lastly, this subject-specific FE simulation was the first investigation of the biomechanical metatarsalgia etiology by quantifying the parametric implications of varying PF stiffness on the load-bearing properties of the internal structures. The important role of the PF in relieving focal metatarsal loading is further emphasized in the current study. In cases where surgical intervention such as fasciotomy is deemed necessary, it is crucial to carefully plan the procedures in order to minimize any potential impact on the structural integrity of the foot as well as its load-bearing and shock-attenuation abilities. This knowledge is crucial for improving current methods of relieving metatarsalgia and surgical treatments for pes cavus, as well as optimizing the design of foot orthotics and footwear.

NEW SCIENTIFIC THESIS POINTS

1st Thesis point

*I compared foot-ankle temporal kinematics characteristics during PGT and UGT in subjects with different ASs based on the SnPM method (**Figure 23**). By measuring three-dimensional arch morphological parameters under different loading conditions, subjects were classified and participated in GT tests to collect MTP and ankle joint kinematics data. The results show that joint angles (MTP and ankle joints) were altered owing to AS and GT factors. These results add additional insights into the morphological arch biomechanical function and the comprehensive compensatory adjustment of lower-limb joints during gait stopping caused by unplanned stimulation.*

*As shown in **Figure 23**, FA exhibits a significantly increased ankle plantarflexion in the sagittal plane during the braking and transitional phases of GT, while external rotation was significantly greater than that of SA during the transitional and stabilization phases. With the lateral longitudinal arch acting as weight-bearing support, the foot tends to compress the MLA, resulting in external rotation of the ankle joint. Similarly, the present experiment found a significant main effect of AS for MTP angles in the transverse plane, i.e., FA exhibited a greater external rotation of the MTP joint than that of SA.*

*Compared with PGT, subjects had significantly smaller ankle plantarflexion angles, greater inversion angles during the braking phase of UGT, and significantly smaller external rotation angles during the transitional phase (**Figure 23**). Given the change in foot balance associated with GT patterns, these kinematic alterations could also lead to gait imbalance and an increased risk of joint injury. Notably, significantly smaller MTP inversion and external rotation angles are exhibited during UGT during braking and transitional phases, which might be related to an integrated response concerning the MTP-ankle coordination pattern to compensate for increased ankle inversion.*

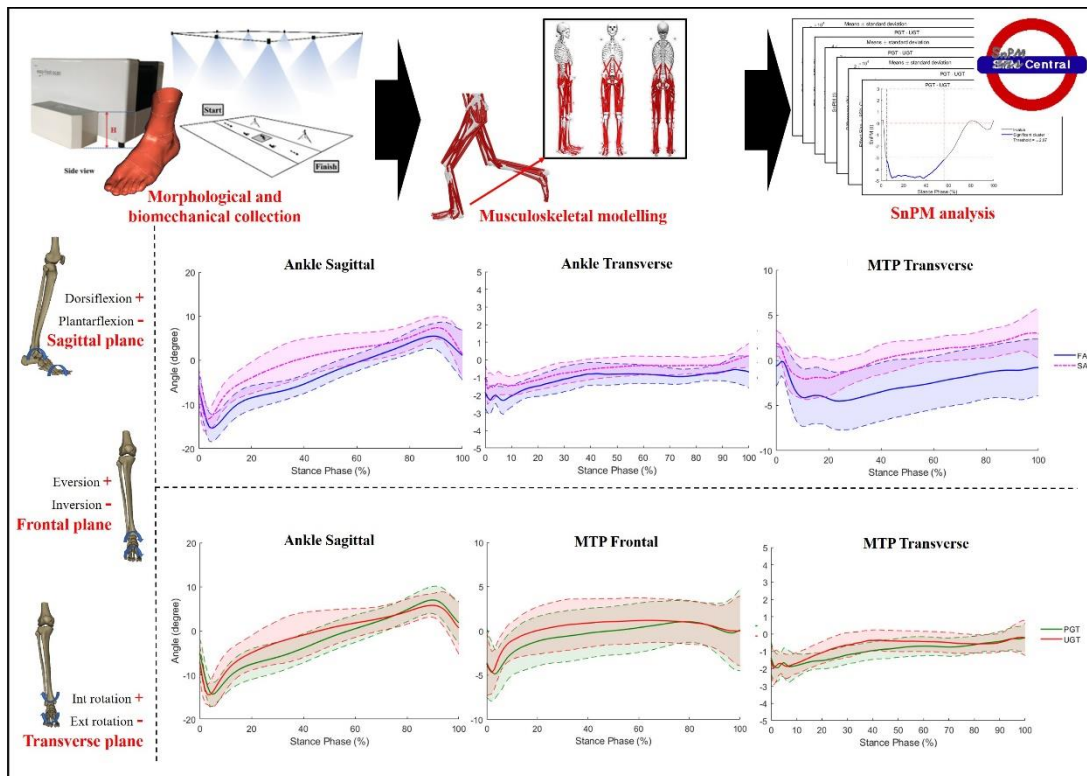


Figure 23 The effect of arch stiffness on the foot-ankle temporal kinematics during gait termination

Related articles to the first thesis point:

1. **Cen, X.**, Yu, P., Song, Y., Sárosi, J., Mao, Z., Bíró, I., & Gu, Y. (2022). The Effect of Arch Stiffness on The Foot–Ankle Temporal Kinematics during Gait Termination: A Statistical Nonparametric Mapping Study. *Bioengineering*, 9(11), 703.
2. **Cen, X.**, Lu, Z., Baker, J. S., István, B., & Gu, Y. (2021). A Comparative Biomechanical Analysis during Planned and Unplanned Gait Termination in Individuals with Different Arch Stiffnesses. *Applied Sciences*, 11(4), 1871.

2nd Thesis point

A causal link exists between structural differences in the foot and alterations in the lower limb biomechanics, which might predispose an individual to develop characteristic musculoskeletal disorders. In this study, I investigated how the foot structural characteristics, as represented by the AS, affect lower limb joint coupling coordination and AP-GRIs during walking and running. Inter-joint coordination and variability were calculated from the angle-angle plots of knee-hip, ankle-knee, and MTP-ankle couplings based on an optimized vector coding technique (Figure 24).

The results indicate that coupling coordination of interest and its variability, as well as AP-GRIs, could potentially be influenced due to differences in arch height flexibility. Notably, the individuals with stiff arches exhibited significantly greater CVs during the early stance for both ankle-knee and MTP-ankle coordination yet significantly smaller for MTP-ankle CVs during the mid-stance phase. Furthermore, combining the SPM analysis results, the flexible arches experienced a greater proportion of GRIs in the AP direction.

These observations demonstrated that individuals with a flexible arch tend to adopt a conservative coordination strategy that better functions as an arch stabilizer and propeller during the stretch-shortening cycle via the arch-spring mechanism.

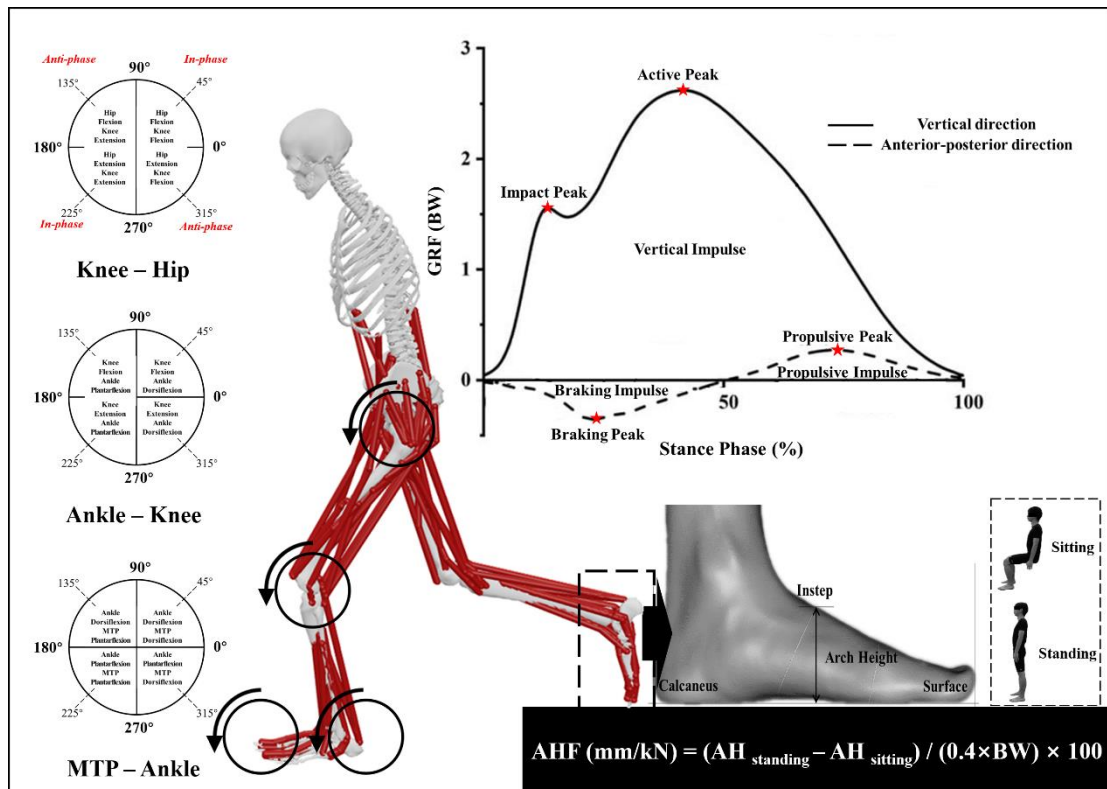


Figure 24 The proposed experimental protocol regarding arch stiffness, lower limb joint coupling coordination, and ground reaction impulse

Related articles to the second thesis point:

1. **Cen, X.**, Gao, L., Yang, M., Liang, M., Bíró, I., & Gu, Y. (2021). Arch-Support Induced Changes in Foot-Ankle Coordination in Young Males with Flatfoot during Unplanned Gait Termination. *Journal of Clinical Medicine*, 10(23), 5539.

3rd Thesis point

I reconstructed a subject-specific FE model of the foot-ankle complex using the actual three-dimensional geometry of foot bones and soft tissues (Figure 25). A sensitivity study was conducted to evaluate the effects of varying elastic modulus (0-700 MPa) of the PF on the metatarsal stress distribution and force transmission. The conclusion regarding potential risk factors for lower extremity overload injury is further supported by my validation results of the foot FE model. Additionally, I also found that the peak plantar pressures are concentrated in the middle forefoot and hindfoot, which might be a kind of compensatory strategy for inadequate load-bearing beneath the midfoot. Such a pattern of plantar pressure distribution might be the source of metatarsalgia owing to musculoskeletal overloading and consequent soft tissue injury, or alternatively, metatarsalgia might be the source of elevated plantar pressure through a modified antalgic loading distribution pattern.

Repeated straining and tearing of the PF may irritate and increase the risk of plantar fasciitis, further exacerbating primary metatarsalgia due to forefoot overload. My FE simulations yielded similar predictions that peak stress of the metatarsals generally increases with increasing PF stiffness (Figure 25). I also quantified the changes in joint contact mechanics through the MTP and TMT joints by FE analysis to further understand its association with the biomechanical mechanisms of metatarsalgia. The simulated results of a general reduction in joint contact forces as Young's modulus of the PF decreases may be related to the fact that PF release leads to arch collapse. Even though focal forces associated with metatarsalgia could be relieved by adjusting PF stiffness, fatigue damage to the metatarsals may be accelerated due to the fact that the dorsal aspects of the medial metatarsals are normally loaded in compression, and the bending loads on these bones would be elevated after fascial release. Therefore, when surgical procedures such as plantar fasciotomy are considered, a decrease in the abilities of load-bearing and shock-attenuation of the pes cavus should be taken into account.

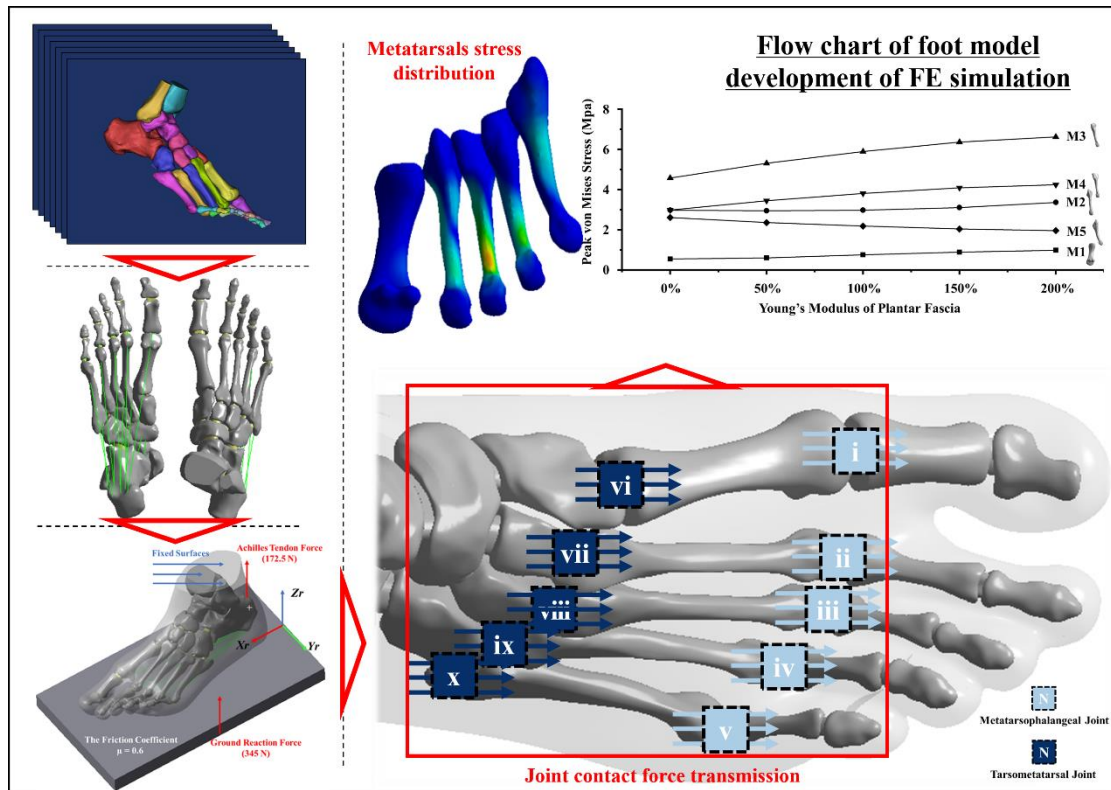


Figure 25 Flow chart of foot model development of FE simulation

Related articles to the third thesis point:

1. **Cen, X.**, Song, Y., Sun, D., Bíró, I., & Gu, Y. (2023). Applications of Finite Element Modeling in Biomechanical Analysis of Foot Arch Deformation: A Scoping Review. *Journal of Biomechanical Engineering*, 145(7), 070801.
2. Song, Y., **Cen, X.**, Chen, H., Sun, D., Munivrana, G., Bálint, K., Bíró, I., & Gu, Y. (2023). The Influence of Running Shoe with Different Carbon-Fiber Plate Designs on Internal Foot Mechanics: A Pilot Computational Analysis. *Journal of Biomechanics*, 153, 111597.

LIST OF PUBLICATIONS

1. **Cen, X.**, Song, Y., Sun, D., Bíró, I., & Gu, Y. (2023). Applications of finite element modeling in biomechanical analysis of foot arch deformation: a scoping review. *Journal of Biomechanical Engineering*, 145(7), 070801.
2. **Cen, X.**, Sun, D., Rong, M., Fekete, G., Baker, J. S., Song, Y., & Gu, Y. (2020). The online education mode and reopening plans for Chinese schools during the COVID-19 pandemic: a mini review. *Frontiers in Public Health*, 8, 566316.
3. **Cen, X.**, Gao, L., Yang, M., Liang, M., Bíró, I., & Gu, Y. (2021). Arch-support induced changes in foot-ankle coordination in young males with flatfoot during unplanned gait termination. *Journal of Clinical Medicine*, 10(23), 5539.
4. **Cen, X.**, Yu, P., Song, Y., Sárosi, J., Mao, Z., Bíró, I., & Gu, Y. (2022). The effect of arch stiffness on the foot-ankle temporal kinematics during gait termination: a statistical nonparametric mapping study. *Bioengineering*, 9(11), 703.
5. **Cen, X.**, Lu, Z., Baker, J. S., István, B., & Gu, Y. (2021). A comparative biomechanical analysis during planned and unplanned gait termination in individuals with different arch stiffnesses. *Applied Sciences*, 11(4), 1871.
6. **Cen, X.**, Xu, D., Baker, J. S., & Gu, Y. (2020). Effect of additional body weight on arch index and dynamic plantar pressure distribution during walking and gait termination. *PeerJ*, 8, e8998.
7. **Cen, X.**, Xu, D., Baker, J. S., & Gu, Y. (2020). Association of arch stiffness with plantar impulse distribution during walking, running, and gait termination. *International Journal of Environmental Research and Public Health*, 17(6), 2090.
8. **Cen, X.**, Jiang, X., & Gu, Y. (2019). Do different muscle strength levels affect stability during unplanned gait termination?. *Acta of Bioengineering and Biomechanics*, 21(4), 27-35.
9. **Cen, X.**, Liang, Z., Gao, Z., Lian, W., & Wang, Z. (2019). The influence of the

- improvement of calf strength on barefoot loading. *Journal of Biomimetics, Biomaterials and Biomedical Engineering*, 40, 16-25.
10. **Cen, X.**, Li, K., Sun, D., Zhao, L., & Gu, Y. (2020). Research on the application of trackless digital technology in the starting movement specialized training of para snowboard. *China Sport Science and Technology*, 56(12), 83-87. (In Chinese)
 11. **Cen, X.**, & Bíró, I. (2022). Predicting center of pressure velocity based on regional plantar force in elderly men using artificial neural networks. In 2022 2nd International Conference on Bioinformatics and Intelligent Computing (ICBIC 2022) (pp. 114-118).
 12. **Cen, X.**, Biro, I., & Gu, Y. (2022) Impacts of different arch stiffness on lower extremity joint kinematics during unexpected gait termination. In 2022 International Conference on Intelligent Medicine and Health (ICIMH 2022) (pp. 14-18).
 13. **Cen, X.**, Song, Y., & Bíró, I. (2023) One-dimensional statistical parametric mapping identifies plantar regional loading differences related to medial longitudinal arch stiffness. In 2023 4th IEEE International Conference on Computer Engineering and Application (ICCEA 2023) (pp. 490-493).
 14. **Cen, X.**, Sun, D., Bíró, I., & Gu, Y. (2021). A pilot study of the effect of arch stiffness on lower limb joint kinematics during unexpected gait termination. *Osteoporosis International*, 32(S1), S306-S307.
 15. Song, Y., **Cen, X.**, Chen, H., Sun, D., Munivrana, G., Bálint, K., Bíró, I., & Gu, Y. (2023). The influence of running shoe with different carbon-fiber plate designs on internal foot mechanics: a pilot computational analysis. *Journal of Biomechanics*, 153, 111597.
 16. Yu, P., **Cen, X.**, Xiang, L., Mei, Q., Wang, A., Gu, Y., & Fernandez, J. (2023). Regional plantar forces and surface geometry variations of a chronic ankle instability population described by statistical shape modelling. *Gait & Posture*, 106,

11-17.

17. Shen, X. A., **Cen, X.***, & Song, Y. (2022). Investigating temporal kinematic differences caused by unexpected stimulation during gait termination through the waveform-level variance equality test. *BioMed Research International*, 2022, 4043426.
18. Xu, D., **Cen, X.**, Wang, M., Rong, M., István, B., Baker, J. S., & Gu, Y. (2020). Temporal kinematic differences between forward and backward jump-landing. *International Journal of Environmental Research and Public Health*, 17(18), 6669.
19. Song, Y., **Cen, X.**, Zhang, Y., Bíró, I., Ji, Y., & Gu, Y. (2022). Development and validation of a subject-specific coupled model for foot and sports shoe complex: a pilot computational study. *Bioengineering*, 9(10), 553.
20. Zhou, H., **Cen, X.**, Song, Y., Ugbolue, U. C., & Gu, Y. (2020). Lower-limb biomechanical characteristics associated with unplanned gait termination under different walking speeds. *Journal of Visualized Experiments*, (162), e61558.
21. Ying, J., **Cen, X.**, & Yu, P. (2021). Effects of eccentric exercise on skeletal muscle injury: from an ultrastructure aspect: a review. *Physical Activity and Health*, 5(1), 15-20.
22. Liang, Z., **Cen, X.**, Lin, C., Gao, Z., Sun, D., Li, J., & Gu, Y. (2021). Review on the research of sports training, sports monitoring and medical monitoring in bobsleigh/skeleton events. *China Sport Science and Technology*, 57(09), 3-10. (In Chinese)
23. Sun, D., Song, Y., **Cen, X.**, Wang, M., Baker, J. S., & Gu, Y. (2022). Workflow assessing the effect of Achilles tendon rupture on gait function and metatarsal stress: combined musculoskeletal modeling and finite element analysis. *Proceedings of the Institution of Mechanical Engineers, Part H: Journal of Engineering in Medicine*, 236(5), 676-685.
24. Tong, J., Lu, Z., **Cen, X.**, Chen, C., Ugbolue, U. C., & Gu, Y. (2023). The effects of

- ankle dorsiflexor fatigue on lower limb biomechanics during badminton forward forehand and backhand lunge. *Frontiers in Bioengineering and Biotechnology*, 11, 1013100.
25. Fan, H., Song, Y., **Cen, X.**, Yu, P., B  r  , I., & Gu, Y. (2021). The effect of repetitive transcranial magnetic stimulation on lower-limb motor ability in stroke patients: a systematic review. *Frontiers in Human Neuroscience*, 15, 620573.
 26. Li, X., Lu, Z., **Cen, X.**, Zhou, Y., Xuan, R., Sun, D., & Gu, Y. (2023). Effect of pregnancy on female gait characteristics: a pilot study based on portable gait analyzer and induced acceleration analysis. *Frontiers in Physiology*, 14, 706.
 27. Chang, H., Song, Y., & **Cen, X.** (2022). Effectiveness of augmented reality for lower limb rehabilitation: a systematic review. *Applied Bionics and Biomechanics*, 2022, 4047845.
 28. Lin, S., Song, Y., **Cen, X.**, B  lint, K., Fekete, G., & Sun, D. (2022). The implications of sports biomechanics studies on the research and development of running shoes: a systematic review. *Bioengineering*, 9(10), 497.
 29. Lin, Y., Lu, Z., **Cen, X.**, Thirupathi, A., Sun, D., & Gu, Y. (2022). The influence of different rope jumping methods on adolescents' lower limb biomechanics during the ground-contact phase. *Children*, 9(5), 721.
 30. Shao, E., Lu, Z., **Cen, X.**, Zheng, Z., Sun, D., & Gu, Y. (2022). The effect of fatigue on lower limb joint stiffness at different walking speeds. *Diagnostics*, 12(6), 1470.
 31. Xu, D., Jiang, X., **Cen, X.**, Baker, J. S., & Gu, Y. (2020). Single-leg landings following a volleyball spike may increase the risk of anterior cruciate ligament injury more than landing on both-legs. *Applied Sciences*, 11(1), 130.
 32. Li, F., Song, Y., **Cen, X.**, Sun, D., Lu, Z., B  r  , I., & Gu, Y. (2023). Comparative efficacy of vibration foam rolling and cold water immersion in amateur basketball players after a simulated load of basketball game. *Healthcare*, 11(15), 2178.

33. Song, Y., Sárosi, J., **Cen, X.**, & Bíró, I. (2023). Human motion analysis and measurement techniques: current application and developing trend. *Analecta Technica Szegedinensia*, 17(2), 48-58.

34. Sun, D., Song, Y., **Cen, X.**, Sheng, B., Gu, Y. (2021). Research progress of computer vision-based markerless sports motion capture technology. *Journal of Shanghai University of Sport*, 45(09), 70-85. (In Chinese)

35. Song, Y., Sun, D., **Cen, X.**, Bíró, I., & Gu, Y. (2022). Subject-specific finite element modelling of the foot-shoe complex and its application in metatarsal stress research. *Chinese Journal of Applied Mechanics*, 2022, 1-10. (In Chinese)

36. He, Y., Shao, S., Fekete, G., Yang, X., **Cen, X.**, Song, Y., Sun, D., & Gu, Y. (2022). Lower limb muscle forces in table tennis footwork during topspin forehand stroke based on the Opensim musculoskeletal model: a pilot study. *Molecular & Cellular Biomechanics*, 19(4), 221-235.

REFERENCE

- [1] Ker RF, Bennett MB, Bibby SR, et al. The spring in the arch of the human foot. *Nature*. 1987;325:147-149.
- [2] Welte L, Kelly LA, Lichtwark GA, et al. Influence of the windlass mechanism on arch-spring mechanics during dynamic foot arch deformation. *Journal of The Royal Society Interface*. 2018;15:20180270.
- [3] Cen X, Lu Z, Baker JS, et al. A comparative biomechanical analysis during planned and unplanned gait termination in individuals with different arch stiffnesses. *Applied Sciences*. 2021;11:1871.
- [4] Bolgla LA, Malone TR. Plantar fasciitis and the windlass mechanism: a biomechanical link to clinical practice. *Journal of athletic training*. 2004;39:77.
- [5] McDonald KA, Stearne SM, Alderson JA, et al. The role of arch compression and metatarsophalangeal joint dynamics in modulating plantar fascia strain in running. *PLOS ONE*. 2016;11:e0152602.
- [6] Tong JWK, Kong PW. Association between foot type and lower extremity injuries: systematic literature review with meta-analysis. *Journal of Orthopaedic & Sports Physical Therapy*. 2013;43:700-714.
- [7] Powell DW, Long B, Milner CE, et al. Frontal plane multi-segment foot kinematics in high- and low-arched females during dynamic loading tasks. *Human Movement Science*. 2011;30:105-114.
- [8] Shiroshita T. Relationship between the medial longitudinal arch, foot dorsiflexion range of motion, and dynamic gait parameters. *Annals of Physical and Rehabilitation Medicine*. 2018;61:e444-e445.
- [9] Zifchock R, Parker R, Wan W, et al. The relationship between foot arch flexibility and medial-lateral ground reaction force distribution. *Gait & Posture*. 2019;69:46-49.

- [10] Williams DS, McClay IS, Hamill J, et al. Lower extremity kinematic and kinetic differences in runners with high and low arches. *Journal of Applied Biomechanics*. 2001;17:153-163.
- [11] Pataky TC, Vanrenterghem J, Robinson MA. The probability of false positives in zero-dimensional analyses of one-dimensional kinematic, force and EMG trajectories. *Journal of Biomechanics*. 2016;49:1468-1476.
- [12] Robinson MA, Vanrenterghem J, Pataky TC. Statistical Parametric Mapping (SPM) for alpha-based statistical analyses of multi-muscle EMG time-series. *Journal of Electromyography and Kinesiology*. 2015;25:14-19.
- [13] Goudriaan M, Van den Hauwe M, Simon-Martinez C, et al. Gait deviations in Duchenne muscular dystrophy—Part 2. Statistical non-parametric mapping to analyze gait deviations in children with Duchenne muscular dystrophy. *Gait & Posture*. 2018;63:159-164.
- [14] Yu P, He Y, Gu Y, et al. Acute effects of heel-to-toe drop and speed on running biomechanics and strike pattern in male recreational runners: application of statistical nonparametric mapping in lower limb biomechanics. *Frontiers in Bioengineering and Biotechnology*. 2022;9:821530.
- [15] Cen X, Xu D, Baker JS, et al. Association of arch stiffness with plantar impulse distribution during walking, running, and gait termination. *International Journal of Environmental Research and Public Health*. 2020;17:2090.
- [16] Roeing KL, Wajda DA, Motl RW, et al. Gait termination in individuals with multiple sclerosis. *Gait & Posture*. 2015;42:335-339.
- [17] Wikstrom EA, Bishop MD, Inamdar AD, et al. Gait termination control strategies are altered in chronic ankle instability subjects. *Medicine & Science in Sports & Exercise*. 2010;42:197-205.
- [18] Chen TL-W, Wong DW-C, Wang Y, et al. Changes in segment coordination variability and the impacts of the lower limb across running mileages in half marathons:

Implications for running injuries. *Journal of Sport and Health Science*. 2022;11:67-74.

[19] Chang R, Van Emmerik R, Hamill J. Quantifying rearfoot–forefoot coordination in human walking. *Journal of Biomechanics*. 2008;41:3101-3105.

[20] Nawoczenski DA, Saltzman CL, Cook TM. The effect of foot structure on the three-dimensional kinematic coupling behavior of the leg and rear foot. *Physical Therapy*. 1998;78:404-416.

[21] Jafarnezhadgero A, Mousavi SH, Madadi-Shad M, et al. Quantifying lower limb inter-joint coordination and coordination variability after four-month wearing arch support foot orthoses in children with flexible flat feet. *Human Movement Science*. 2020;70:102593.

[22] Bardelli M, Turelli L, Scoccianti G. Definition and classification of metatarsalgia. *Foot and Ankle Surgery*. 2003;9:79-85.

[23] Cen X, Song Y, Sun D, et al. Applications of finite element modeling in biomechanical analysis of foot arch deformation: A scoping review. *Journal of Biomechanical Engineering*. 2023;145:070801.

[24] Song Y, Cen X, Chen H, et al. The influence of running shoe with different carbon-fiber plate designs on internal foot mechanics: A pilot computational analysis. *Journal of Biomechanics*. 2023;153:111597.

[25] Donatelli R. Normal biomechanics of the foot and ankle. *Journal of Orthopaedic & Sports Physical Therapy*. 1985;7:91-95.

[26] Zifchock RA, Davis I, Hillstrom H, et al. The effect of gender, age, and lateral dominance on arch height and arch stiffness. *Foot & Ankle International*. 2006;27:367-372.

[27] Sun P-C, Shih S-L, Chen Y-L, et al. Biomechanical analysis of foot with different foot arch heights: a finite element analysis. *Computer Methods in Biomechanics and Biomedical Engineering*. 2012;15:563-569.

- [28] Kelly LA, Cresswell AG, Racinais S, et al. Intrinsic foot muscles have the capacity to control deformation of the longitudinal arch. *Journal of The Royal Society Interface*. 2014;11:20131188.
- [29] McKeon PO, Hertel J, Bramble D, et al. The foot core system: a new paradigm for understanding intrinsic foot muscle function. *British Journal of Sports Medicine*. 2015;49:290.
- [30] Mann RA, Hagy JL. The function of the toes in walking, jogging and running. *Clinical Orthopaedics and Related Research*. 1979;24-29.
- [31] López-López D, Becerro-de-Bengoa-Vallejo R, Losa-Iglesias ME, et al. Evaluation of foot health related quality of life in individuals with foot problems by gender: a cross-sectional comparative analysis study. *BMJ Open*. 2018;8:e023980.
- [32] Dawe EJC, Davis J. (vi) Anatomy and biomechanics of the foot and ankle. *Orthopaedics and Trauma*. 2011;25:279-286.
- [33] Sarrafian SK. Functional characteristics of the foot and plantar aponeurosis under tibiotalar loading. *Foot & Ankle*. 1987;8:4-18.
- [34] Lynn SK, Padilla RA, Tsang KKW. Differences in static- and dynamic-balance task performance after 4 weeks of intrinsic-foot-muscle training: the short-foot exercise versus the towel-curl exercise. *Journal of Sport Rehabilitation*. 2012;21:327-333.
- [35] Kruger KM, Graf A, Flanagan A, et al. Segmental foot and ankle kinematic differences between rectus, planus, and cavus foot types. *Journal of Biomechanics*. 2019;94:180-186.
- [36] Cen X, Xu D, Baker JS, et al. Effect of additional body weight on arch index and dynamic plantar pressure distribution during walking and gait termination. *PeerJ*. 2020;8:e8998.
- [37] Sparrow W, Tirosh O. Gait termination: a review of experimental methods and the effects of ageing and gait pathologies. *Gait & Posture*. 2005;22:362-371.

- [38] Bishop MD, Brunt D, Pathare N, et al. The interaction between leading and trailing limbs during stopping in humans. *Neuroscience letters*. 2002;323:1-4.
- [39] Jaeger RJ, Vanitchatchavan P. Ground reaction forces during termination of human gait. *Journal of Biomechanics*. 1992;25:1233-1236.
- [40] Williams Iii DS, McClay IS, Hamill J. Arch structure and injury patterns in runners. *Clinical Biomechanics*. 2001;16:341-347.
- [41] Chuckpaiwong B, Nunley JA, Mall NA, et al. The effect of foot type on in-shoe plantar pressure during walking and running. *Gait & Posture*. 2008;28:405-411.
- [42] Williams DS, McClay IS. Measurements used to characterize the foot and the medial longitudinal arch: reliability and validity. *Physical Therapy*. 2000;80:864-871.
- [43] Boyer ER, Ward ED, Derrick TR. Medial longitudinal arch mechanics before and after a 45-minute run. *Journal of the American Podiatric Medical Association*. 2014;104:349-356.
- [44] Zifchock RA, Theriot C, Hillstrom HJ, et al. The relationship between arch height and arch flexibility: A proposed arch flexibility classification system for the description of multidimensional foot structure. *Journal of the American Podiatric Medical Association*. 2017;107:119-123.
- [45] Fernández-Seguín LM, Diaz Mancha JA, Sánchez Rodríguez R, et al. Comparison of plantar pressures and contact area between normal and cavus foot. *Gait & Posture*. 2014;39:789-792.
- [46] Burns J, Crosbie J, Ouvrier R, et al. Effective orthotic therapy for the painful cavus foot: A randomized controlled trial. *Journal of the American Podiatric Medical Association*. 2006;96:205-211.
- [47] Aminian A, Sangeorzan BJ. The anatomy of cavus foot deformity. *Foot and Ankle Clinics*. 2008;13:191-198.
- [48] Cen X, Gao L, Yang M, et al. Arch-support induced changes in foot-ankle

coordination in young males with flatfoot during unplanned gait termination. *Journal of Clinical Medicine*. 2021;10:5539.

[49] Richie DH. Biomechanics and clinical analysis of the adult acquired flatfoot. *Clinics in Podiatric Medicine and Surgery*. 2007;24:617-644.

[50] Dubbeldam R, Nester C, Nene AV, et al. Kinematic coupling relationships exist between non-adjacent segments of the foot and ankle of healthy subjects. *Gait & Posture*. 2013;37:159-164.

[51] Canseco K, Long J, Marks R, et al. Quantitative characterization of gait kinematics in patients with hallux rigidus using the Milwaukee foot model. *Journal of Orthopaedic Research*. 2008;26:419-427.

[52] Kawakami W, Iwamoto Y, Takeuchi Y, et al. Young females with hallux valgus show lower foot joint movement stability compared to controls: An investigation of coordination patterns and variability. *Clinical Biomechanics*. 2022;94:105624.

[53] DeLeo AT, Dierks TA, Ferber R, et al. Lower extremity joint coupling during running: a current update. *Clinical Biomechanics*. 2004;19:983-991.

[54] Eslami M, Begon M, Farahpour N, et al. Forefoot–rearfoot coupling patterns and tibial internal rotation during stance phase of barefoot versus shod running. *Clinical Biomechanics*. 2007;22:74-80.

[55] Nigg BM, Cole GK, Nachbauer W. Effects of arch height of the foot on angular motion of the lower extremities in running. *Journal of Biomechanics*. 1993;26:909-916.

[56] Hamill J, van Emmerik REA, Heiderscheit BC, et al. A dynamical systems approach to lower extremity running injuries. *Clinical Biomechanics*. 1999;14:297-308.

[57] Stergiou N, Jensen JL, Bates BT, et al. A dynamical systems investigation of lower extremity coordination during running over obstacles. *Clinical Biomechanics*. 2001;16:213-221.

[58] Li L, van den Bogert ECH, Caldwell GE, et al. Coordination patterns of walking

and running at similar speed and stride frequency. *Human Movement Science*. 1999;18:67-85.

[59] Trezise J, Bartlett R, Bussey M. Coordination variability changes with fatigue in sprinters. *International Journal of Sports Science & Coaching*. 2011;6:357-363.

[60] Seay JF, Van Emmerik REA, Hamill J. Influence of low back pain status on pelvis-trunk coordination during walking and running. *Spine*. 2011;36:E1070-E1079.

[61] Cappozzo A. Gait analysis methodology. *Human Movement Science*. 1984;3:27-50.

[62] Fukuchi CA, Fukuchi RK, Duarte M. Effects of walking speed on gait biomechanics in healthy participants: a systematic review and meta-analysis. *Systematic Reviews*. 2019;8:153.

[63] Whittle MW. Clinical gait analysis: A review. *Human Movement Science*. 1996;15:369-387.

[64] Chan CW, Rudins A. Foot biomechanics during walking and running. *Mayo Clinic Proceedings*. 1994;69:448-461.

[65] Moe-Nilssen R, Helbostad JL. Spatiotemporal gait parameters for older adults – An interactive model adjusting reference data for gender, age, and body height. *Gait & Posture*. 2020;82:220-226.

[66] Park YS, Kim J-W, Kwon Y, et al. Effect of age and sex on gait characteristics in the Korean elderly people. *Iranian journal of public health*. 2018;47:666-673.

[67] Stephan Y, Sutin AR, Terracciano A. “Feeling younger, walking faster”: subjective age and walking speed in older adults. *AGE*. 2015;37:86.

[68] Sittichoke C, Buasord J, Boripuntakul S, et al. Effects of compliant flooring on dynamic balance and gait characteristics of community-dwelling older persons. *The journal of nutrition, health & aging*. 2019;23:665-668.

[69] Scaglioni-Solano P, Aragón-Vargas LF. Gait characteristics and sensory abilities

of older adults are modulated by gender. *Gait & Posture*. 2015;42:54-59.

[70] Rowe E, Beauchamp MK, Astephen Wilson J. Age and sex differences in normative gait patterns. *Gait & Posture*. 2021;88:109-115.

[71] Kennedy PM, Inglis JT. Distribution and behaviour of glabrous cutaneous receptors in the human foot sole. *The Journal of Physiology*. 2002;538:995-1002.

[72] Trinkaus E. Anatomical evidence for the antiquity of human footwear use. *Journal of Archaeological Science*. 2005;32:1515-1526.

[73] Trinkaus E, Shang H. Anatomical evidence for the antiquity of human footwear: Tianyuan and Sunghir. *Journal of Archaeological Science*. 2008;35:1928-1933.

[74] Sinclair J, Atkins S, Taylor PJ. The effects of barefoot and shod running on limb and joint stiffness characteristics in recreational runners. *Journal of Motor Behavior*. 2016;48:79-85.

[75] Rao U, Joseph B. The influence of footwear on the prevalence of flat foot. A survey of 2300 children. *The Journal of Bone & Joint Surgery British Volume*. 1992;74-B:525-527.

[76] Cronin NJ, Barrett RS, Carty CP. Long-term use of high-heeled shoes alters the neuromechanics of human walking. *Journal of Applied Physiology*. 2012;112:1054-1058.

[77] Wolf S, Simon J, Patikas D, et al. Foot motion in children shoes—A comparison of barefoot walking with shod walking in conventional and flexible shoes. *Gait & Posture*. 2008;27:51-59.

[78] Hsu AR. Topical review: barefoot running. *Foot & Ankle International*. 2012;33:787-794.

[79] Lieberman DE. Those feet in ancient times. *Nature*. 2012;483:550-551.

[80] Lieberman DE, Venkadesan M, Werbel WA, et al. Foot strike patterns and collision forces in habitually barefoot versus shod runners. *Nature*. 2010;463:531-535.

- [81] Hall JPL, Barton C, Jones PR, et al. The biomechanical differences between barefoot and shod distance running: A systematic review and preliminary meta-analysis. *Sports Medicine*. 2013;43:1335-1353.
- [82] Cochrum RG, Connors RT, Coons JM, et al. Comparison of running economy values while wearing no shoes, minimal shoes, and normal running shoes. *Journal of Strength and Conditioning Research*. 2017;31:595-601.
- [83] Bonacci J, Saunders PU, Hicks A, et al. Running in a minimalist and lightweight shoe is not the same as running barefoot: a biomechanical study. *British Journal of Sports Medicine*. 2013;47:387-392.
- [84] Chard A, Greene A, Hunt A, et al. Effect of thong style flip-flops on children's barefoot walking and jogging kinematics. *Journal of Foot and Ankle Research*. 2013;6:8.
- [85] Scott LA, Murley GS, Wickham JB. The influence of footwear on the electromyographic activity of selected lower limb muscles during walking. *Journal of Electromyography and Kinesiology*. 2012;22:1010-1016.
- [86] Zhang X, Paquette MR, Zhang S. A comparison of gait biomechanics of flip-flops, sandals, barefoot and shoes. *Journal of Foot and Ankle Research*. 2013;6:45.
- [87] Keenan GS, Franz JR, Dicharry J, et al. Lower limb joint kinetics in walking: The role of industry recommended footwear. *Gait & Posture*. 2011;33:350-355.
- [88] Sacco ICN, Akashi PMH, Hennig EM. A comparison of lower limb EMG and ground reaction forces between barefoot and shod gait in participants with diabetic neuropathic and healthy controls. *BMC Musculoskeletal Disorders*. 2010;11:24.
- [89] Carl TJ, Barrett SL. Computerized analysis of plantar pressure variation in flip-flops, athletic shoes, and bare feet. *Journal of the American Podiatric Medical Association*. 2008;98:374-378.
- [90] Echarri JJ, Forriol F. The development in footprint morphology in 1851 Congolese children from urban and rural areas, and the relationship between this and

wearing shoes. *Journal of Pediatric Orthopaedics B*. 2003;12:141-146.

[91] Holowka NB, Wallace IJ, Lieberman DE. Foot strength and stiffness are related to footwear use in a comparison of minimally- vs. conventionally-shod populations. *Scientific Reports*. 2018;8:3679.

[92] Shu Y, Mei Q, Fernandez J, et al. Foot morphological difference between habitually shod and unshod runners. *PLOS ONE*. 2015;10:e0131385.

[93] Mei Q, Fernandez J, Fu W, et al. A comparative biomechanical analysis of habitually unshod and shod runners based on a foot morphological difference. *Human Movement Science*. 2015;42:38-53.

[94] Lieberman DE. What we can learn about running from barefoot running: an evolutionary medical perspective. *Exercise and Sport Sciences Reviews*. 2012;40:63-72.

[95] Shih Y, Lin K-L, Shiang T-Y. Is the foot striking pattern more important than barefoot or shod conditions in running? *Gait & Posture*. 2013;38:490-494.

[96] Divert C, Mornieux G, Baur H, et al. Mechanical comparison of barefoot and shod running. *International journal of sports medicine*. 2004;593-598.

[97] Crowell HP, Davis IS. Gait retraining to reduce lower extremity loading in runners. *Clinical Biomechanics*. 2011;26:78-83.

[98] Daoud AI, Geissler GJ, Wang F, et al. Foot strike and injury rates in endurance runners: a retrospective study. *Medicine & Science in Sports & Exercise*. 2012;44:1325-1334.

[99] Salzler MJ, Bluman EM, Noonan S, et al. Injuries observed in minimalist runners. *Foot & Ankle International*. 2012;33:262-266.

[100] Conte C, Serrao M, Casali C, et al. Planned gait termination in cerebellar ataxias. *The Cerebellum*. 2012;11:896-904.

[101] Cen X, Jiang X, Gu Y. Do different muscle strength levels affect stability during unplanned gait termination? *Acta Bioeng Biomech*. 2019;21:27-35.

- [102] Cao C, A. Ashton-Miller J, Schultz AB, et al. Effects of age, available response time and gender on ability to stop suddenly when walking. *Gait & Posture*. 1998;8:103-109.
- [103] Pai Y-C, Patton J. Center of mass velocity-position predictions for balance control. *Journal of Biomechanics*. 1997;30:347-354.
- [104] Tirosh O, Sparrow WA. Gait termination in young and older adults: effects of stopping stimulus probability and stimulus delay. *Gait & Posture*. 2004;19:243-251.
- [105] Jian Y, Winter DA, Ishac MG, et al. Trajectory of the body COG and COP during initiation and termination of gait. *Gait & Posture*. 1993;1:9-22.
- [106] Pai Y-C, Iqbal K. Simulated movement termination for balance recovery: can movement strategies be sought to maintain stability in the presence of slipping or forced sliding? *Journal of Biomechanics*. 1999;32:779-786.
- [107] Perry SD, Santos LC, Patla AE. Contribution of vision and cutaneous sensation to the control of centre of mass (COM) during gait termination. *Brain Research*. 2001;913:27-34.
- [108] Gehring WJ, Gratton G, Coles MGH, et al. Probability effects on stimulus evaluation and response processes. *Journal of Experimental Psychology: Human Perception and Performance*. 1992;18:198-216.
- [109] Tirosh O, Sparrow WA. Age and walking speed effects on muscle recruitment in gait termination. *Gait & Posture*. 2005;21:279-288.
- [110] Bishop M, Brunt D, Pathare N, et al. The effect of velocity on the strategies used during gait termination. *Gait & Posture*. 2004;20:134-139.
- [111] Hase K, Stein RB. Analysis of rapid stopping during human walking. *Journal of Neurophysiology*. 1998;80:255-261.
- [112] Meier MR, Desrosiers J, Bourassa P, et al. Effect of Type II diabetic peripheral neuropathy on gait termination in the elderly. *Diabetologia*. 2001;44:585-592.

- [113] O'Kane FW, McGibbon CA, Krebs DE. Kinetic analysis of planned gait termination in healthy subjects and patients with balance disorders. *Gait & Posture*. 2003;17:170-179.
- [114] Bishop MD, Brunt D, Kukulka C, et al. Braking impulse and muscle activation during unplanned gait termination in human subjects with parkinsonism. *Neuroscience letters*. 2003;348:89-92.
- [115] Cameron D, Murphy A, Morris ME, et al. Planned stopping in people with Parkinson. *Parkinsonism & Related Disorders*. 2010;16:191-196.
- [116] Oates AR, Frank JS, Patla AE, et al. Control of dynamic stability during gait termination on a slippery surface in Parkinson's disease. *Movement Disorders*. 2008;23:1977-1983.
- [117] Oates AR, Van Ooteghem K, Frank JS, et al. Adaptation of gait termination on a slippery surface in Parkinson's disease. *Gait & Posture*. 2013;37:516-520.
- [118] Bishop M, Brunt D, Marjama-Lyons J. Do people with Parkinson's disease change strategy during unplanned gait termination? *Neuroscience letters*. 2006;397:240-244.
- [119] Serrao M, Conte C, Casali C, et al. Sudden stopping in patients with cerebellar ataxia. *The Cerebellum*. 2013;12:607-616.
- [120] Roeing KL, Moon Y, Sosnoff JJ. Unplanned gait termination in individuals with multiple sclerosis. *Gait & Posture*. 2017;53:168-172.
- [121] Givon U, Zeilig G, Achiron A. Gait analysis in multiple sclerosis: Characterization of temporal-spatial parameters using GAITRite functional ambulation system. *Gait & Posture*. 2009;29:138-142.
- [122] Cimolin V, Cau N, Galli M, et al. Gait initiation and termination strategies in patients with Prader-Willi syndrome. *Journal of NeuroEngineering and Rehabilitation*. 2017;14:44.

- [123] Zhao X, Gu Y, Yu J, et al. The influence of gender, age, and body mass index on arch height and arch stiffness. *The Journal of Foot and Ankle Surgery*. 2020;59:298-302.
- [124] Tao K, Ji W-T, Wang D-M, et al. Relative contributions of plantar fascia and ligaments on the arch static stability: a finite element study. *Biomedical Engineering-Biomedizinische Technik*. 2010;55:265-271.
- [125] Liang J, Yang Y, Yu G, et al. Deformation and stress distribution of the human foot after plantar ligaments release: A cadaveric study and finite element analysis. *Science China Life Sciences*. 2011;54:267-271.
- [126] Dahle LK, Mueller M, Delitto A, et al. Visual assessment of foot type and relationship of foot type to lower extremity injury. *Journal of Orthopaedic & Sports Physical Therapy*. 1991;14:70-74.
- [127] Burns J, Crosbie J, Hunt A, et al. The effect of pes cavus on foot pain and plantar pressure. *Clinical Biomechanics*. 2005;20:877-882.
- [128] Rao S, Song J, Kraszewski A, et al. The effect of foot structure on 1st metatarsophalangeal joint flexibility and hallucal loading. *Gait & Posture*. 2011;34:131-137.
- [129] Levy JC, Mizel MS, Wilson LS, et al. Incidence of foot and ankle injuries in west point cadets with pes planus compared to the general cadet population. *Foot & Ankle International*. 2006;27:1060-1064.
- [130] Bus SA, Lange Ad. A comparison of the 1-step, 2-step, and 3-step protocols for obtaining barefoot plantar pressure data in the diabetic neuropathic foot. *Clinical Biomechanics*. 2005;20:892-899.
- [131] Sun D, Song Y, Cen X, et al. Workflow assessing the effect of Achilles tendon rupture on gait function and metatarsal stress: Combined musculoskeletal modeling and finite element analysis. *Proceedings of the Institution of Mechanical Engineers, Part H: Journal of Engineering in Medicine*. 2022;236:676-685.

- [132] Gu YD, Ren XJ, Li JS, et al. Computer simulation of stress distribution in the metatarsals at different inversion landing angles using the finite element method. *International Orthopaedics*. 2010;34:669-676.
- [133] Behforootan S, Chatzistergos P, Naemi R, et al. Finite element modelling of the foot for clinical application: A systematic review. *Medical Engineering & Physics*. 2017;39:1-11.
- [134] Song Y, Shao E, Bíró I, et al. Finite element modelling for footwear design and evaluation: A systematic scoping review. *Heliyon*. 2022;8:e10940.
- [135] Wong DW-C, Chen TL-W, Peng Y, et al. An instrument for methodological quality assessment of single-subject finite element analysis used in computational orthopaedics. *Medicine in Novel Technology and Devices*. 2021;11:100067.
- [136] Song Y, Cen X, Zhang Y, et al. Development and validation of a subject-specific coupled model for foot and sports shoe complex: a pilot computational study. *Bioengineering*. 2022;9:553.
- [137] Cifuentes-De la Portilla C, Larrainzar-Garijo R, Bayod J. Analysis of the main passive soft tissues associated with adult acquired flatfoot deformity development: A computational modeling approach. *Journal of Biomechanics*. 2019;84:183-190.
- [138] Chen TL-W, Wong DW-C, Wang Y, et al. Foot arch deformation and plantar fascia loading during running with rearfoot strike and forefoot strike: A dynamic finite element analysis. *Journal of Biomechanics*. 2019;83:260-272.
- [139] Zhang Y-j, Guo Y, Long X, et al. Analysis of the main soft tissue stress associated with flexible flatfoot deformity: a finite element study. *Biomechanics and Modeling in Mechanobiology*. 2021;20:2169-2177.
- [140] Cheung JT-M, Zhang M, An K-N. Effects of plantar fascia stiffness on the biomechanical responses of the ankle-foot complex. *Clinical Biomechanics*. 2004;19:839-846.

- [141] Wang Y, Wong DW-C, Zhang M. Computational models of the foot and ankle for pathomechanics and clinical applications: a review. *Annals of Biomedical Engineering*. 2016;44:213-221.
- [142] Malakoutikhah H, de Cesar Netto C, Madenci E, et al. Evaluation of assumptions in foot and ankle biomechanical models. *Clinical Biomechanics*. 2022;100:105807.
- [143] Chen Y-N, Chang C-W, Li C-T, et al. Finite element analysis of plantar fascia during walking: a quasi-static simulation. *Foot & Ankle International*. 2015;36:90-97.
- [144] Malakoutikhah H, Madenci E, Latt LD. A computational model of force within the ligaments and tendons in progressive collapsing foot deformity. *Journal of Orthopaedic Research*. 2023;41:396-406.
- [145] Malakoutikhah H, Madenci E, Latt LD. The contribution of the ligaments in progressive collapsing foot deformity: A comprehensive computational study. *Journal of Orthopaedic Research*. 2022;40:2209-2221.
- [146] Malakoutikhah H, Madenci E, Latt LD. The impact of ligament tears on joint contact mechanics in progressive collapsing foot deformity: A finite element study. *Clinical Biomechanics*. 2022;94:105630.
- [147] Cifuentes-De la Portilla C, Larrainzar-Garijo R, Bayod J. Biomechanical stress analysis of the main soft tissues associated with the development of adult acquired flatfoot deformity. *Clinical Biomechanics*. 2019;61:163-171.
- [148] Cifuentes-De la Portilla C, Pasapula C, Gutiérrez-Narvarte B, et al. Peroneus Longus overload caused by soft tissue deficiencies associated with early adult acquired flatfoot: A finite element analysis. *Clinical Biomechanics*. 2021;86:105383.
- [149] Wang C, He X, Zhang Z, et al. Three-dimensional finite element analysis and biomechanical analysis of midfoot von mises stress levels in Flatfoot, Clubfoot, and Lisfranc Joint Injury. *Medical Science Monitor: International Medical Journal of Experimental and Clinical Research*. 2021;27:e931969-931961.

- [150] Cheung JT-M, Zhang M, An K-N. Effect of Achilles tendon loading on plantar fascia tension in the standing foot. *Clinical Biomechanics*. 2006;21:194-203.
- [151] Wong DW-C, Wang Y, Leung AK-L, et al. Finite element simulation on posterior tibial tendinopathy: Load transfer alteration and implications to the onset of pes planus. *Clinical Biomechanics*. 2018;51:10-16.
- [152] Guo J, Wang L, Mo Z, et al. Biomechanical behavior of valgus foot in children with cerebral palsy: A comparative study. *Journal of Biomechanics*. 2015;48:3170-3177.
- [153] Phan PK, Vo ATN, Bakhtiarydavijani A, et al. In silico finite element analysis of the foot ankle complex biomechanics: a literature review. *Journal of Biomechanical Engineering*. 2021;143:090802.
- [154] Morales-Orcajo E, Bayod J, Barbosa de Las Casas E. Computational foot modeling: scope and applications. *Archives of Computational Methods in Engineering*. 2016;23:389-416.
- [155] Zhu J, Forman J. A review of finite element models of ligaments in the foot and considerations for practical application. *Journal of Biomechanical Engineering*. 2022;144:080801.
- [156] Viceconti M, Olsen S, Nolte L-P, et al. Extracting clinically relevant data from finite element simulations. *Clinical Biomechanics*. 2005;20:451-454.
- [157] Nie B, Panzer MB, Mane A, et al. A framework for parametric modeling of ankle ligaments to determine the in situ response under gross foot motion. *Computer Methods in Biomechanics and Biomedical Engineering*. 2016;19:1254-1265.
- [158] Arangio GA, Reinert KL, Salathe EP. A biomechanical model of the effect of subtalar arthroereisis on the adult flexible flat foot. *Clinical Biomechanics*. 2004;19:847-852.
- [159] Wang M, Li S, Teo E-C, et al. The influence of heel height on strain variation of plantar fascia during high heel shoes walking-combined musculoskeletal modeling and

finite element analysis. *Frontiers in Bioengineering and Biotechnology*. 2021;9:821530.

[160] Xiang L, Mei Q, Wang A, et al. Evaluating function in the hallux valgus foot following a 12-week minimalist footwear intervention: A pilot computational analysis. *Journal of Biomechanics*. 2022;132:110941.

[161] Iaquineto JM, Wayne JS. Effects of surgical correction for the treatment of adult acquired flatfoot deformity: A computational investigation. *Journal of Orthopaedic Research*. 2011;29:1047-1054.

[162] Smyth NA, Aiyer AA, Kaplan JR, et al. Adult-acquired flatfoot deformity. *European Journal of Orthopaedic Surgery & Traumatology*. 2017;27:433-439.

[163] Lee Y-C, Lin G, Wang M-JJ. Comparing 3D foot scanning with conventional measurement methods. *Journal of Foot and Ankle Research*. 2014;7:44.

[164] England SA, Granata KP. The influence of gait speed on local dynamic stability of walking. *Gait & Posture*. 2007;25:172-178.

[165] Delp SL, Anderson FC, Arnold AS, et al. OpenSim: Open-source software to create and analyze dynamic simulations of movement. *IEEE Transactions on Biomedical Engineering*. 2007;54:1940-1950.

[166] Park H-J, Sim T, Suh S-W, et al. Analysis of coordination between thoracic and pelvic kinematic movements during gait in adolescents with idiopathic scoliosis. *European Spine Journal*. 2016;25:385-393.

[167] Needham R, Naemi R, Chockalingam N. Quantifying lumbar–pelvis coordination during gait using a modified vector coding technique. *Journal of Biomechanics*. 2014;47:1020-1026.

[168] Sparrow WA, Donovan E, van Emmerik R, et al. Using relative motion plots to measure changes in intra-limb and inter-limb coordination. *Journal of Motor Behavior*. 1987;19:115-129.

[169] Kido M, Ikoma K, Hara Y, et al. Effect of therapeutic insoles on the medial

longitudinal arch in patients with flatfoot deformity: A three-dimensional loading computed tomography study. *Clinical Biomechanics*. 2014;29:1095-1098.

[170] Hamill J, Haddad JM, McDermott WJ. Issues in quantifying variability from a dynamical systems perspective. *Journal of Applied Biomechanics*. 2000;16:407-418.

[171] Pataky TC, Vanrenterghem J, Robinson MA. Zero- vs. one-dimensional, parametric vs. non-parametric, and confidence interval vs. hypothesis testing procedures in one-dimensional biomechanical trajectory analysis. *Journal of Biomechanics*. 2015;48:1277-1285.

[172] Zhang Y, Awrejcewicz J, Szymanowska O, et al. Effects of severe hallux valgus on metatarsal stress and the metatarsophalangeal loading during balanced standing: A finite element analysis. *Computers in Biology and Medicine*. 2018;97:1-7.

[173] Gefen A. Stress analysis of the standing foot following surgical plantar fascia release. *Journal of Biomechanics*. 2002;35:629-637.

[174] Cho J-R, Park S-B, Ryu S-H, et al. Landing impact analysis of sports shoes using 3-D coupled foot-shoe finite element model. *Journal of Mechanical Science and Technology*. 2009;23:2583-2591.

[175] Siegler S, Block J, Schneck CD. The mechanical characteristics of the collateral ligaments of the human ankle joint. *Foot & Ankle*. 1988;8:234-242.

[176] Brilakis E, Kaselouris E, Xypnitos F, et al. Effects of Foot Posture on Fifth Metatarsal Fracture Healing: A Finite Element Study. *The Journal of Foot and Ankle Surgery*. 2012;51:720-728.

[177] Zhang Y, Baker JS, Ren X, et al. Metatarsal strapping tightness effect to vertical jump performance. *Human Movement Science*. 2015;41:255-264.

[178] Shen X-a, Cen X, Song Y. Investigating temporal kinematic differences caused by unexpected stimulation during gait termination through the waveform-level variance equality test. *BioMed Research International*. 2022;2022:4043426.

- [179] Hafer JF, Boyer KA. Age related differences in segment coordination and its variability during gait. *Gait & Posture*. 2018;62:92-98.
- [180] Svoboda Z, Janura M, Kutilek P, et al. Relationships between movements of the lower limb joints and the pelvis in open and closed kinematic chains during a gait cycle. *Journal of Human Kinetics*. 3916;51:37-43.
- [181] Grozier CD, Cagle GK, Pantone L, et al. Effects of medial longitudinal arch flexibility on propulsion kinetics during drop vertical jumps. *Journal of Biomechanics*. 2021;118:110322.
- [182] Hafer JF, Peacock J, Zernicke RF, et al. Segment coordination variability differs by years of running experience. *Medicine & Science in Sports & Exercise*. 2019;51:1438-1443.
- [183] Baida SR, Gore SJ, Franklyn-Miller AD, et al. Does the amount of lower extremity movement variability differ between injured and uninjured populations? A systematic review. *Scandinavian Journal of Medicine & Science in Sports*. 2018;28:1320-1338.
- [184] Sakata H, Hashizume S, Amma R, et al. Anterior-posterior ground reaction forces across a range of running speeds in unilateral transfemoral amputees. *Sports Biomechanics*. 2020;1-12.
- [185] Riddick R, Farris DJ, Kelly LA. The foot is more than a spring: human foot muscles perform work to adapt to the energetic requirements of locomotion. *Journal of The Royal Society Interface*. 2019;16:20180680.
- [186] Powell DW, Long B, Milner CE, et al. Effects of vertical loading on arch characteristics and intersegmental foot motions. *Journal of Applied Biomechanics*. 2012;28:165-173.
- [187] May TJ, Judy TA, Conti M, et al. Current treatment of plantar fasciitis. *Current Sports Medicine Reports*. 2002;1:278-284.

[188] Singh AK, Briggs PJ. Metatarsal extension osteotomy without plantar aponeurosis release in cavus feet. The effect on claw toe deformity a radiographic assessment. *Foot and Ankle Surgery*. 2012;18:210-212.

ABBREVIATION

AHI: arch height index	M1: first metatarsal
AP: anterior-posterior	M2: second metatarsal
ART: available response time	M3: third metatarsal
AS: arch stiffness	M4: forth metatarsal
ASI: arch stiffness index	M5: fifth metatarsal
BW: bodyweight	ML: medial-lateral
CA: coupling angle	MLA: medial longitudinal arch
COM: center of mass	MRI: magnetic resonance imaging
COP: center of pressure	MS: middle stance
CRP: continuous relative phase	MTP: metatarsophalangeal
CT: computer tomography	PF: plantar fascia
CV: coordination variability	PGT: planned gait termination
EMG: electromyography	ROM: range of motion
ES: early stance	SA: stiff arch
EV/TIR: eversion / tibial internal rotation	SnPM: statistical nonparametric mapping
FA: flexible arch	SOL: soleus
FE: finite element	SPM: statistical parametric mapping
GM: gluteus medius	TMT: tarsometatarsal
GRF: ground reaction force	UGT: unplanned gait termination
GRI: ground reaction impulse	VL: vastus lateralis
GT: gait termination	
LS: late stance	

LIST OF TABLES

Table 1 Anthropometric characteristics of two groups	43
Table 2 Material properties of the components in the finite element model	50
Table 3 Coupling angle between different arch flexibility in each sub-phase.....	56
Table 4 Ground reaction forces and impulses between different arch flexibility...	59

LIST OF FIGURES

Figure 1 The windlass mechanism of the human foot.....	5
Figure 2 The triangular truss model for medial longitudinal arch support.....	6
Figure 3 Illustration of foot morphology variables and arch indexes.....	8
Figure 4 Comparison of impulse distribution between different arch stiffness index	9
Figure 5 Illustration of continuous relative phase calculation [53]	14
Figure 6 Classification of coordination model based on the coupling angle in sagittal, frontal, and transverse planes.....	16
Figure 7 Phase division of the normal gait cycle.....	17
Figure 8 The main components of the foot finite element model.....	29
Figure 9 Experimental and computational process flowchart	40
Figure 10 The human informed consent form and institutional review board procedures.....	42
Figure 11 Illustration of reflective markers attached to the human body	45
Figure 12 The three-dimensional finite element model and the application of boundary and loading conditions.....	49

Figure 13 Kinematic differences of ankle angles in the sagittal plane	52
Figure 14 Kinematic differences of ankle angles in the frontal plane	53
Figure 15 Kinematic differences of ankle angles in the transverse plane	54
Figure 16 Kinematic differences of MTP angles in the frontal plane	55
Figure 17 Kinematic differences of MTP angles in the transverse plane.....	55
Figure 18 Comparison of coordination variabilities between different arch flexibilities.....	57
Figure 19 Comparison of ground reaction forces and impulses between different ASI.....	58
Figure 20 Comparison of FE predicted (left) and experimentally measured (right) peak pressure during balanced standing for model validation	60
Figure 21 Effects of varying Young’s modulus of the plantar fascia on peak von Mises stress of metatarsals	61
Figure 22 Effects of varying Young’s modulus of the plantar fascia on changes in the force transmission through the metatarsophalangeal and tarsometatarsal joints	62
Figure 23 The effect of arch stiffness on the foot–ankle temporal kinematics during gait termination.....	74
Figure 24 The proposed experimental protocol regarding arch stiffness, lower limb joint coupling coordination, and ground reaction impulse.....	76
Figure 25 Flow chart of foot model development of FE simulation	78

ACKNOWLEDGEMENTS

The winds that began from China in the autumn of 2021 have finally blown into Hungary's summer in 2024.

This doctoral journey has been a remarkable mix of challenges and rewards, and I am deeply humbled by the unwavering support and encouragement I have received along the way. As it now draws to a close, my heart is filled with both reluctance to bid farewell and profound nostalgia.

First and foremost, I extend my deepest thanks to my esteemed supervisors, Prof. Dr. István Bíró and Prof. Dr. Yaodong Gu, for their invaluable guidance, insightful contributions, and boundless patience. Their expertise and dedication have been instrumental in shaping the course of this research.

I also want to express my sincere appreciation to the staff and faculty at the Doctoral School on Safety and Security Sciences, Óbuda University (OE), the Faculty of Engineering, University of Szeged (SZTE), and the Faculty of Sports Science, Ningbo University (NBU), for providing me with a conducive research environment and the necessary resources to conduct this study. Moreover, I extend my heartfelt thanks to the Stipendium Hungaricum Programme, Tempus Public Foundation, and China Scholarship Council (CSC) for their generous financial support, which has been instrumental in making this journey possible.

To my family, I am eternally thankful for your unwavering love, encouragement, and unyielding belief in me. Your constant support and understanding throughout this entire journey have been an unshakable source of strength and motivation.

Last but not least, I want to express my deep appreciation to the countless researchers, scholars, and academics whose contributions and insights have profoundly shaped my thinking and laid a solid foundation for this work. I feel truly indebted to the broader academic community for their collective efforts in advancing knowledge in the field of *Biomechanics*.

I am profoundly grateful to each one of you for being part of this significant milestone in my academic journey.

Xuanzhen Cen